


NUREG/CR-1636, Vol. 4
SAND79-1909

Printed December 1981

Risk Methodology for Geologic Disposal of Radioactive Waste: Effects of Variable Hydrologic Patterns on the Environmental Transport Model

Jack B. Brown, Jon C. Helton

Prepared by
Sandia National Laboratories
Albuquerque, New Mexico 87185 and Livermore, California 94550
for the United States Department of Energy
under Contract DE-AC04-76DP00789



Prepared for **8205030642**
U. S. NUCLEAR REGULATORY COMMISSION

NOTICE

This report was prepared as an account of work sponsored by an agency of the United States Government. Neither the United States Government nor any agency thereof, or any of their employees, makes any warranty, expressed or implied, or assumes any legal liability or responsibility for any third party's use, or the results of such use, of any information, apparatus product or process disclosed in this report, or represents that its use by such third party would not infringe privately owned rights.

Available from
GPO Sales Program
Division of Technical Information and Document Control
U.S. Nuclear Regulatory Commission
Washington, D.C. 20555

and
National Technical Information Service
Springfield, Virginia 22161

NUREG/CR-1636, Vol. 4
SAND79-1909
GF

RISK METHODOLOGY FOR GEOLOGIC DISPOSAL OF
RADIOACTIVE WASTE:
EFFECTS OF VARIABLE HYDROLOGIC PATTERNS ON
THE ENVIRONMENTAL TRANSPORT MODEL

Jack B. Brown
Sandia National Laboratories
and
Auburn University

Jon C. Helton
Sandia National Laboratories
and
Arizona State University

Date Published: December 1981

Sandia National Laboratories
Albuquerque, New Mexico 87185
operated by
Sandia Corporation
for the
U.S. Department of Energy

Prepared for
Division of Risk Analysis
Office of Nuclear Regulatory Research
U.S. Nuclear Regulatory Commission
Washington, DC 20555
Under Memorandum of Understanding DOE 40-550-75
NRC FIN No. 1192

ABSTRACT

The Environmental Transport Model is a compartment model which represents radionuclide movement through a surface hydrologic system. Some of the parameters in the model are based on water and solid flow rates between various compartments in the system. Mean yearly flow rates have been used in the calculation of these parameters, whereas the flow rates are (at best) periodic functions of time or (more realistically) periodic stochastic processes. This report presents the results of an investigation into the effects that these variable hydrologic patterns have on the Environmental Transport Model.

ACKNOWLEDGEMENT

The work reported here was performed while the first author was employed at Sandia National Laboratories on Summer University Faculty Appointments during the summers of 1978 and 1979, and he would not have been able to make much progress on the problem without excellent guidance and assistance from the regular staff members involved in the project (project leader J. E. Campbell, in particular). Special thanks are due H. E. Anderson for his assistance in helping the first author become familiar with the computing system at Sandia.

TABLE OF CONTENTS

	<u>Page</u>
1. Introduction	1
2. General Description of A, X and Y	8
3. Computer Simulation Results	14
4. Comparison of X and Y	70
5. Further Discussion of the Stochastic Case	90
6. Summary and Conclusion	94
Appendix	96
References	103

LIST OF FIGURES

	Page
1-1 Division of a Zone Into Subzones	2
1-2 Compartments and Flows Associated with the Movement of a Chain of N Radionuclides Through a System of M Zones	3
3-1 Asymptotic Behavior of X (Units: Atoms) for Radionuclide Input to Groundwater Subzone of River Zone	21
3-2 Asymptotic Behavior of X (Units: Atoms) for Radionuclide Input to Soil Subzone of River Zone	23
3-3 Asymptotic Behavior of X (Units: Atoms) for Radionuclide Input to Surface Water Subzone of River Zone	25
3-4 Asymptotic Behavior of X (Units: Atoms) for Radionuclide Input to Sediment Subzone of River Zone	27
3-5 Behavior of X, Y, EZ, and EZ + SDZ (Units: Atoms) for Year 100 with Radionuclide Input to Groundwater Subzone of River Zone	29
3-6 Behavior of X, Y, EZ, and EZ + SDZ (Units: Atoms) for Year 100 with Radionuclide Input to Soil Subzone of River Zone	31
3-7 Behavior of X, Y, EZ, and EZ + SDZ (Units: Atoms) for Year 100 with Radionuclide Input to Surface Water Subzone of River Zone	33
3-8 Behavior of X, Y, EZ, and EZ + SDZ (Units: Atoms) for Year 100 with Radionuclide Input to Sediment Subzone of River Zone	35
3-9 Behavior of X, Y, EZ, and EZ + SDZ (Units: Atoms) for Year 1000 with Radionuclide Input to Groundwater Subzone of River Zone	37

LIST OF FIGURES

	Page
3-10 Behavior of X, Y, EZ, and EZ + SDZ (Units: Atoms) for Year 1000 with Radionuclide Input to Soil Subzone of River Zone	39
3-11 Behavior of X, Y, EZ, and EZ + SDZ (Units: Atoms) for Year 1000 with Radionuclide Input to Surface Water Subzone of River Zone	41
3-12 Behavior of X, Y, EZ, and EZ + SDZ (Units: Atoms) for Year 1000 with Radionuclide Input to Sediment Subzone of River Zone	43
3-13 Asymptotic Behavior of X (Units: Atoms) for Radionuclide Input to Groundwater Subzone of Lake Zone	45
3-14 Asymptotic Behavior of X (Units: Atoms) for Radionuclide Input to Soil Subzone of Lake Zone	47
3-15 Asymptotic Behavior of X (Units: Atoms) for Radionuclide Input to Surface Water Subzone of Lake Zone	49
3-16 Asymptotic Behavior of X (Units: Atoms) for Radionuclide Input to Sediment Subzone of Lake Zone	51
3-17 Behavior of X, Y, EZ, and EZ + SDZ (Units: Atoms) for Year 100 with Radionuclide Input to Groundwater Subzone of Lake Zone	53
3-18 Behavior of X, Y, EZ, and EZ + SDZ (Units: Atoms) for Year 100 with Radionuclide Input to Soil Subzone of Lake Zone	55
3-19 Behavior of X, Y, EZ, and EZ + SDZ (Units: Atoms) for Year 100 with Radionuclide Input to Surface Water Subzone of Lake Zone	57

LIST OF FIGURES

	Page
3-20 Behavior of X, Y, EZ, and EZ + SDZ (Units: Atoms) for Year 100 with Radionuclide Input to Sediment Subzone of Lake Zone	59
3-21 Behavior of X, Y, EZ, and EZ + SDZ (Units: Atoms) for Year 1000 with Radionuclide Input to Groundwater Subzone of Lake Zone	61
3-22 Behavior of X, Y, EZ, and EZ + SDZ (Units: Atoms) for Year 1000 with Radionuclide Input to Soil Subzone of Lake Zone	63
3-23 Behavior of X, Y, EZ, and EZ + SDZ (Units: Atoms) for Year 1000 with Radionuclide Input to Surface Water Subzone of Lake Zone	65
3-24 Behavior of X, Y, EZ, and EZ + SDZ (Units: Atoms) for Year 1000 with Radionuclide Input to Sediment Sub- zone of Lake Zone	67

LIST OF TABLES

	Page
Table 3-1 $\text{Max}[EZ_k(t) + 2 \cdot \text{SDZ}_K(t) - X_k(t)]/X_k(t)$ Expressed as a Percentage	69

Chapter 1

Introduction

The following report presents the results of an investigation into the effects that variable hydrologic patterns have on the Environmental Transport Model. The Environmental Transport Model is a compartment model which is used to represent how radionuclides would move through a given surface water system of lakes and rivers and how they would build up in the adjacent soil layers, the upper groundwater aquifers beneath the soil layers, and the sediment layers beneath the surface water system. Detailed discussions of the model are given in Campbell, et al., (Ca78) and Helton and Kaestner (Hel81b).

The model is based on the vector differential equation

$$dX/dt = AX + R, \quad (1.1)$$

where, if $1 < i < n$, then $X_i(t)$ denotes the number of atoms of a particular radionuclide which are present at time t in a certain subzone (GW ~ groundwater, SOIL ~ soil, SW ~ surface water, SED ~ sediment) of one of the hydrologic zones in the system being considered. The preceding terminology is explained in greater detail in the next paragraph. The matrix A (called an Environmental Transport or ET-matrix here) contains the transfer coefficients (units: yr^{-1}) between the subzones and has a special character which will be indicated. The vector R represents the rates (units: atoms/yr) at which the radionuclides under consideration are entering the subzones in the system being considered. In the following, R is assumed to be constant.

The elements of the matrix A are derived from the flow rates for water and solid material between the various subzones in the system. These flows are shown for a single zone in Figure 1-1. Further, the linkage of zones to represent the movement of a decay chain containing N radionuclides through a system of M zones is shown in Figure 1-2. As discussed in Campbell, et al., (Ca78, Chapter 4) a total of $4MN$ compartments is used to represent the movement of a decay chain with N radionuclides through a system of M zones. With

$$L = 4N(I - 1) + 4(J - 1) + K$$

and under the notation used in conjunction with the computer program (Hel81b) which implements model, the Lth compartment is the compartment associated with the presence of Radionuclide J in Subzone K (1 ~ GW, 2 ~ SOIL, 3 ~ SW, 4 ~ SED) of Zone I. That is, the function X_L in the radionuclide transport equations represents the amount of Radionuclide J in Subzone K of Zone I.

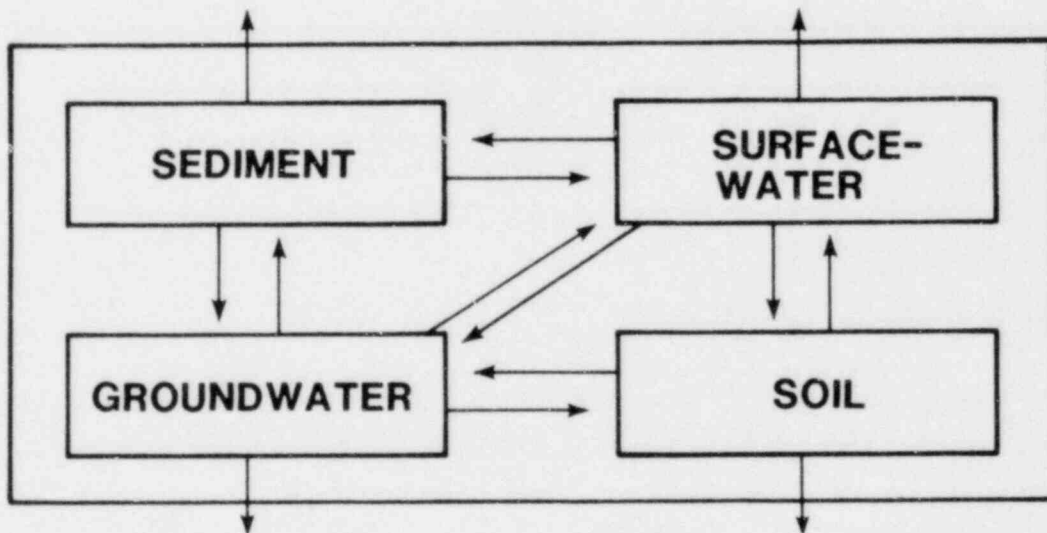


Figure 1-1. Division of a Zone Into Subzones. Arrows represent potential directions of movement for water and solid material. Radionuclide movement should follow the same pattern since it is these flows that dominate radionuclide transport.

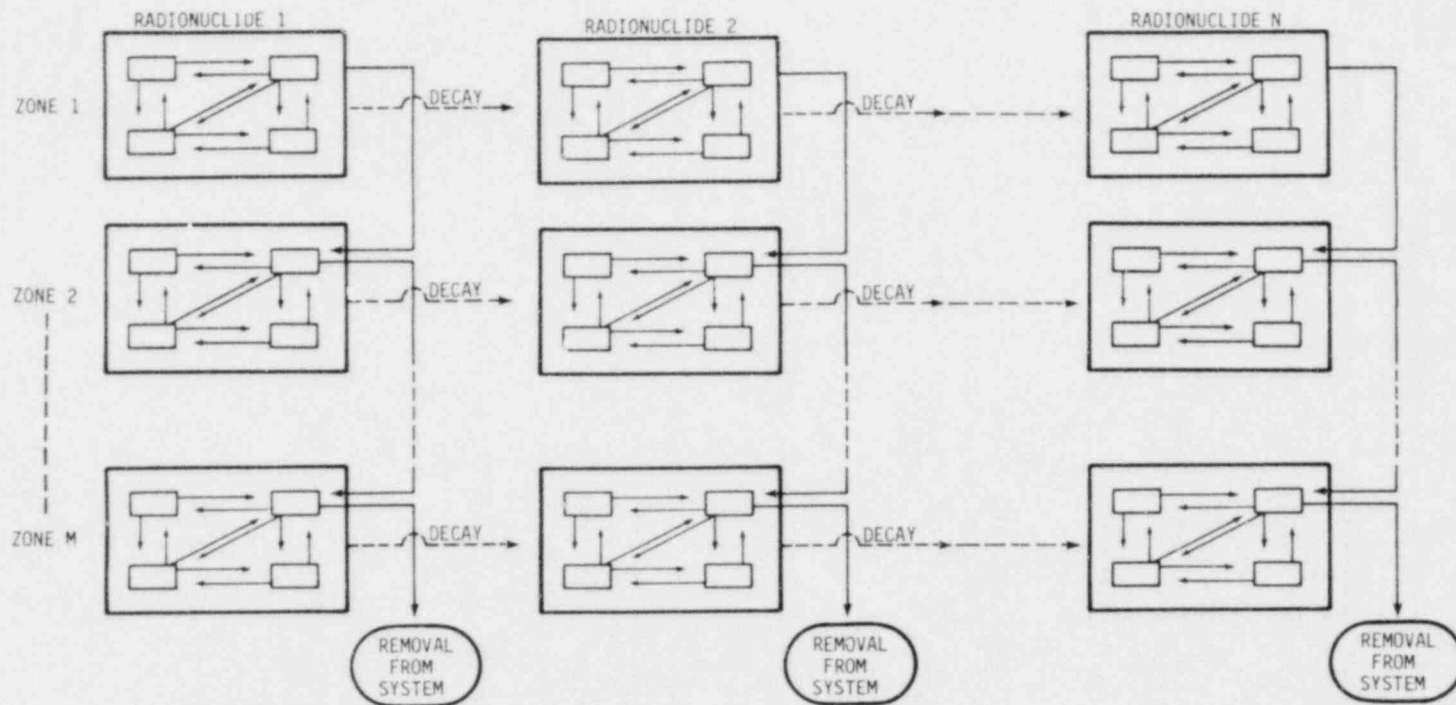


Figure 1-2. Compartments and Flows Associated With the Movement of a Chain of N Radionuclides Through a System of M Zones. Each subzone has N compartments associated with it. Each radionuclide has $4M$ compartments associated with it. Solid lines represent physical flows of radionuclides; dotted lines represent decay. With the exception of the surface-water subzone of Zone M , arrows which represent possible physical flows out of the system are omitted.

In the simplest case where only one zone and one radionuclide are considered, $A = [a_{ij}]$ is a 4x4 matrix. Then, $X_1(t)$, $X_2(t)$, $X_3(t)$ and $X_4(t)$ represent the number of atoms of the radionuclide in question present at time t in the groundwater, soil, surface water and sediment subzones, respectively. The flow rate constant a_{ij} (units: yr^{-1}), representing flow from Subzone J to Subzone I , is defined by the equation

$$a_{ij} = (1 - S_j)RW_{ij}/VW_j + (S_j)RS_{ij}/MS_j,$$

where VW_j is the volume (units: L) of water in Subzone J , MS_j is the mass (units: kg) of solid material in Subzone J , RW_{ij} is the rate of water movement (units: L/yr) from Subzone J to Subzone I and RS_{ij} is the rate of solid movement (units: kg/yr) from Subzone J to Subzone I . The term S_j is a weighting factor based on the distribution coefficient (KD -value) for the particular radionuclide and subzone under consideration. Specifically,

$$S_j = KD_j MS_j / (KD_j MS_j + VW_j),$$

where KD_j is the distribution coefficient for the radionuclide in Subzone J . The distribution coefficient (units: ci/kg per ci/L) is a measure of the tendency of the radionuclide to become sorbed to solids and has generally been found to range between 10^0 and 10^5 (To79, Ap77). If the distribution coefficient is large, S is close to 1; if the distribution coefficient is small, S is closer to 0. For $i = 5$, the term a_{ij} defines a movement out of Subzone J and out of the zone. Such terms do not appear by themselves as elements of A as do the other a_{ij} ; however, they are used in the calculation of the diagonal elements of A . Specifically, such diagonal elements are given by

$$a_{jj} = - \sum_{i \neq j} a_{ij} - \lambda,$$

where λ is the decay constant for the radionuclide. With respect to the preceding equality, each diagonal element is the rate constant for movement out of a particular subzone and thus is the sum of all rate constants for movement out of that subzone.

The preceding paragraph describes the elements of A for one zone and one radionuclide. That is, A is defined for a system of the form represented in Figure 1-1. The elements of A are defined similarly for a system of the form represented in Figure 1-2. Here, A is a 4MNx4MN matrix and it is necessary to incorporate into the elements of A the linkages which result from radioactive decay and from physical flow through the system.

In the Environmental Transport Model, mean yearly values for the flow rates RW_{ij} and RS_{ij} are used in the calculation of the a_{ij} and A is treated as a constant matrix. These flow rates are (at best) periodic functions of time or (more realistically) periodic stochastic processes. Here, the designation periodic stochastic process is used to indicate a stochastic process for which the expected values of the individual random variables form a periodic function. This study examines the rates at which radionuclide buildup occurs when this variability in A is taken into account. The desire is to determine if such variability has sufficient effects on predictions by the Environmental Transport Model to require some method for its incorporation into model predictions. In investigating these processes, the intent is to perform bounding calculations to develop a feeling for the extent of their effects rather than to develop detailed models which incorporate these effects into the Environmental Transport Model.

For this study, the solutions Y to the following equations are considered as models of the periodic case:

$$dY/dt = p(t)AY + R \quad (1.2)$$

and

$$dY/dt = (p(t)F + D)Y + R. \quad (1.3)$$

The function $p(t)$ is called a hydrologic pattern and is a continuous (or, at least piecewise-continuous), periodic (with period 1 year), positive-valued function with

$$\int_0^1 p(t)dt = 1.$$

The function $p(t)$ is unitless and thus the units for the preceding integral are years. The matrix A is the Environmental Transport Matrix computed with mean yearly values for the flow rates as previously indicated. Further, F is the resulting matrix when the decay rates are not included and D is the decay rate matrix; that is, $A = F + D$. The matrix D is a lower triangular matrix with nonpositive diagonal elements and nonnegative off-diagonal elements. The diagonal elements correspond to radioactive decay rates; the positive off-diagonal elements correspond to generation rates of daughter isotopes due to the radioactive decay of parent radionuclides.

Replacements of the form indicated in the preceding paragraph are common in biological and ecological modeling. Specifically, a periodic parameter $A(t)$ with period τ may be replaced by its mean value

$$A = \int_0^{\tau} A(t) dt / \tau .$$

Or, a periodic stochastic parameter $A(t, \bullet)$ with period τ may be replaced by its expected value

$$A = E \left(\int_0^{\tau} A(t, \bullet) dt / \tau \right) = \int_0^{\tau} E[A(t, \bullet)] dt / \tau .$$

See Rykiel and Kuenzel (Ry71), Heathcote (Hea73) and Tiwari, et al., (Ti78) for some linear and nonlinear models where this is done and some comparisons are made.

It is obviously assumed in Equations (1.2) and (1.3) that variations in flow rates of water and sediments occur simultaneously in all subzones of the system. This is only an approximation of true hydrologic phenomenon and tends to overestimate flow rates for other subzones relative to those for the surface water subzone. As discussed in Section 4.1, this does cause some potentially misleading results. It is also inherently assumed in (1.2) that, if the decay rates are included in the computation of the diagonal elements of A , then they vary along with the flow rates; this obviously does not agree with reality.

Equation (1.3) avoids this difficulty. However, Equation (1.2) yields to a certain change of variables which greatly simplifies the analytical comparison of its solution to the solution X of (1.1). Also, certain computational difficulties are encountered in generating solutions to (1.3) which do not occur in generating solutions to (1.2). Therefore, this study concentrates primarily on (1.2). For a radionuclide chain with equal distribution coefficients, it is possible to omit consideration of the decay rates, in which case a comparison of the solutions to (1.1) and (1.2) is the pertinent comparison. In most cases of interest in geologic waste disposal, the decay rates in D are much smaller than the elements of F , so that $p(t)A$ is almost the same as $p(t)F + D$. Indeed, it will be shown that in the case of a single radionuclide with long half life, there is limited difference between the solutions to (1.2) and (1.3).

As a model of the stochastic case, the solution to the following equation is considered:

$$dZ(t,\omega)/dt = S(t,\omega)p(t)AZ(t,\omega) + R, \quad (1.4)$$

where $p(t)$ is a hydrologic pattern and $S(t,\omega)$ is a certain kind of stochastic process with $E[S(t,\cdot)] = 1$. The particular stochastic process considered is described in Chapter 3.

Chapter 2

General Description of A, X and Y

An Environmental Transport Matrix is an example of a class of matrices each of which is a square matrix with (1) off-diagonal elements nonnegative, (2) diagonal elements nonpositive, and (3) the j th diagonal element $a_{jj} = -d_j$ satisfying

$$d_j \geq \sum_{i \neq j} a_{ij}.$$

With respect to the structure of an Environmental Transport Matrix A, each element a_{ij} , $i \neq j$, corresponds to a movement from Compartment J to Compartment I; thus, strict inequality holds in the preceding relation only if there is a direct movement of radionuclide (due to radioactive decay or physical transport) out of Compartment J and out of the system under consideration. A compartment system such as the one represented in Figure 1-2 is said to be open if material can move out of the system; conversely, a system is said to be closed if it is not open. Further, a system is said to be completely open if it is open and contains no closed subsystem. If all the flows represented in Figure 1-2 are nonzero, then the indicated system is completely open. If the system represented by an Environmental Transport Matrix is completely open, then (4) each diagonal element is negative and (5) there exists at least one diagonal element $a_{jj} = -d_j$ such that

$$d_j > \sum_{i \neq j} a_{ij}.$$

But, validity of conditions (1) through (5) does not necessarily imply that the underlying system is completely open. However, if the system is completely open, then the corresponding Environmental Transport Matrix A is nonsingular and all eigenvalues of A have negative real part. Additional discussion is available in Franklin (Fr68, Section 6.8), Thron (Thr72) and Helton, et al., (Hel81a, Section 1.2).

The general mathematical nature of the solutions to (1.1), (1.2) and (1.3) is now discussed. For convenience, the terminology and notation of Brauer and Noel (Br69) are used. There will be scalar, vector and matrix quantities mixed in various equations. It should be clear from context which is which. For example, in the expression $p(t)e^{At}R$, the following is intended: t and $p(t)$ are scalars; A , At and e^{At} are matrices; R is a vector; and so the product is a vector. The equivalent expressions e^{At} and $\exp(At)$ are used to represent matrix exponentials. As discussed in Bellman (Bel70) and Dollard and Friedman (Do79), such functions can be represented as infinite series or multiplicative integrals. If $V \geq a$ is used to indicate that every element of V is greater than or equal to a . In the following, the underlying system is always assumed to be completely open.

The solution to (1.1) is examined first. A convenient representation for the solution X to (1.1) with $X(0) = V_0$ is

$$X(t) = e^{At}V_0 + \int_0^t e^{(t-s)A}R ds \quad (2.1)$$

[Br69, p. 72]. The equality in (2.1) remains valid when R is assumed to be a function rather than a constant. Further, the vector function $e^{At}V_0$ can be expressed as a linear combination of elements of the form $p_i(t)e^{\lambda_i t}$, where the $p_i(t)$ are vector polynomials in t and the λ_i are the eigenvalues of A (Th72, Theorem 8). Since the eigenvalues of A have negative real part, it follows that

$$e^{At}V_0 \rightarrow 0 \text{ as } t \rightarrow \infty. \quad (2.2)$$

It is easily shown by direct substitution that the constant vector

$$SX = -A^{-1}R$$

is a solution for (1.1). Now, by using the relations in (2.1) and (2.2), it follows that SX is the constant asymptotic solution for (1.1) to which every solution converges.

The following relationship involving the nonnegativity of solutions to (1.1) with initial value $X(0) = V_0$ is often useful:

$$\text{if } V_0 \geq 0, \text{ then } e^{At}V_0 \geq 0. \quad (2.3)$$

This result can be established by using the equality

$$e^{At}V_0 = \lim_{j \rightarrow \infty} (I + At/j)^j V_0.$$

Once j is sufficiently large, all elements of $(I + At/j)$, and hence of $(I + At/j)^j$, are nonnegative. The result now follows readily.

The solutions to (1.2) and (1.3) are examined next. The unique solution to a nonhomogeneous system

$$dY/dt = M(t)Y + G(t), \quad Y(0) = Y_0$$

is given by

$$Y(t) = \Phi(t)Y_0 + \Phi(t) \int_0^t \Phi^{-1}(s)G(s)ds, \quad (2.4)$$

where Φ is the fundamental matrix solution for the corresponding homogeneous system $dY/dt = M(t)Y$ with $\Phi(0) = I$ (Br69, Section 2.4). The preceding result is now used to show that there exists a unique periodic asymptotic solution SY to (1.2) to which every solution of (1.2) converges. For convenience, the functions P and Q are introduced, where

$$P(t) = \int_0^t p(s)ds = \int_0^t 1ds + \int_0^t (p(s) - 1)ds = t + Q(t). \quad (2.5)$$

The function P is increasing with $P(n) = n$ for each positive integer n , and the function Q is periodic with

$$Q(n) = 0 \text{ and } |Q(s) - Q(t)| \leq 1$$

for all s and t . Since

$$\frac{d}{dt}(e^{P(t)A}) = p(t)Ae^{P(t)A},$$

it follows that¹

$$e^{P(t)A} = e^{Q(t)A}e^{tA}$$

is a fundamental matrix solution to the homogeneous equation $dX/dt = p(t)AX$. Thus, since every eigenvalue of A has negative real part, the relation indicated in (2.2) implies that every solution to the preceding homogeneous equation must converge to zero and so the equation can have no nonzero periodic solutions. This is sufficient to imply that (1.2) has at least one periodic solution (Br69, Theorem 2.14). Now, by using the relations in (2.2) and (2.4) and noting that $G(s) = R$ is a constant, it follows that this periodic solution SY is unique and that every solution to (1.2) converges to SY . For (1.2) with the initial value condition $Y(0) = V_0$, the representation in (2.4) becomes

$$Y(t) = e^{P(t)A}V_0 + \int_0^t e^{(P(t)-P(s))A}Rds. \quad (2.6)$$

¹The matrix function $e^{Q(t)A}$ is the periodic function appearing in Floquet's Theorem (Br69, Theorem 2.12).

The preceding discussion of the behavior of (1.2) would not be valid if $p(t)$ were replaced by a periodic matrix $B(t)$ due to complications associated with the noncommutativity of matrix multiplication.

In general, it is not possible to express the solution to (1.3) in a form involving matrix exponentials as is done in (2.6) for the solution to (1.2). This results because it is not necessarily true that $FD = DF$. However, in the l-radionuclide case, such commutativity holds because D is a diagonal matrix, and in this case, the solution to (1.3) with initial value V_0 can be expressed as

$$Y(t) = e^{(P(t)F+TD)}V_0 + \int_0^t e^{(P(t)F+TD-P(s)-SD)}Rds. \quad (2.7)$$

It has now been shown that both (1.1) and (1.2) have unique asymptotic solutions to which all other solutions converge.² The manner in which individual solutions to these equations approach their asymptotic limits is now considered. For (1.1) with $X(0) = 0$, the components of X are nondecreasing functions on $[0, \infty]$. To establish this statement, the equality in (2.1) is used to show that, if $0 < t < t + \epsilon$, then

$$\begin{aligned} X(t+\epsilon) - X(t) &= \int_0^{t+\epsilon} e^{(t+\epsilon-s)A}Rds - \int_0^t e^{(t-s)A}Rds \\ &= \int_0^\epsilon e^{(t+\epsilon-s)A}Rds + \int_\epsilon^{t+\epsilon} e^{(t+\epsilon-s)A}Rds - \int_0^t e^{(t-s)A}Rds. \end{aligned}$$

²A definition of convergence which is applicable for both (1.1) and (1.2) is the following: The statement that the function F converges asymptotically to the function G means, if $\epsilon > 0$, then there exists a positive number N such that, if $t > N$, then $\|F(t) - G(t)\| < \epsilon$.

Now, the change of variable $s = z + \epsilon$ in the second integral cancels the last integral and thus leads to the relationship

$$X(t+\epsilon) - X(t) = \int_0^\epsilon e^{(t+\epsilon-s)A} R ds \geq 0,$$

where the inequality follows from (2.3). This establishes the result.

The behavior of solutions for (1.2) is considered next. As the asymptotic solution SY to (1.2) is periodic, the components of other solutions cannot "increase monotonically to their limits." However, the following result is true. For (1.2) with $Y(0) = 0$, the inequality $Y(t) < Y(t+1)$ is valid for $t > 0$, and hence, if Y_i is a component of Y , then $Y_i(t) < SY_i(t)$ for $t > 0$. The first inequality can be established by an argument similar to that used to establish the nondecreasing nature of the components of X . The second inequality follows immediately since its failure would contradict the convergence of Y to SY .

Chapter 3

Computer Simulation Results

The results of a number of simulations using the Environmental Transport Model are presented in this chapter. Specifically, solutions to the equations in (1.1), (1.2) and (1.4) are given. The intent is to illustrate the behavior of solutions to (1.1) as the asymptotic solution SX is approached and to provide comparisons of representations for a given site with (1.1), (1.2) and (1.4).

Each simulation involves a representation for one zone and one radionuclide. Two different sites are considered. The first site is a "typical river zone" and is the zone designated as Zone 1 in the Reference Site defined by Helton and Iman (Hel80, Chapter 2). The second site is a "typical lake zone" and is the zone designated as Zone 2 in the preceding Reference Site (Hel80). The radionuclide used is Cm245 (Half Life = 8.3×10^3 yr, Decay Constant = 8.4×10^{-5} yr⁻¹). With an assumed distribution coefficient of 1000 L/kg, the resulting Environmental Transport Matrices for these two sites are

$$A = \begin{bmatrix} -3.2 \times 10^{-4} & 8.9 \times 10^{-4} & 0. & 0. \\ 0. & -2.3 \times 10^{-3} & 5.9 & 0. \\ 2.3 \times 10^{-4} & 1.4 \times 10^{-3} & -960.0 & 1.0 \times 10^{-1} \\ 0. & 0. & 90.0 & -1.0 \times 10^{-1} \end{bmatrix} \quad (3.1)$$

and

$$A = \begin{bmatrix} -3.2 \times 10^{-4} & 8.9 \times 10^{-4} & 0. & 0. \\ 0. & -1.4 \times 10^{-3} & 2.5 \times 10^{-3} & 0. \\ 2.3 \times 10^{-4} & 4.5 \times 10^{-4} & -1.6 & .10 \\ 0. & 0. & 4.0 \times 10^{-1} & -.15 \end{bmatrix} \quad (3.2)$$

respectively. The units for the elements of the preceding matrices are yr⁻¹. The input data for the Environmental Transport Model which defines the two preceding matrices are derived in Helton and Iman (Hel80, Chapter 2).

Solutions for (1.1) were obtained using the coefficient matrices in (3.1) and (3.2). However, to consider (1.2) and (1.4) it was first necessary to define the hydrologic pattern $p(t)$. Initially, a study was made of stream hydrographs available from the United States Geological Survey and data in the recent literature on synthetic hydrology (appearing mostly in the journal Water Resources Research) to determine what assumptions were reasonable with respect to $p(t)$. Such patterns are usually bimodal (sometimes unimodal), typically attaining a minimum value, $\min p$, in the fall and a maximum value, $\max p$, in the spring. For examples, see Harms and Campbell (Ha67), Thomas and Fiering (Tho62) and Moreau and Pyatt (Mo70). The intervals ($\min p$, $\max p$) generally range from (.4, 2.0), see Harms and Campbell (Ha67, Figure 4), to more extreme values like (.2, 3.8), see Thomas and Fiering (Tho62, Table 12.2). Although one might imagine an environment so extreme that $p(t)$ would be less than .1 for 11 months of the year and then greater than 10.9 for one month, this appears to be an unusual case. In all computations of the solutions $Y(t)$ and $Z(t)$ to (1.2) and (1.4), respectively, the hydrologic pattern is assumed to be the following mildly extreme one:

$$\begin{aligned}
 p_1 = .4, p_2 = .3, p_3 = .6, p_4 = 2.0, p_5 = 3.8, p_6 = 2.5, \\
 p_7 = .7, p_8 = .2, p_9 = .2, p_{10} = .3, p_{11} = .4, p_{12} = .6,
 \end{aligned}
 \tag{3.3}$$

where $p_m = p(t)$, $(m-1)/12 \leq t < m/12$, and can be considered as the level of hydrologic activity during the m th month. This is essentially the $p(t)$ appearing in Table 12.2 of Thomas and Fiering (Tho62).

To generate solutions for the equations in (1.2) and (1.4), it is assumed that the hydrologic activity throughout the m th month of the n th year is equal to

$$(1) \quad p_m \text{ in incrementing } Y(t) \text{ for (1.2)}$$

and

$$(2) \quad v_{12n+m} p_m \text{ in incrementing } Z(t) \text{ for (1.4),}$$

where the v_i are elements of a suitably defined Markov process. The definition of this process is now considered.

Discussions of accepted methods of simulating the stochastic process $S(t, \omega)$ appearing in (1.4) are given by Yevdjovich (Ye72, pp. 252-253) and in greater detail by Matalas (Mata67). For such simulations, Thomas and Fiering (Tho62) proposed a model for the mathematical synthesis of streamflow data which would preserve the monthly means and variances and the month to month serial correlation³ and also give the monthly streamflow variable a (truncated) normal distribution. Harms and Campbell (Ha67) extended the Thomas-Fiering model to give the monthly streamflow variable a log normal distribution. However, as Matalas (Mata67) pointed out, the model preserves the means, variances and month to month serial correlations of the logarithms of the monthly streamflow rather than the corresponding parameters of the streamflow itself. Matalas (Mata67, p. 939) gave the formulas to be used in synthesizing a monthly streamflow sequence which preserves means, variances and lag-1 correlations of historical streamflow data and also gives the streamflow variable a log normal distribution. It is this technique given by Matalas which is used to define the stochastic process $S(t, \omega)$.

³For a sequence $\{x_i\}_{i=1}^n$, the lag-1 or serial correlation

coefficient is defined to be the quotient

$$\rho = \frac{\frac{1}{n-1} \sum_{i=1}^{n-1} (x_i - \bar{x})(x_{i+1} - \bar{x})}{\frac{1}{n} \sum_{i=1}^n (x_i - \bar{x})^2}$$

where $\bar{x} = \frac{1}{n} \sum_{i=1}^n x_i$. This number provides a measure of the extent to which x_i and x_{i+1} vary together. Additional discussion is given by Yevdjovich (Ye72, Chapter 2).

Specifically, after an examination of the literature, it was decided to define the v_i such that each v_i has a log normal distribution and also such that $E(v_i) = 1.0$, $\text{var}(v_i) = 0.25$ and the month to month serial correlation is 0.5. The sequence $\{v_i\}$ is generated by first defining a sequence $\{u_i\}$ such that

$$u_1 = \sigma \epsilon_1 \text{ and } u_{i+1} = \mu + \rho(u_i - \mu) + (1 - \rho^2)^{1/2} \sigma \epsilon_{i+1},$$

where $\sigma^2 = 0.2231$, $\mu = -0.1116$, $\rho = 0.5278$ and $\{\epsilon_i\}$ is a sequence of independent, standard (i.e., mean 0 and variance 1), normal variates. The preceding values for σ^2 , μ and ρ were obtained by solving the following equations:

$$1.0 = E(v_i) = \exp(1/2\sigma^2 + \mu) \quad (3.4)$$

$$0.25 = \text{var}(v_i) = \exp[2(\sigma^2 + \mu)] - \exp[\sigma^2 + 2\mu] \quad (3.5)$$

$$0.5 = [\exp(\sigma^2\rho) - 1]/[\exp(\sigma^2) - 1]. \quad (3.6)$$

The preceding equations are Equations (7), (8) and (12), respectively, of Matalas (Mata67), where $a = 0$ is assumed in Equation (7). In the solution of these equations, (3.4) and (3.5) are solved first; then, the value for σ so obtained is used in the solution of (3.6). Each v_i is defined by $v_i = \exp(u_i)$. As indicated by Matalas (Mata67, p. 939), the sequence $\{v_i\}$ has the properties stated at the beginning of this paragraph.

The following simulations were performed with the coefficient matrix appearing in (3.1). This is the matrix for the "typical river zone." First, calculations were performed to illustrate the manner in which the solution X of (1.1) approaches its asymptotic solution SX . Specifically, (1.1) was solved four times. For each solution, the initial value is taken as $X(0) = 0$ and a different subzone is assumed to receive a radionuclide input of 1 atom/year. For example, this yields $R = [1, 0, 0, 0]^T$ when radionuclide input is to the groundwater subzone; the units for R are atoms/yr. As the solution of (1.1) is linear with respect to R with the initial value condition $X(0) = 0$, the solutions obtained here can be scaled to represent other rates of input. Then, components of X and the corresponding components of SX were

graphed. Each graph illustrates the behavior of a single component of X from time $t = 0$ until the time at which the component of X has reached approximately 90% of its asymptotic value. These graphs appear in Figures 3-1 through 3-4.

Second, calculations were performed to compare the solutions of (1.1), (1.2), and (1.4) for the 100th year after the initiation of radionuclide input. Specifically, plots were generated which show (1) a component of the solution X of (1.1) for that period, (2) the corresponding component of the solution Y of (1.2), (3) the average value EZ of the corresponding component of 100 Monte Carlo simulations of the solution Z of (1.4), and (4) $EZ + SDZ$, where $SDZ(t)$ is the standard deviation of the 100 observed values of the component of $Z(t)$. These plots appear in Figures 3-5 through 3-8.

Third, similar plots were generated for the 1000th year after the initiation of radionuclide input. These plots appear in Figures 3-9 through 3-12.

Next, the same sequence of simulations was performed with the coefficient matrix appearing in (3.2). This is the matrix for the "typical lake zone." These plots appear in Figures 3-13 through 3-24.

A listing of the program XYZ1 which generated the data used in preparing the plots of X, Y, EZ, and $EZ + SDZ$ is given in the Appendix in the form used for the following case: Year 1000 of input to the soil subzone of the River Zone. Figure 3-10 presents the results generated by this version of the program. Each of the 8 "Year 1000" runs (each run involving 100 Monte Carlo simulations of 1000 years for Z) took approximately 34 minutes of CDC 6600 CPU time. The "Year 100" runs were of course shorter by a factor of 10. It is a fairly expensive proposition to simulate repeatedly over long time periods, but if it is deemed desirable to do so, the program XYZ1 is adaptable to fit the estimated hydrologic parameters of other sites.

The computational results presented in Figures 3-1 through 3-24 are now discussed. First, Figures 3-1 through 3-4 and 3-13 through 3-16 indicate the asymptotic behavior of solutions to (1.1). As discussed in Chapter 2, such solutions increase monotonically towards a constant solution. For radionuclide input to the groundwater subzone, it takes approximately 10,000 years for the systems to reach equilibrium. For radionuclide input to the soil

subzone, it takes approximately 1000 years for the soil subzone in the River Zone to reach equilibrium and approximately twice as long for the soil subzone in the Lake Zone to reach equilibrium. This difference results from the fact that the soil subzone of the River Zone was defined with more active processes that influence radionuclide movement. Also, it takes approximately 5000 years for the surface water and sediment subzones to reach equilibrium in the River Zone and somewhat longer for these subzones to reach equilibrium in the Lake Zone. As indicated in a previous sensitivity analysis (Hel81a) for radionuclide input to the soil subzone, the surface water and sediment subzones approach their equilibrium concentrations more slowly than the soil subzone due to radionuclide movement through the groundwater subzone. For radionuclide input to the surface water or sediment subzones, both the surface water and sediment subzones move rapidly towards their equilibrium concentrations. Here, the times required to reach equilibrium vary from a year to a few tens of years. In contrast, it requires on the order of 1000 to 2000 years for the soil subzones to reach equilibrium.

Figures 3.5 through 3.12 and 3.17 through 3.24 contain comparisons of X, Y and Z, the solutions to (1.1), (1.2) and (1.4), respectively. The most striking feature of these figures is the relatively small differences indicated in these solutions.

The comparisons of X and Y are considered first. With the exception of the surface water component for radionuclide input to the surface water subzone, there is little discernable difference between X and Y. For input to the surface water subzone of the River Zone, Y_3 appears to oscillate between $1/(\max p) SX_3$ and $1/(\min p) SX_3$. In fact, $Y_3(t)$ behaves approximately as $SX_3/p(t)$. A similar but less pronounced pattern holds for Y_3 when radionuclide input is to the surface water subzone of the Lake Zone. This behavior can be related to the large rate constants associated with radionuclide movement out of the surface water subzones. An explanation of the observed behavior of X and Y is provided in Chapter 4.

The comparisons of X and Z are now considered. These comparisons are similar to those for X and Y. Again with the exception of the surface water component for radionuclide input to the surface water subzone,

there is little difference between X and Z . The following is presented in justification of the preceding statement. First, let us assume that it is "unlikely" that a random variable will exceed its mean plus 2 times its standard deviation. Chebyshev's inequality guarantees that the probability is less than .25, and it is usually more like .0228, which is the value for normal variables. Let us also assume that the estimates $EZ_k(t)$ and $SDZ_k(t)$ are good estimates of the true moments $E(Z_k(t, \cdot))$ and $SD(Z_k(t, \cdot))$. If one examines each graph to determine the maximum amount that $EZ_k(t) + 2 \cdot SDZ_k(t)$ exceeds $X_k(t)$, it is found that in most cases this is a small percentage of the value of $X_k(t)$. The results of such a comparison are listed in Table 3-1. In every case except for the surface water component with radionuclide input to the surface water subzone, it can be said that it is unlikely that $Z_k(t, \omega)$ exceeds $1.2X_k(t)$. In the case of input to the surface water subzone of the Lake Zone, it appears unlikely that $Z_3(t, \omega)$ will exceed $1.8X_3(t)$; even for the case of input to the surface water subzone of the River Zone, it appears unlikely that $Z_3(t, \omega)$ will exceed $1.2X_3(t)$. Further, the expected behavior of Z is very close to that for Y . Additional discussion of (1.4) is provided in Chapter 5.

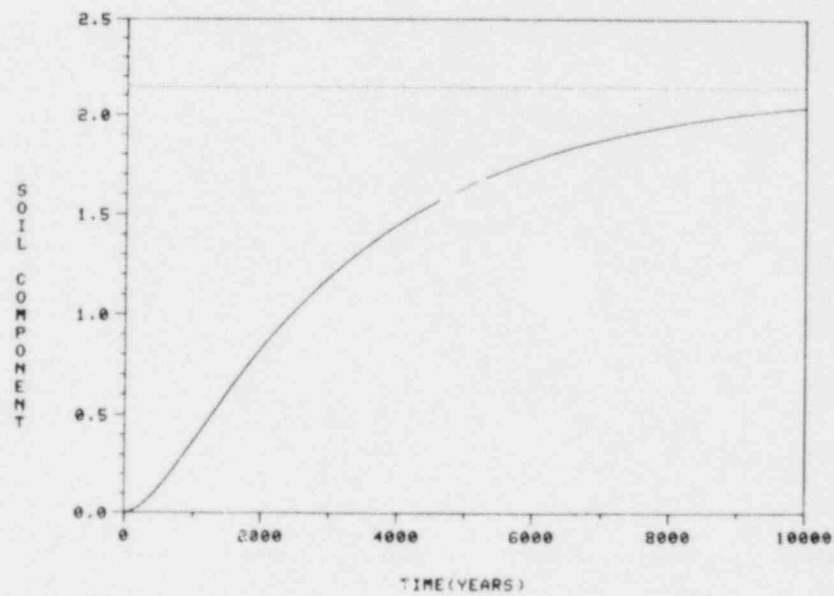
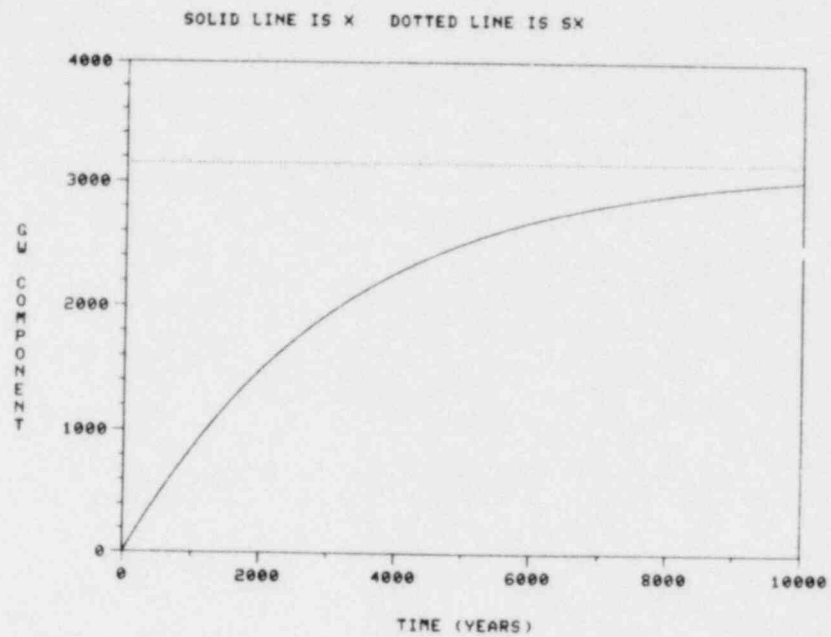


Figure 3-1. Asymptotic Behavior of X (Units: Atoms) for Radionuclide Input to Groundwater Subzone of River Zone.

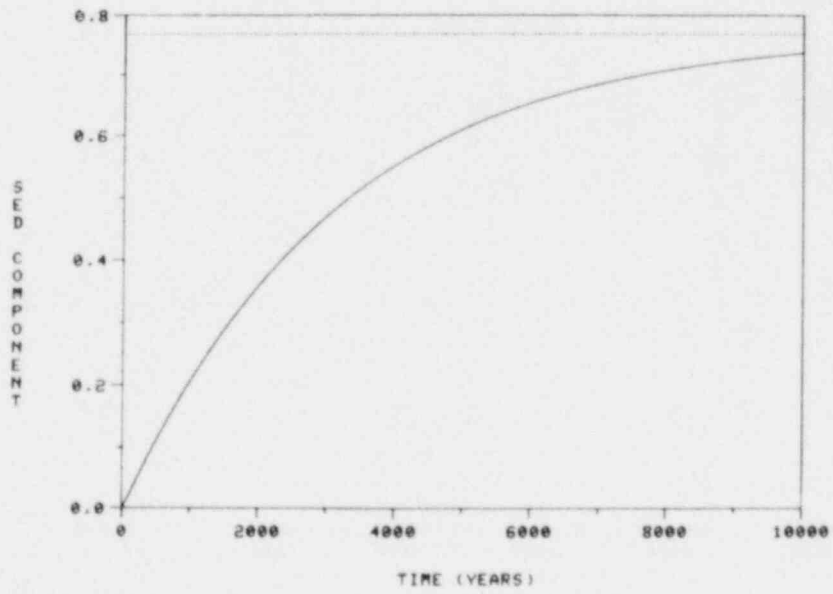
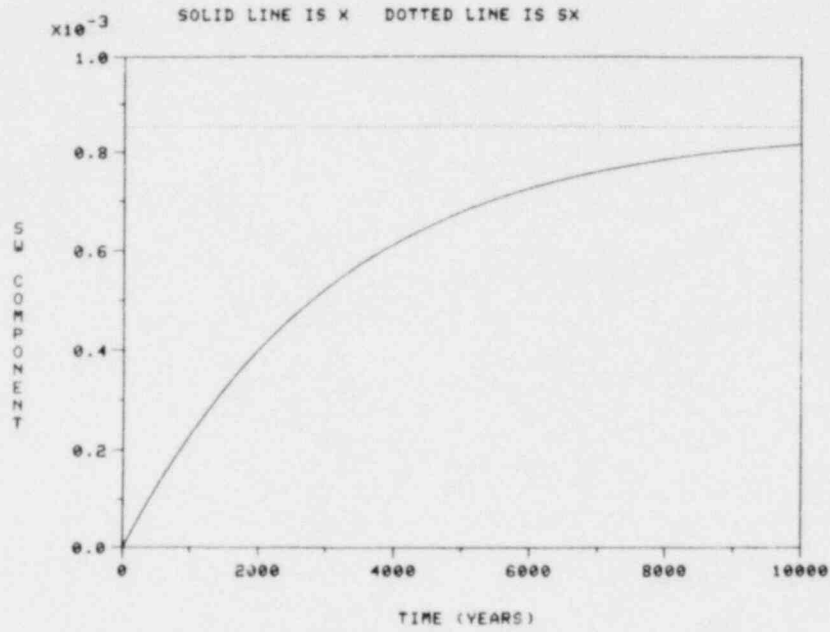


Figure 3-1. Continued

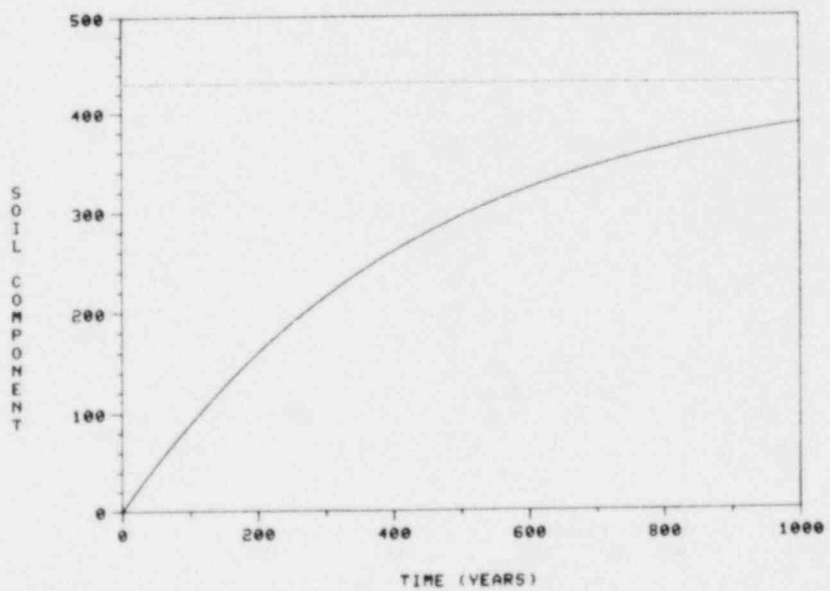
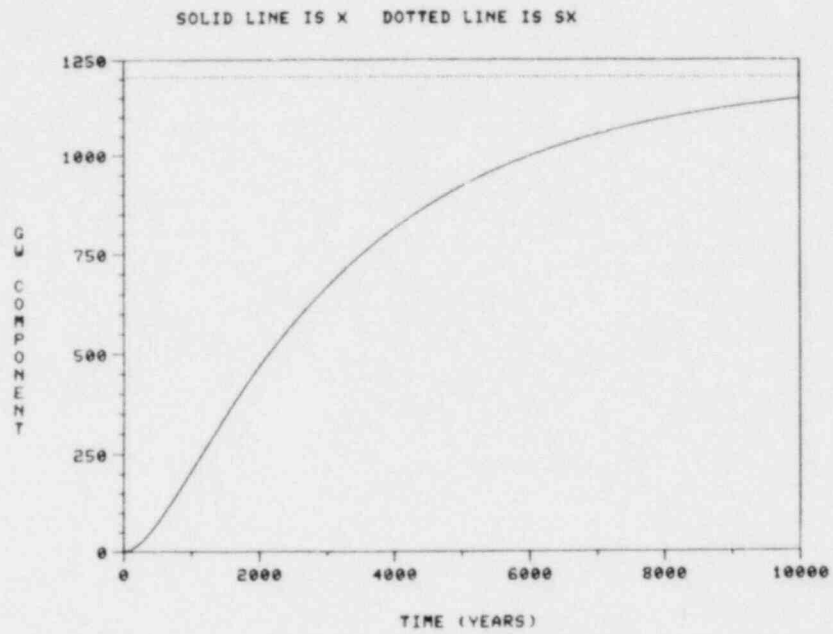


Figure 3.2. Asymptotic Behavior of X (Units: Atoms) for Radionuclide Input to Soil Subzone of River Zone.

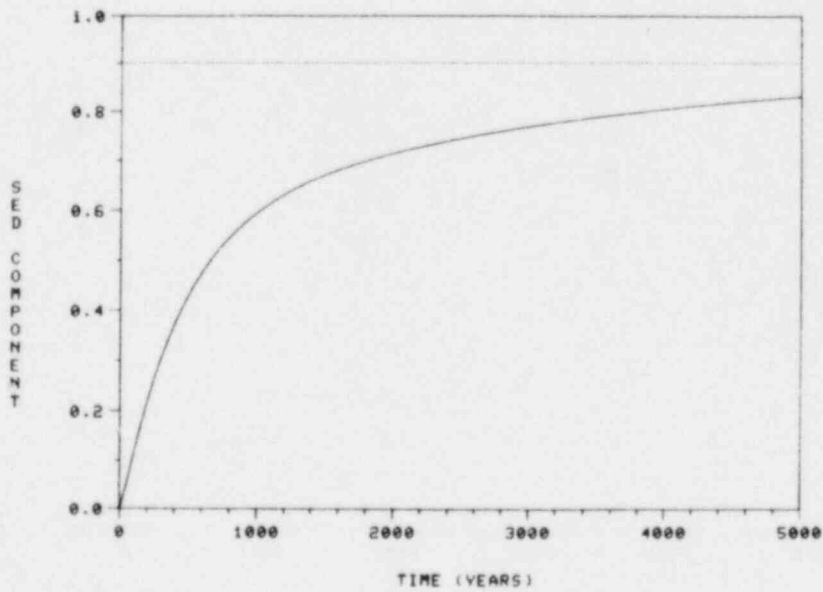
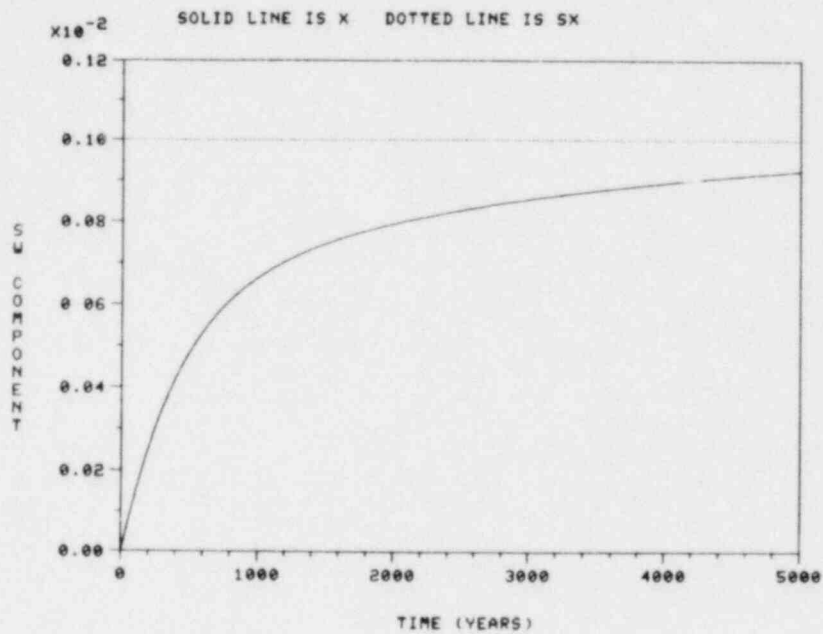


Figure 3-2. Continued

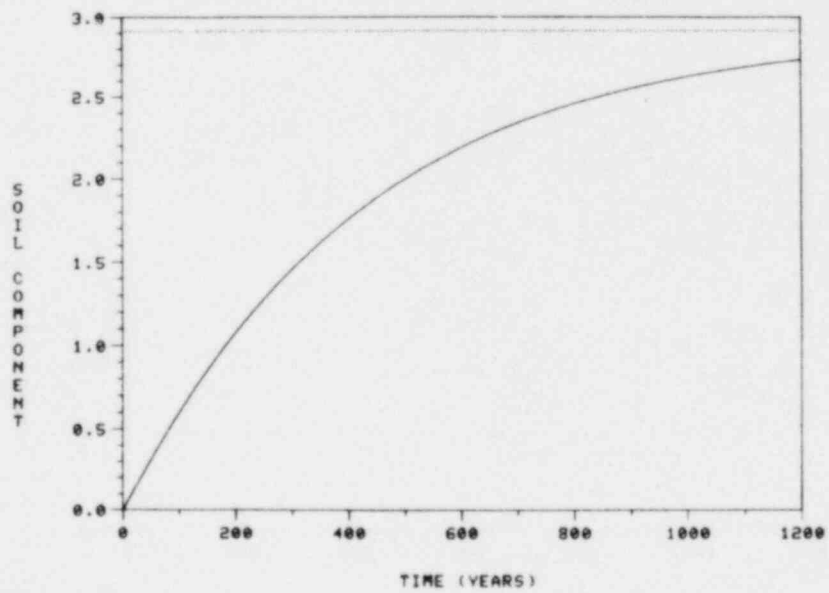
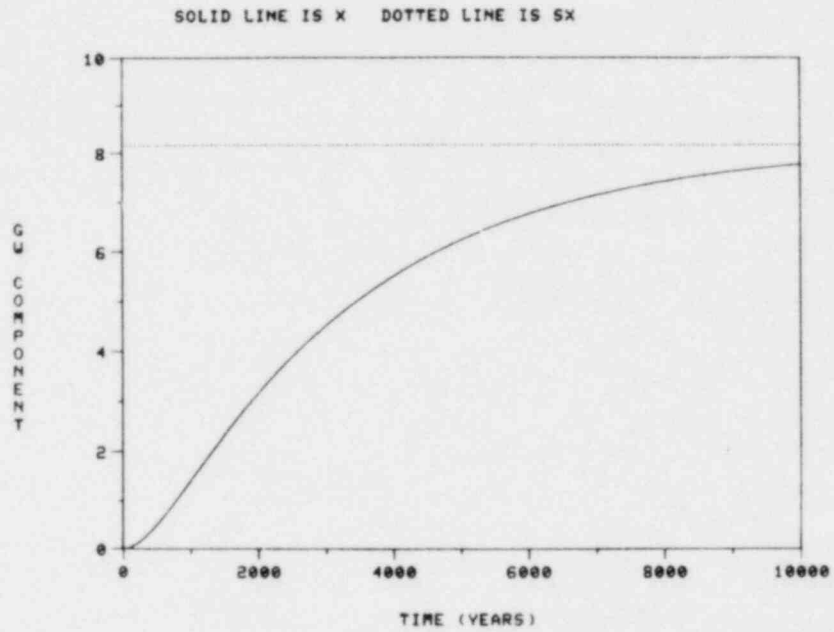


Figure 3-3. Asymptotic Behavior of X (Units: Atoms) for Radionuclide Input to Surface Water Subzone of River Zone.

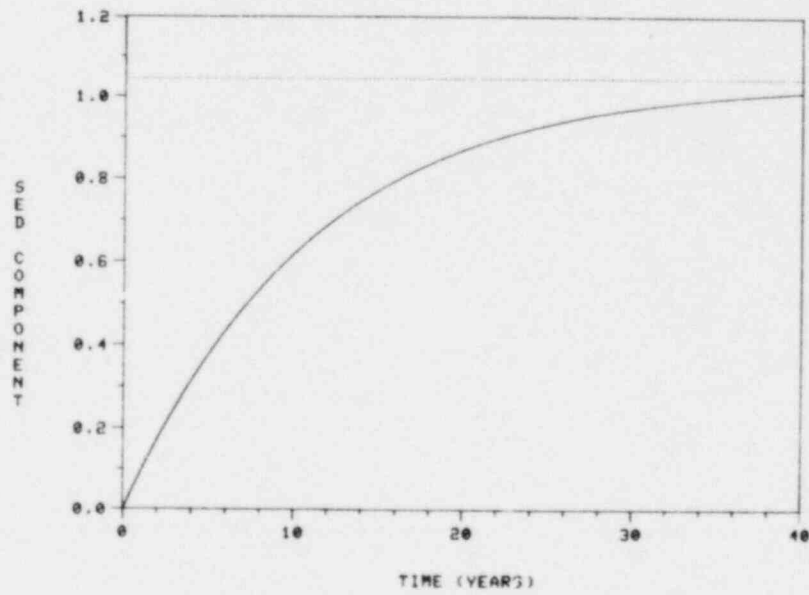
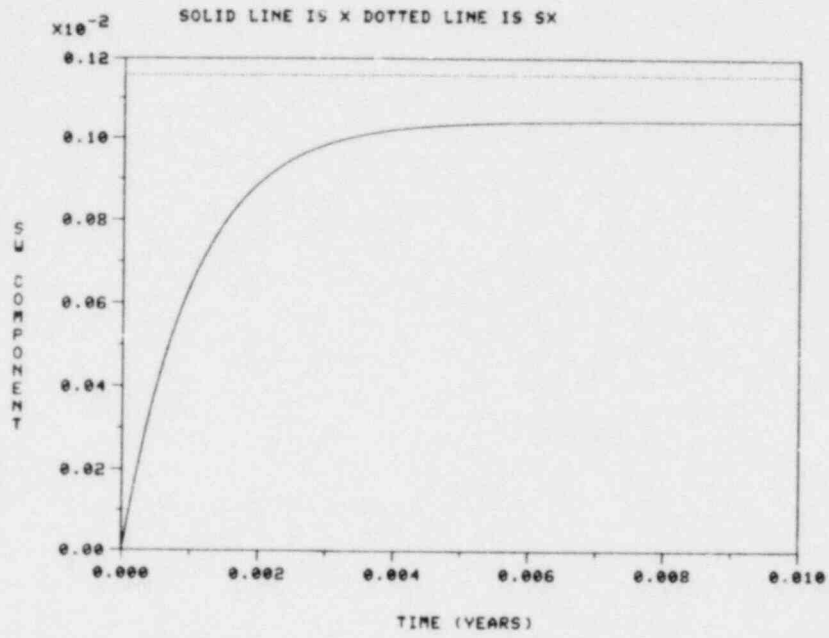


Figure 3-3. Continued

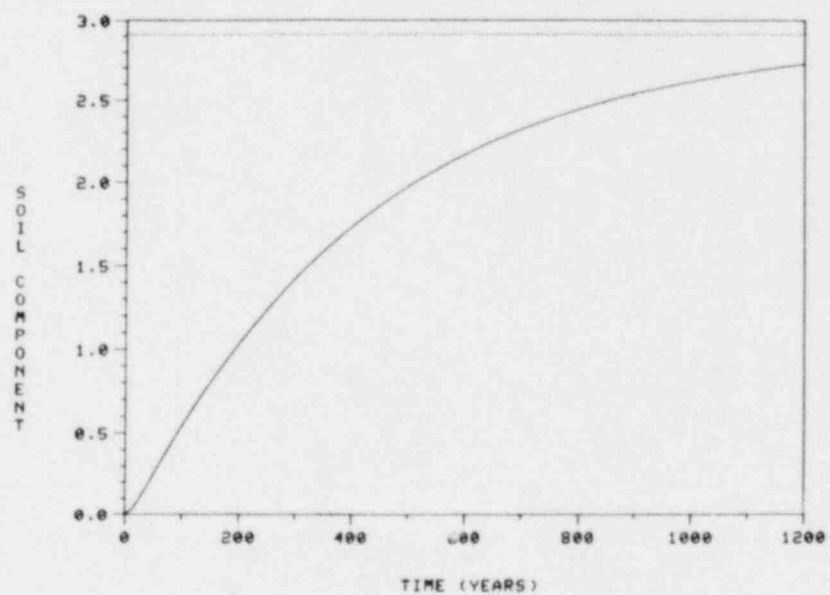
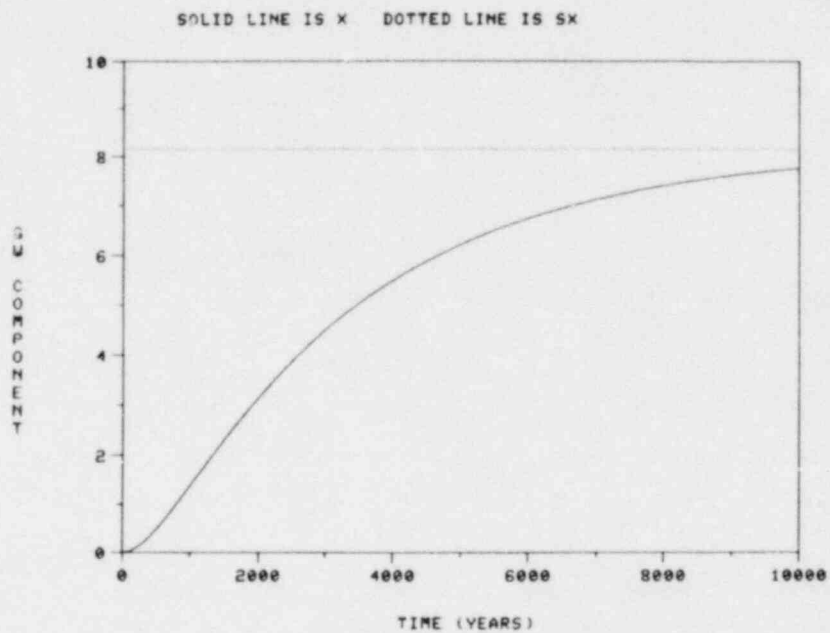


Figure 3-4. Asymptotic Behavior of X (Units: Atoms) for Radionuclide Input to Sediment Sub-zone of River Zone.

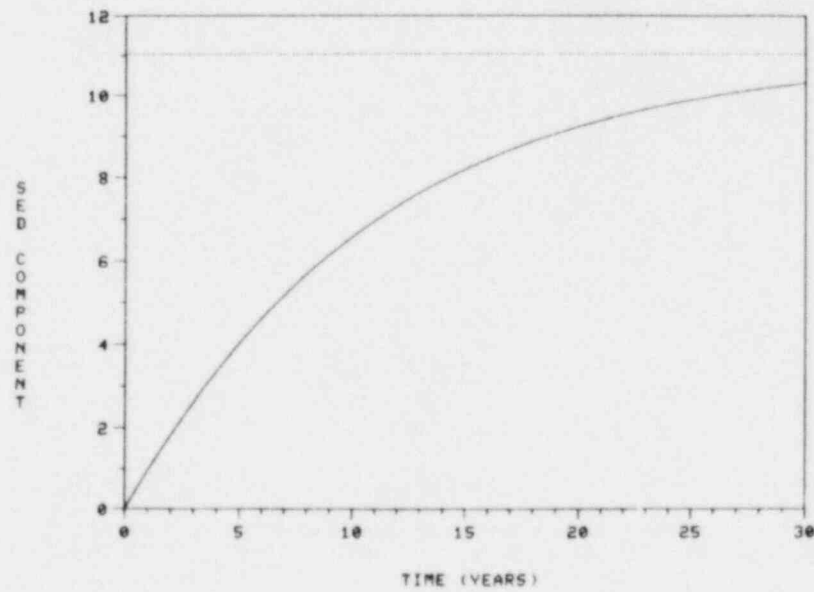
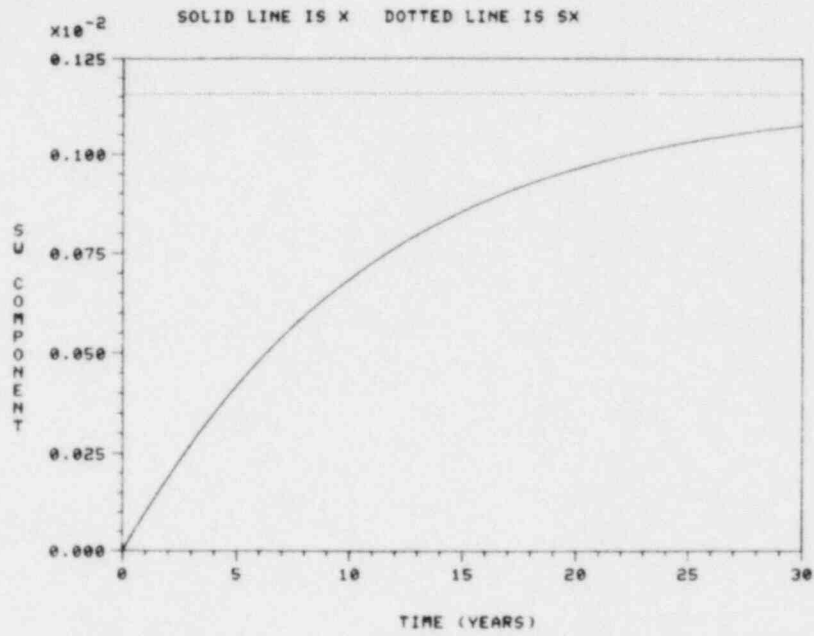


Figure 3-4. Continued

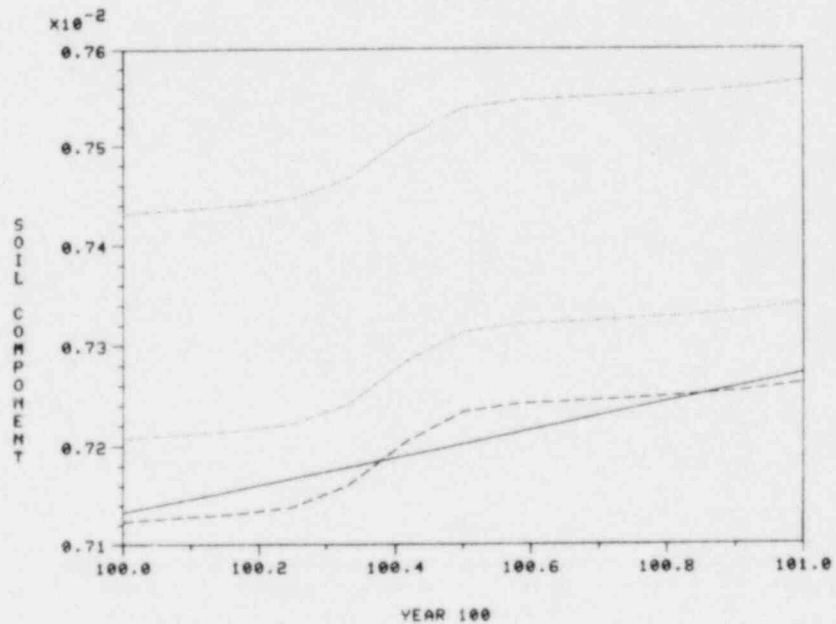
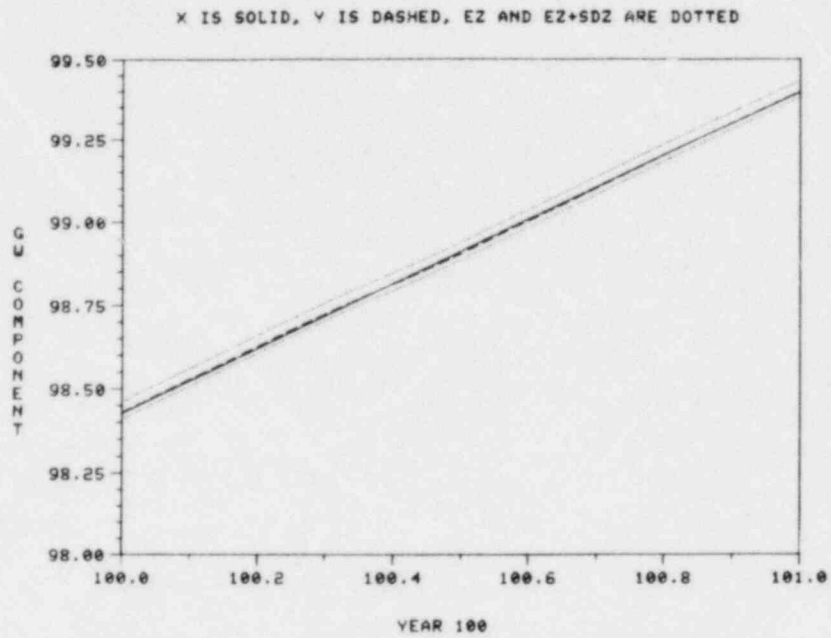


Figure 3-5. Behavior of X, Y, EZ, and EZ + SDZ (Units: Atoms) for Year 100 With Radionuclide Input to Groundwater Subzone of River Zone.

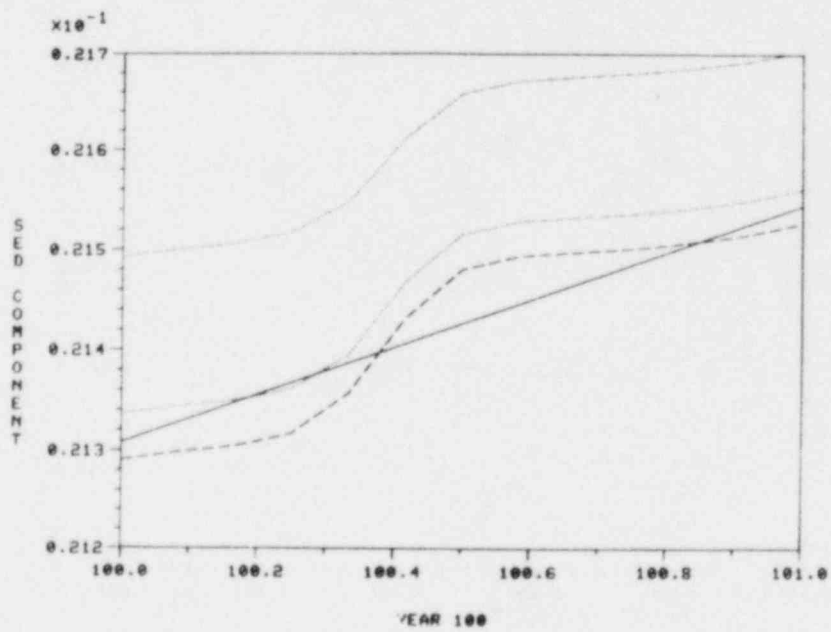
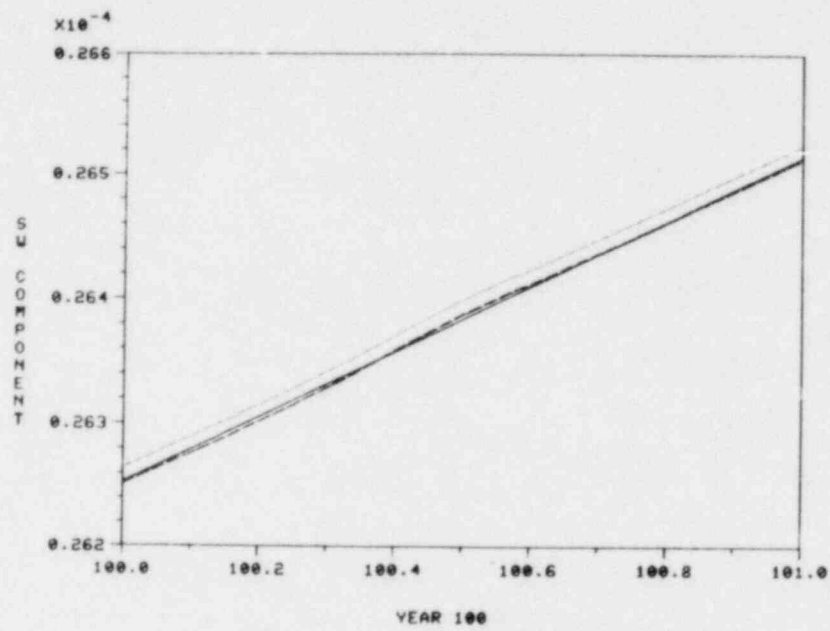


Figure 3-5. Continued

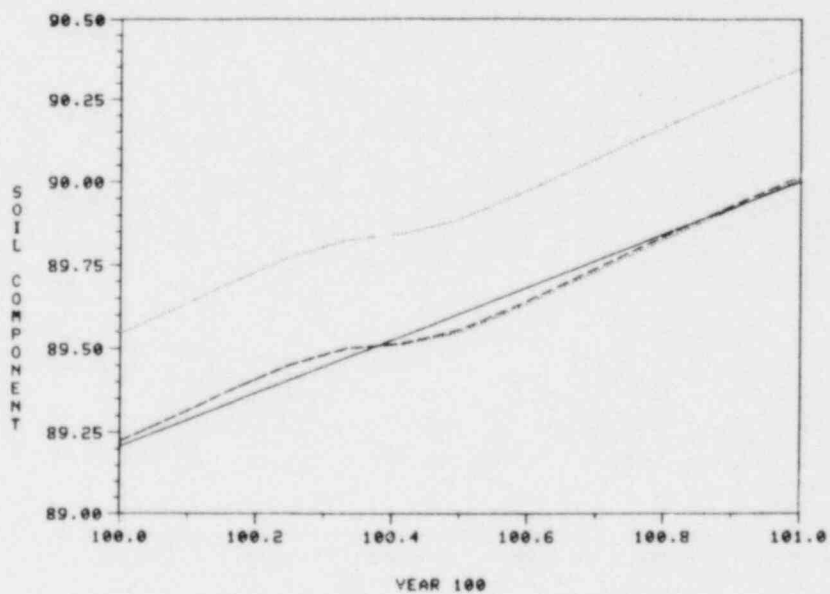
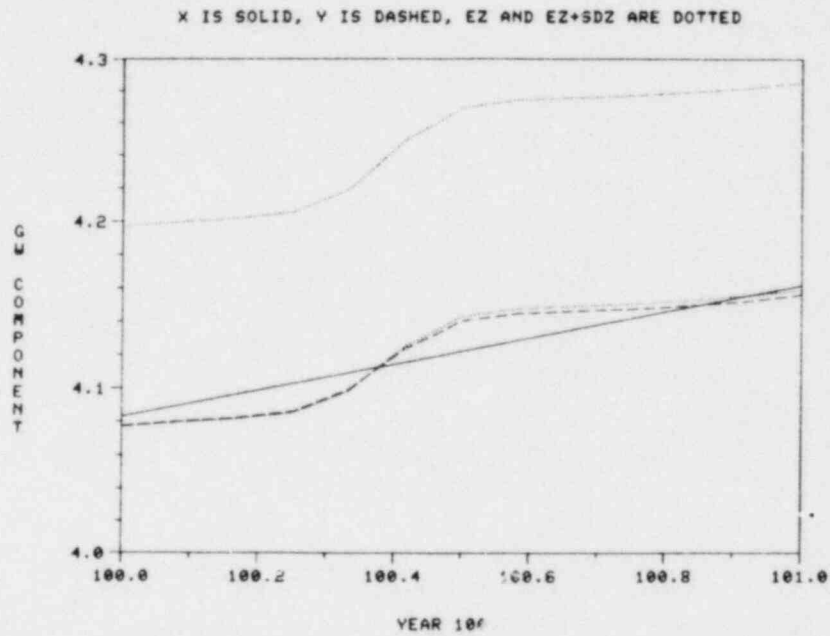


Figure 3-6. Behavior of X, Y, EZ, and EZ + SDZ (Units: Atoms) for Year 100 With Radionuclide Input to Soil Subzone of River Zone.

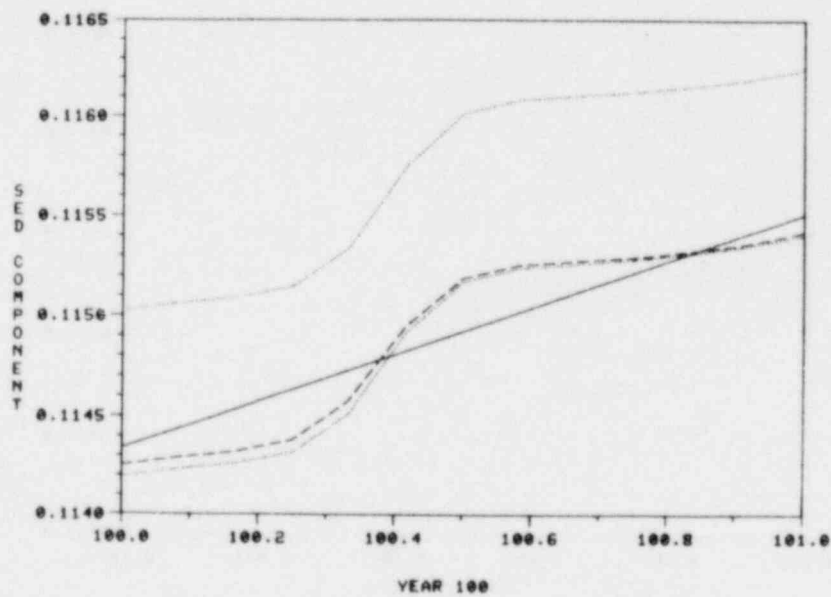
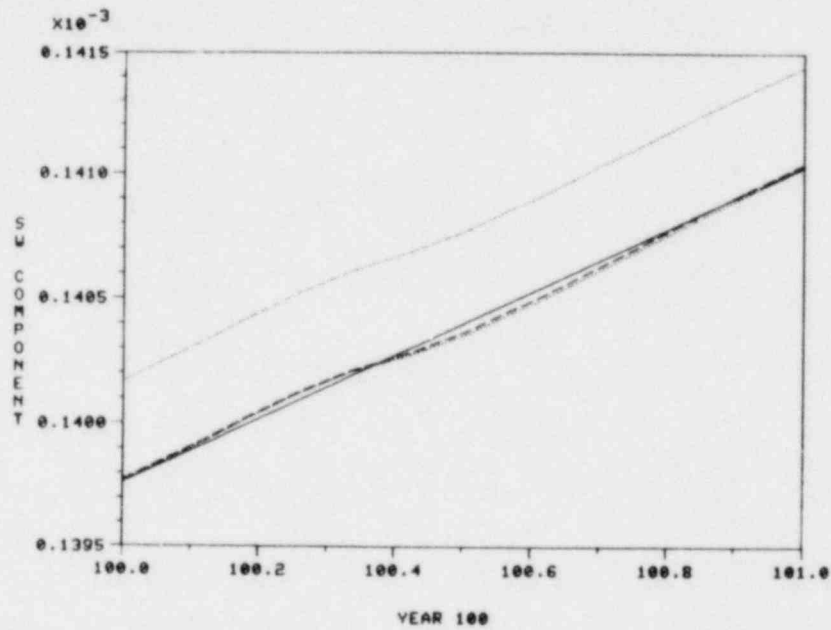


Figure 3-6. Continued

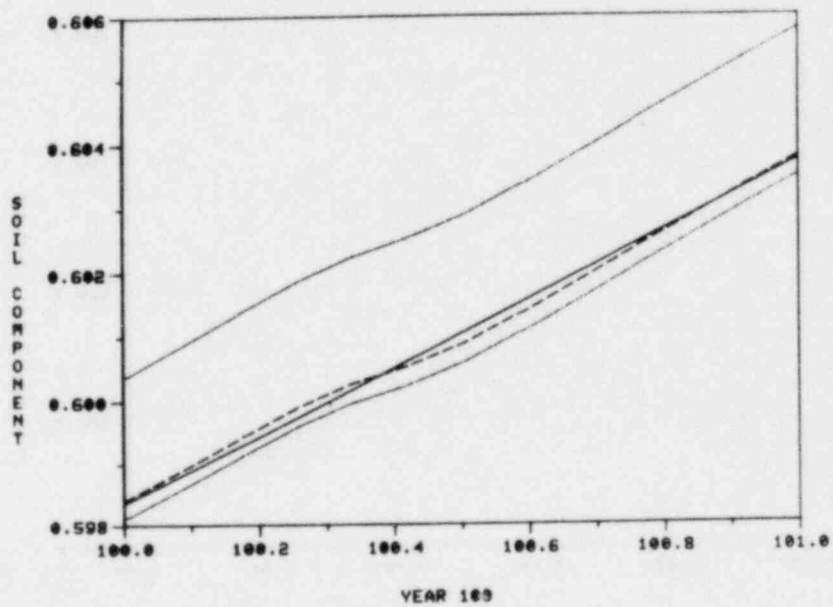
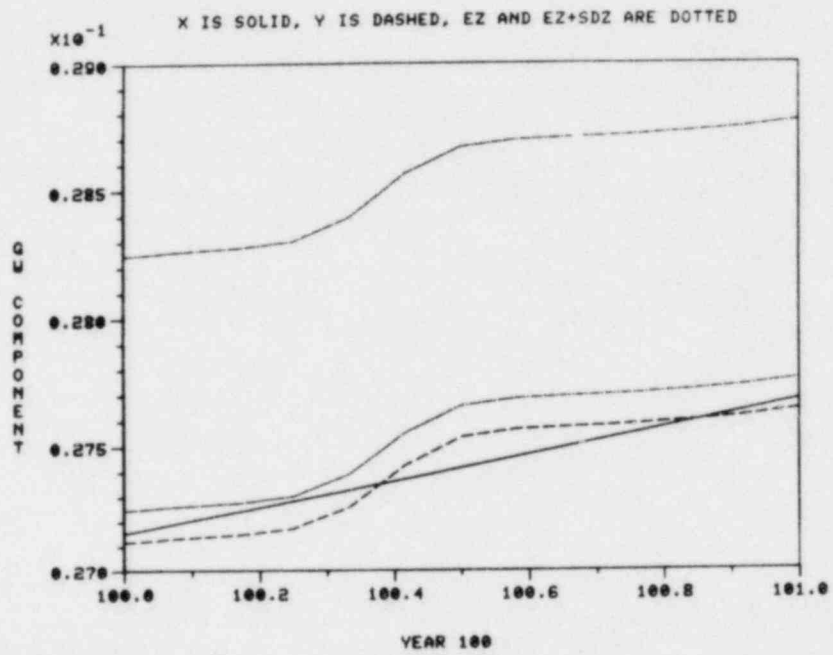


Figure 3-7. Behavior of X, Y, EZ, and EZ + SDZ (Units: Atoms) for Year 100 With Radionuclide Input to Surface Water Subzone of River Zone.

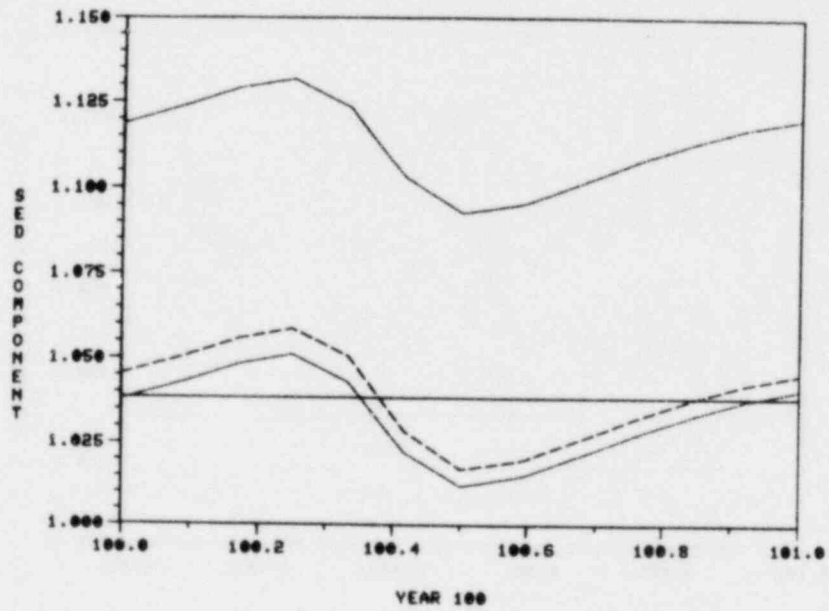
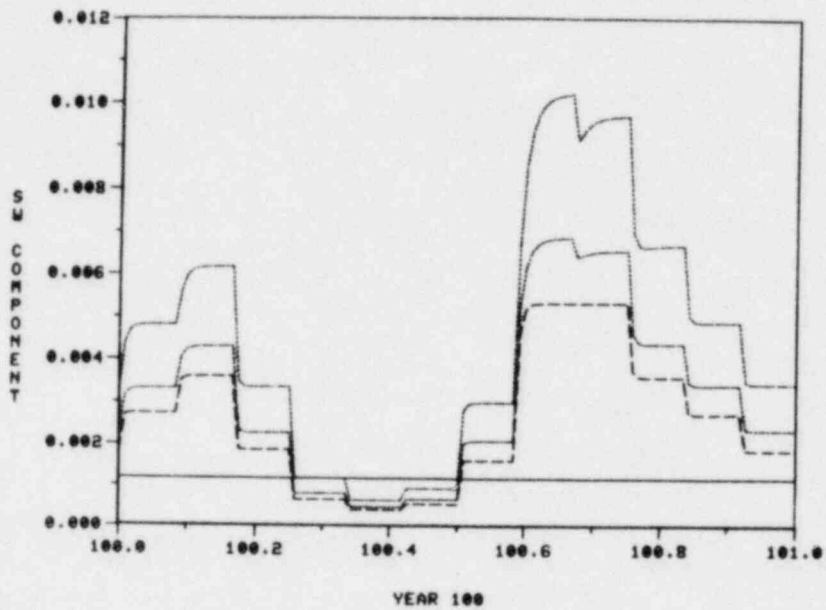


Figure 3-7. Continued

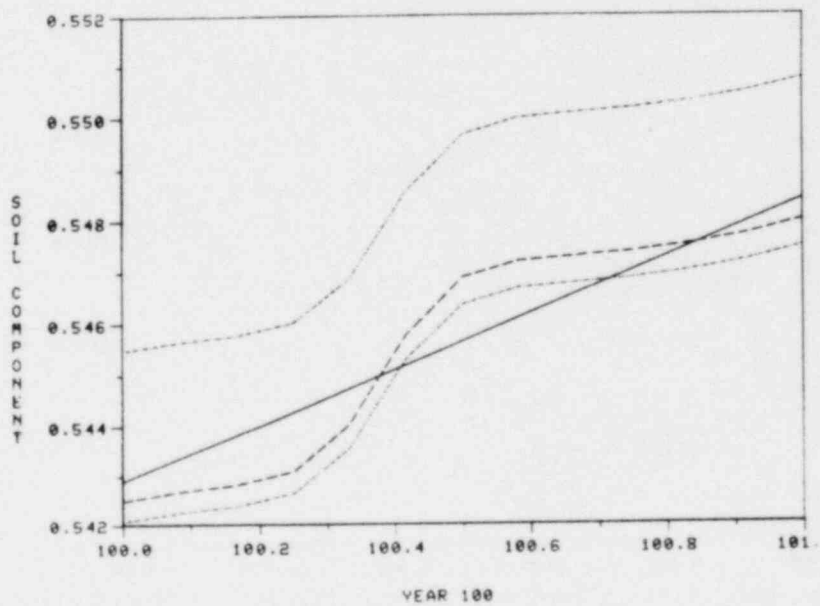
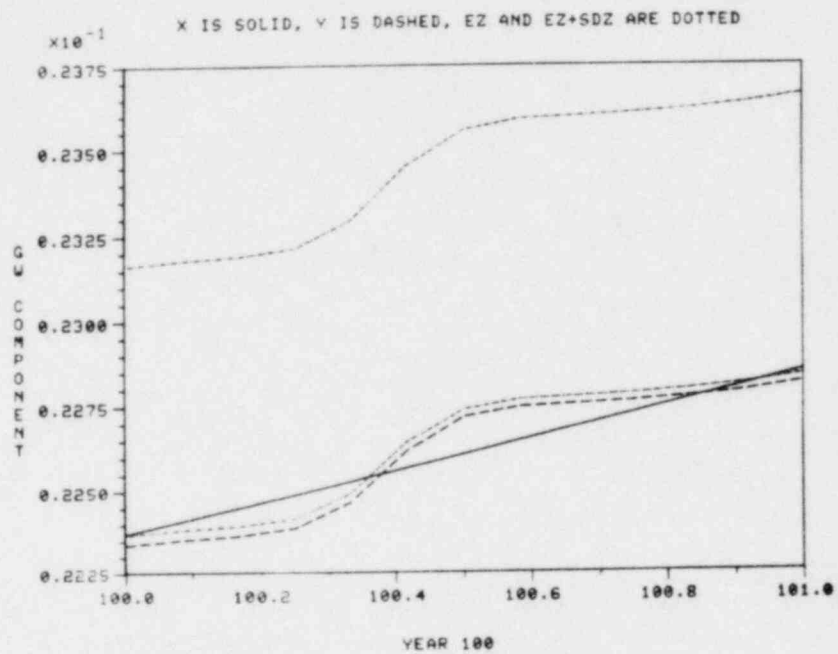


Figure 3-8. Behavior of X, Y, EZ, and EZ + SDZ (Units: Atoms) for Year 100 With Radionuclide Input to Sediment Subzone of River Zone.

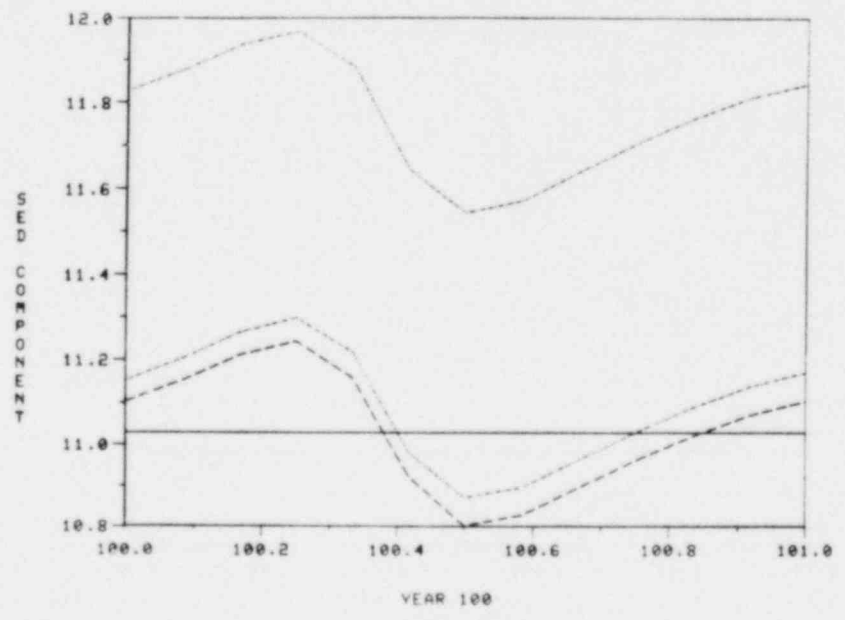
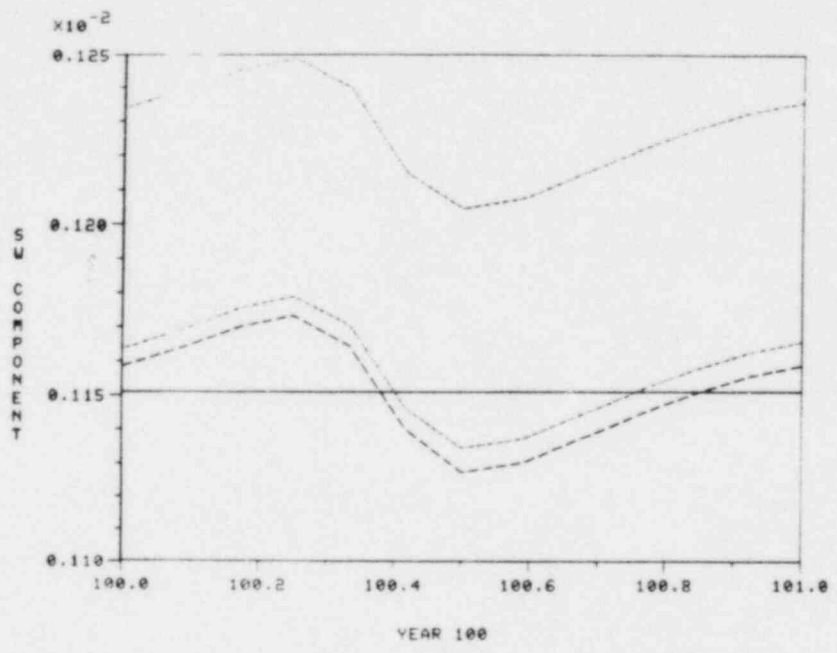


Figure 3-8. Continued

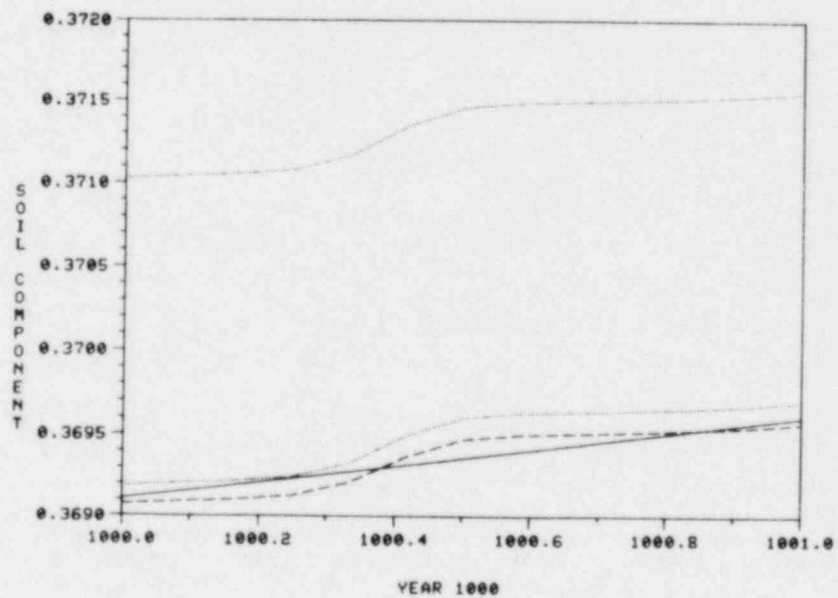
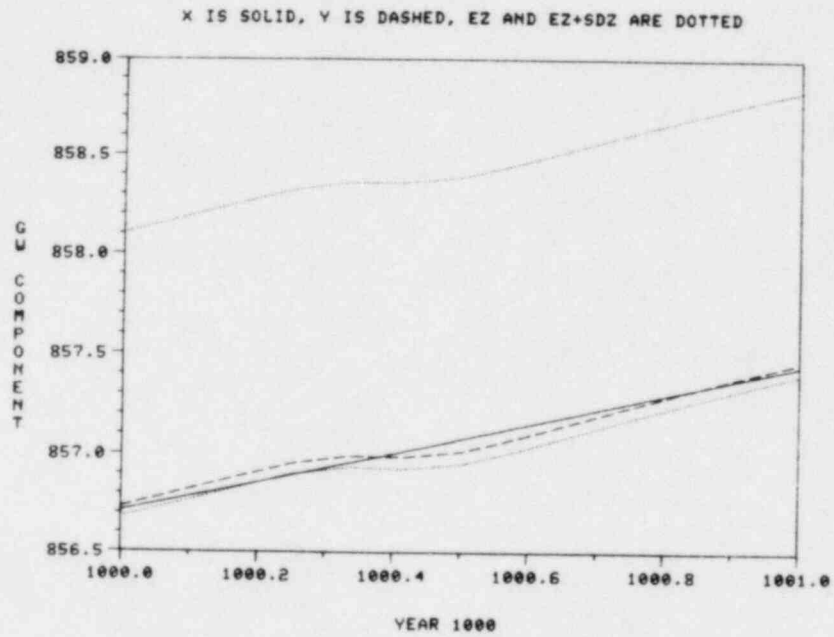


Figure 3-9. Behavior of X, Y, EZ, and EZ + SDZ (Units: Atoms) for Year 1000 With Radionuclide Input to Groundwater Subzone of River Zone.

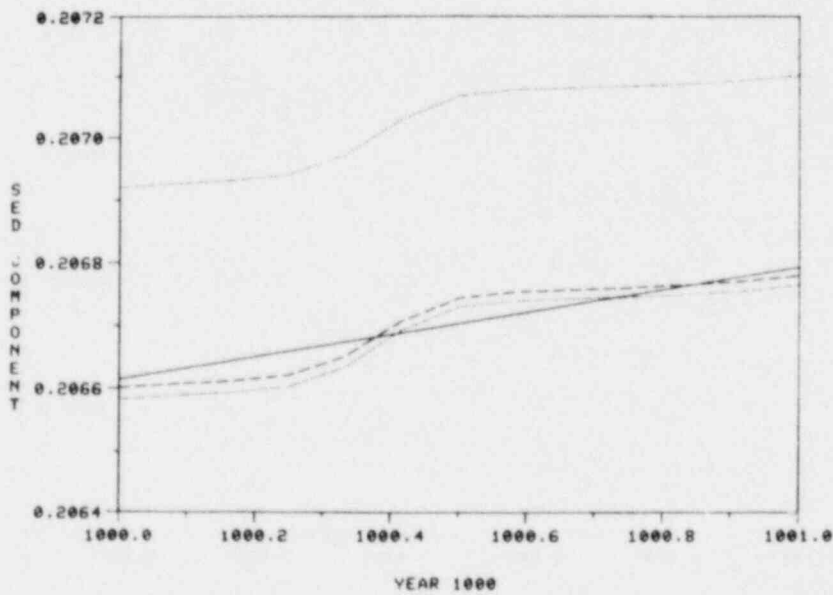
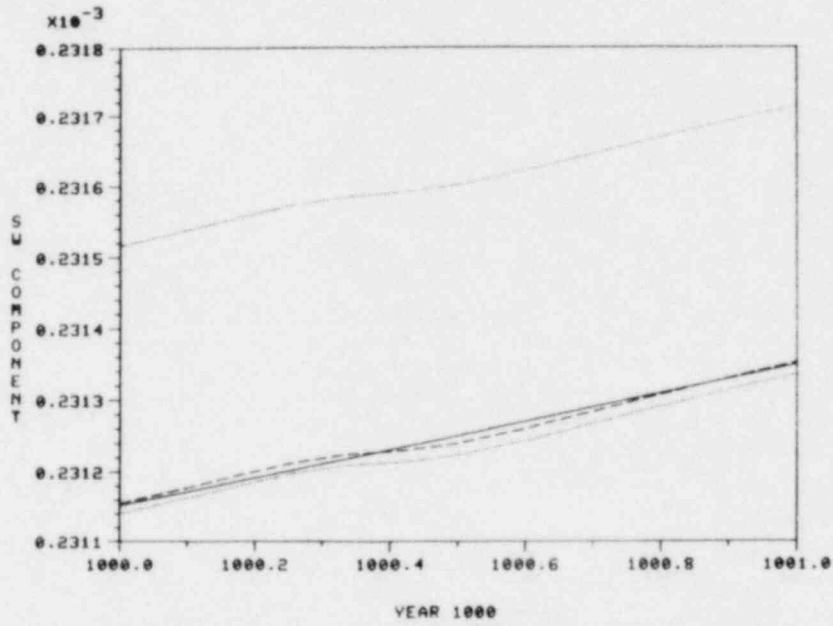


Figure 3-9. Continued

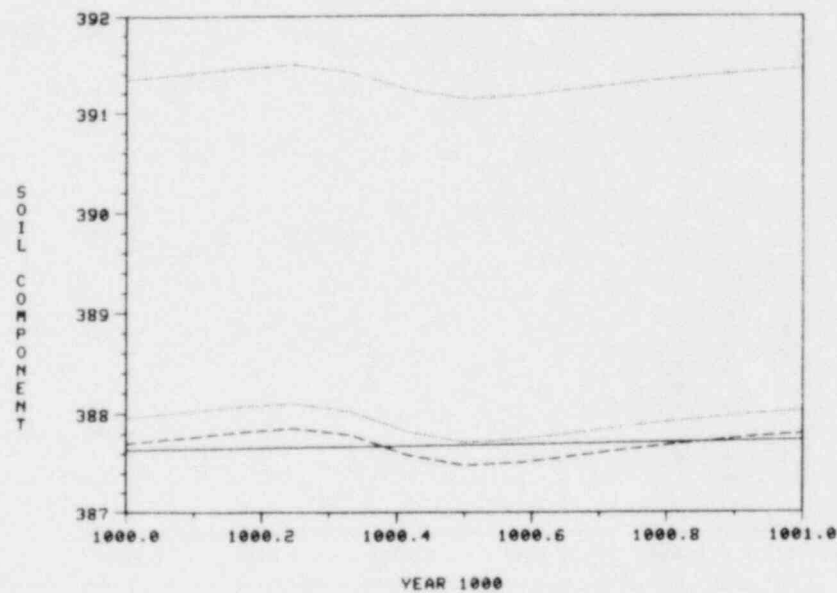
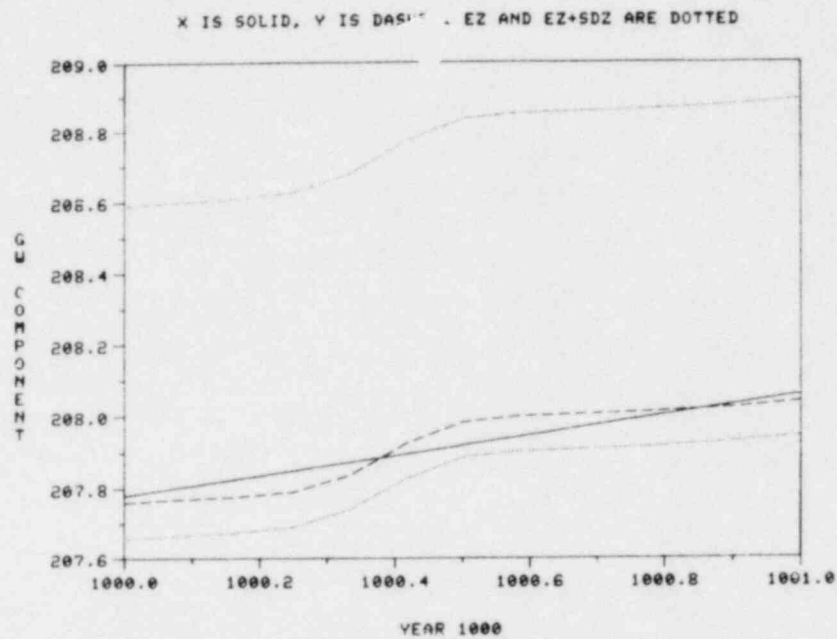


Figure 3-10. Behavior of X, Y, EZ, and EZ + SDZ (Units: Atoms) for Year 1000 With Radionuclide Input to Soil Subzone of River Zone.

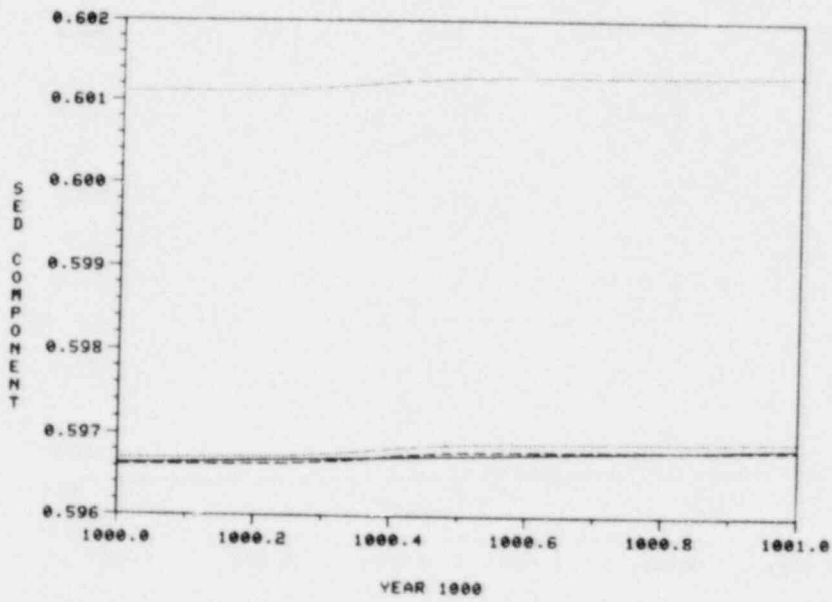
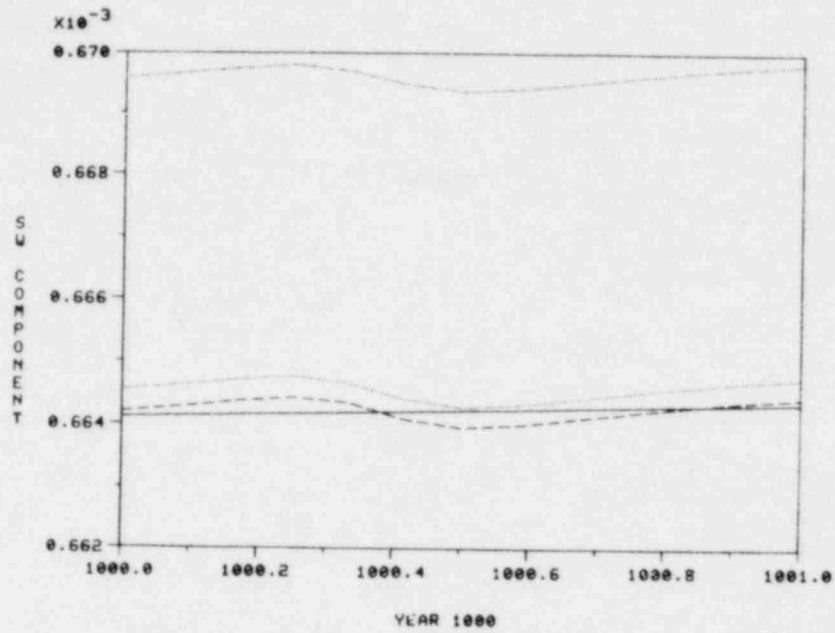


Figure 3-10. Continued

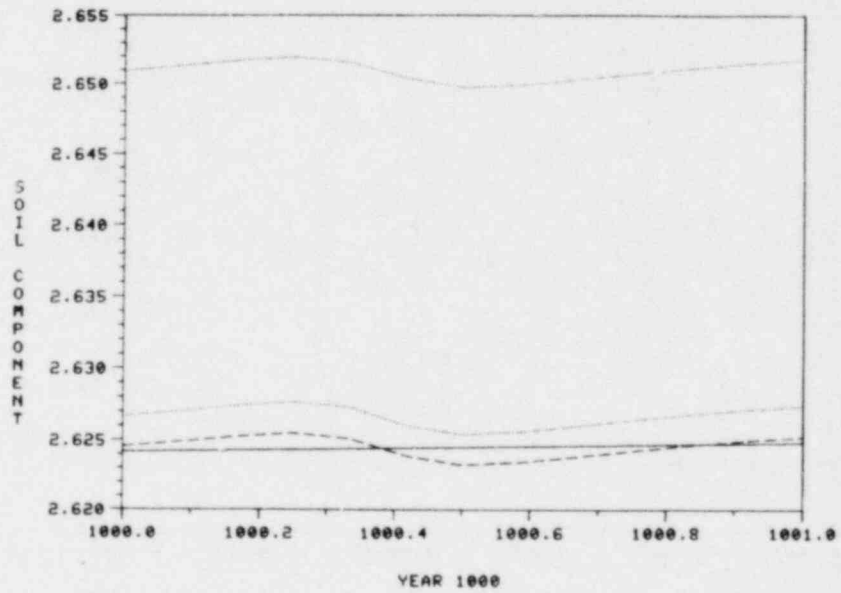
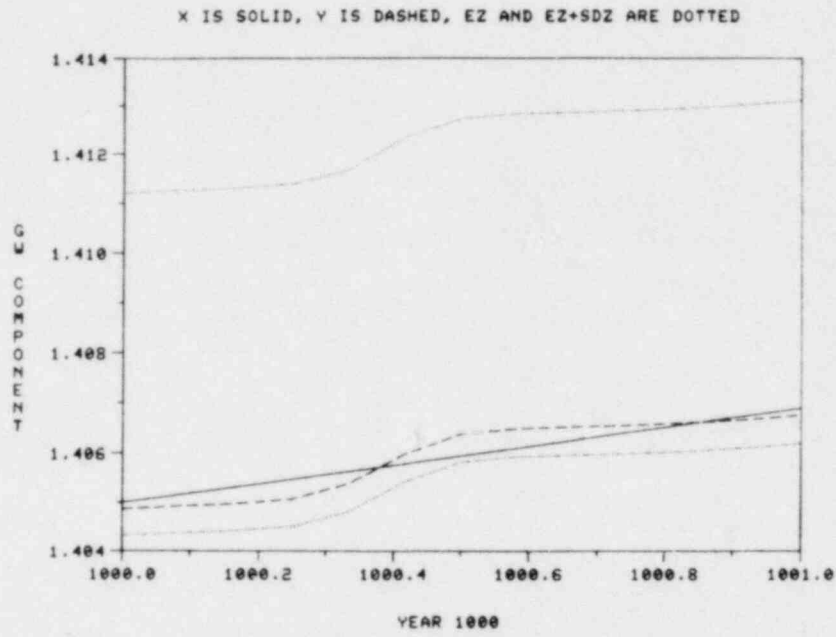


Figure 3-11. Behavior of X, Y, EZ, and EZ + SDZ (Units: Atoms) for Year 1000 With Radionuclide Input to Surface Water Subzone of River Zone.

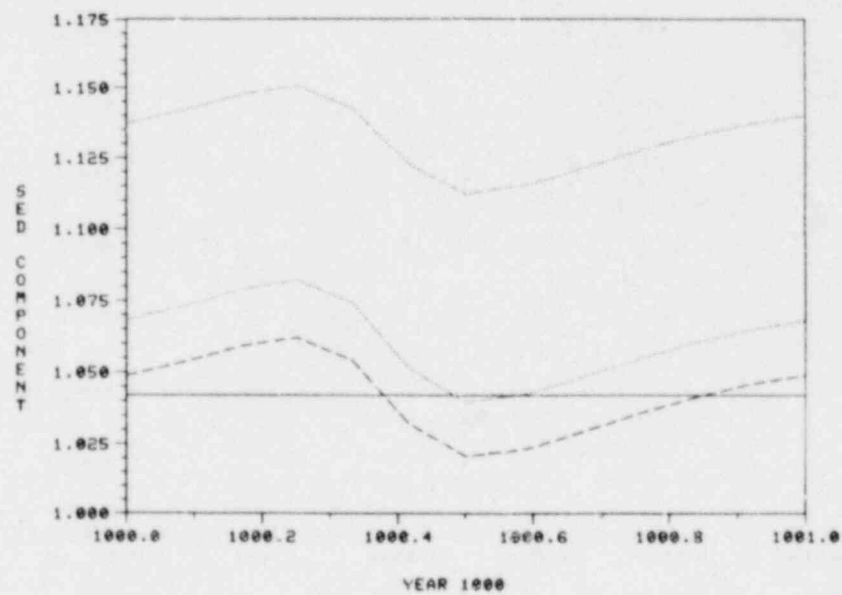
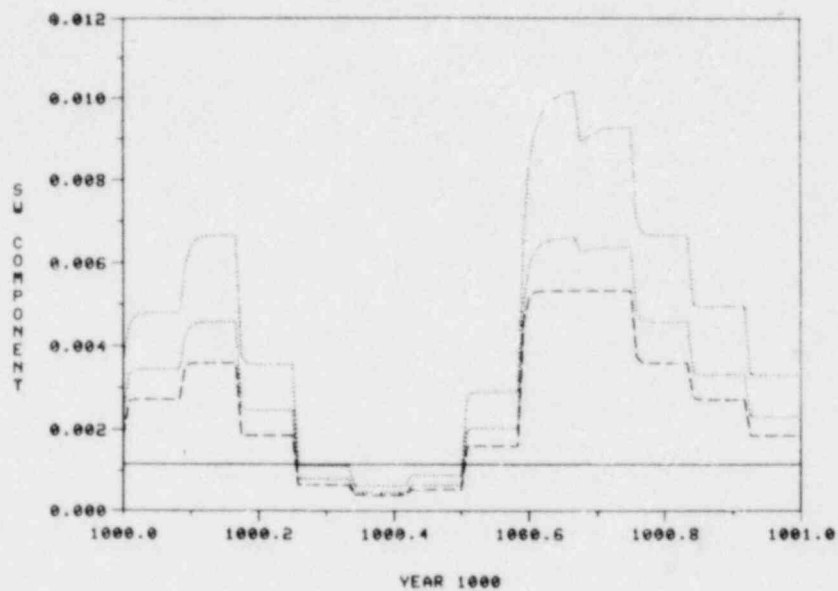


Figure 3-11. Continued

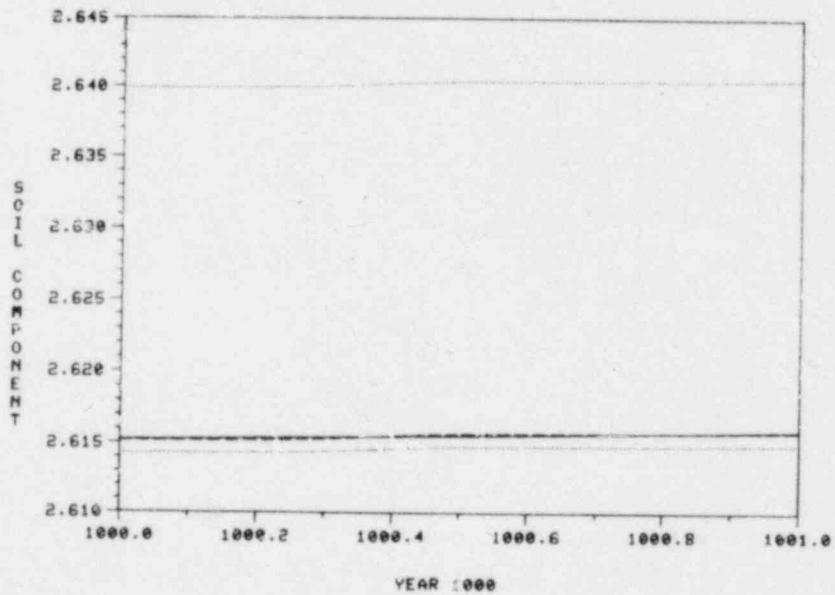
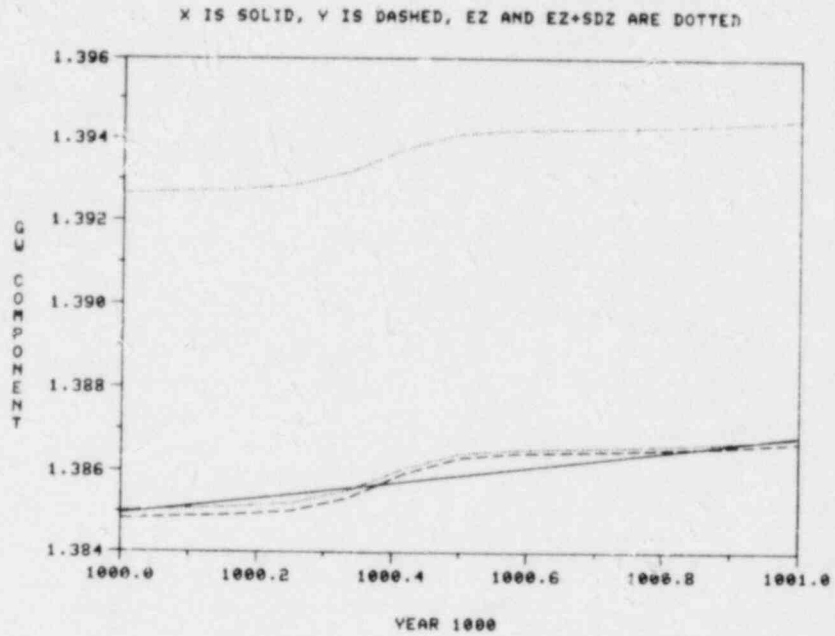


Figure 3-12. Behavior of X, Y, EZ, and EZ + SDZ (Units: Atoms) for Year 1000 With Radionuclide Input to Sediment Subzone of River Zone.

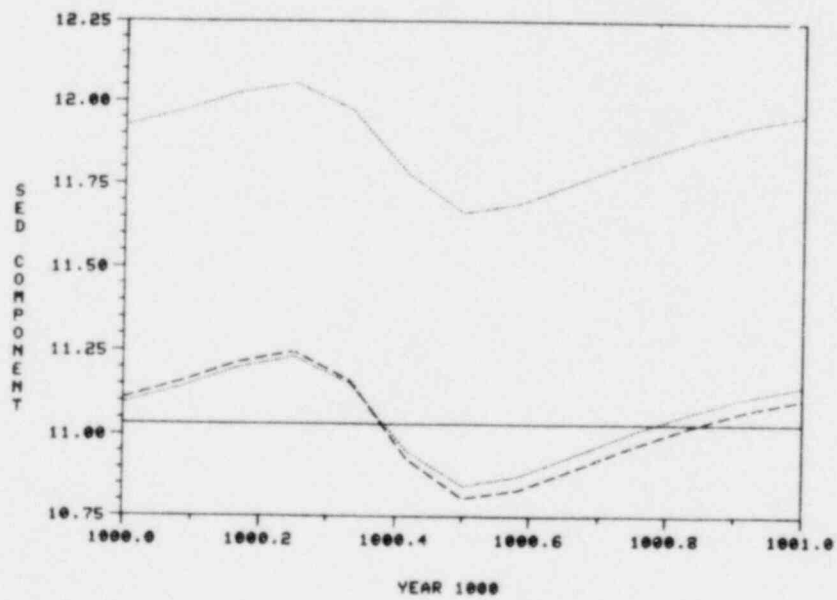
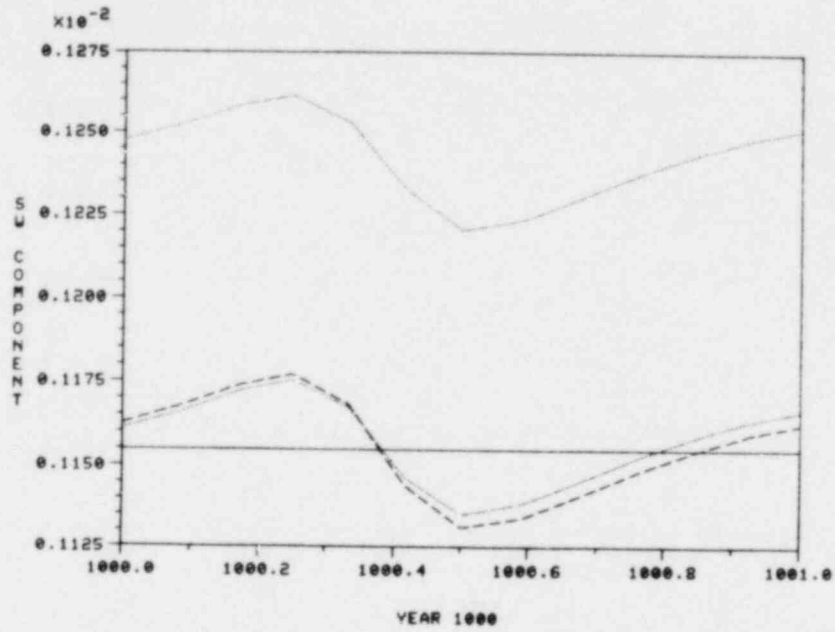


Figure 3-12. Continued

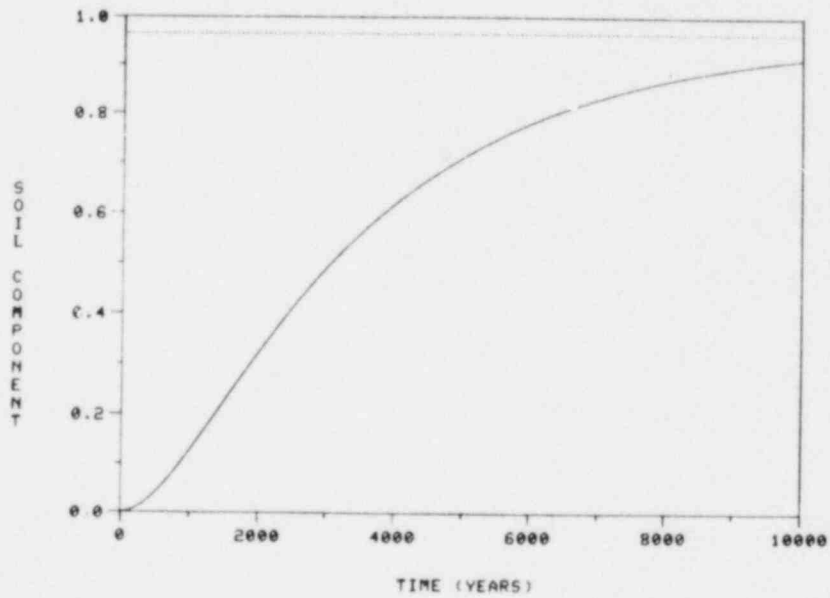
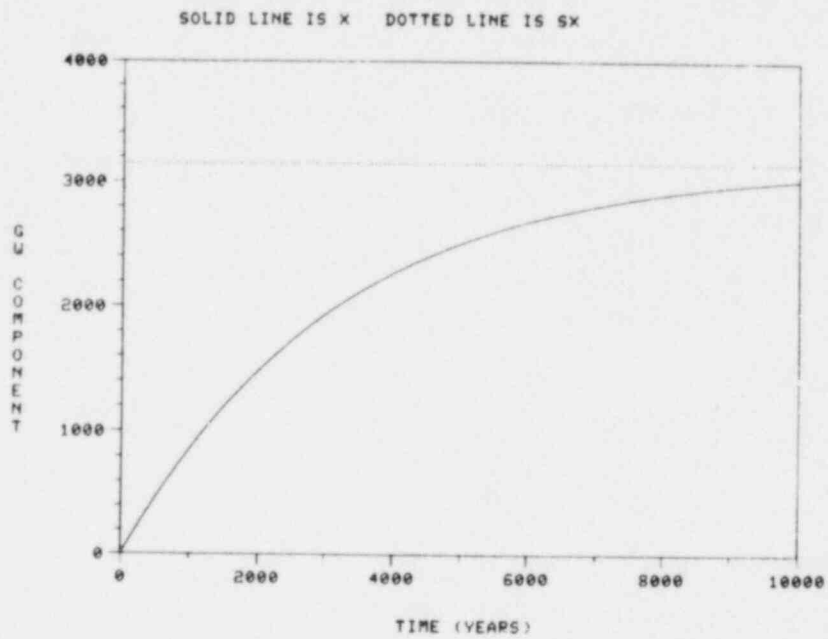


Figure 3-13. Asymptotic Behavior of X (Units: Atoms) for Radionuclide Input to Groundwater Subzone of Lake Zone.

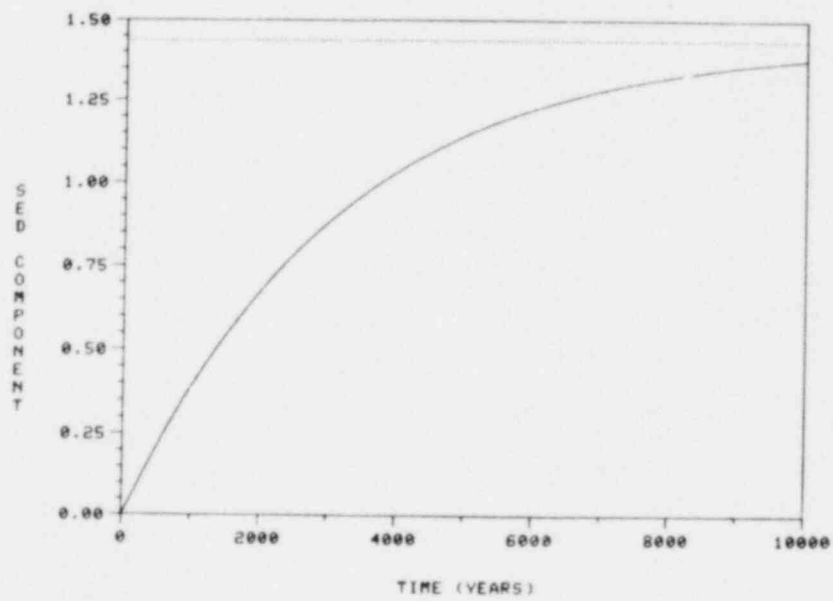
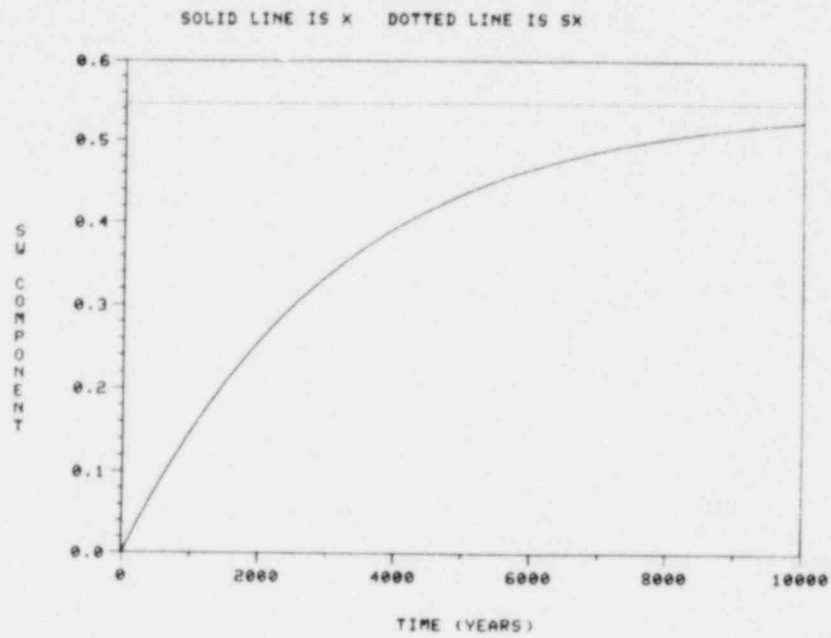


Figure 3-13. Continued

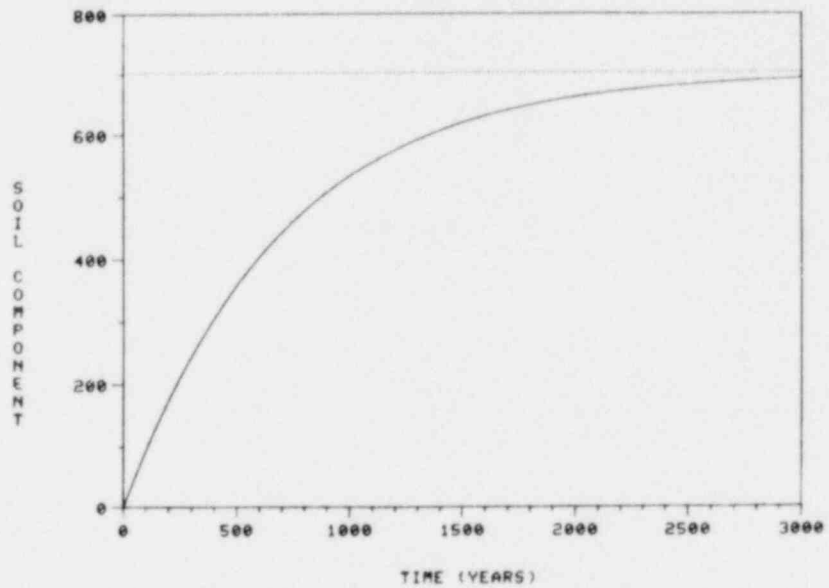
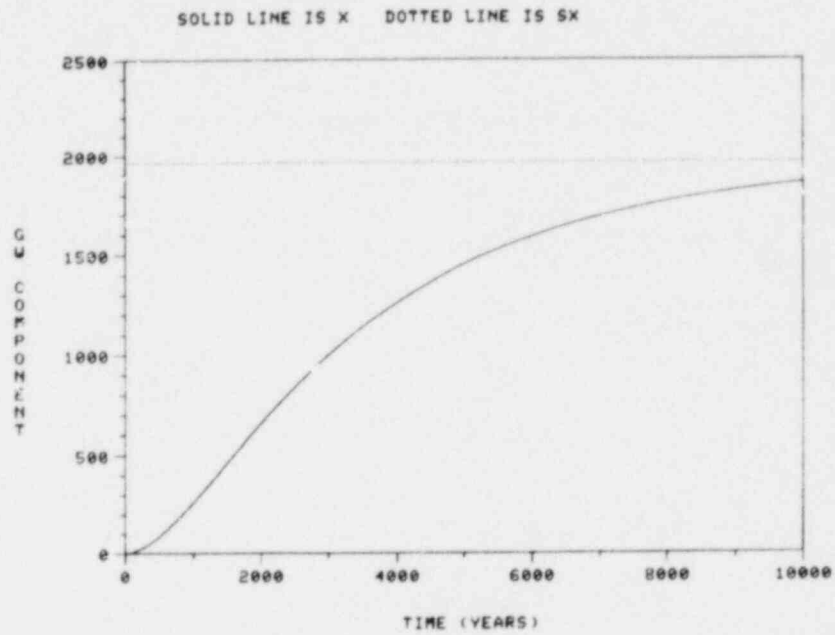


Figure 3-14. Asymptotic Behavior of X (Units: Atoms) for Radionuclide Input to Soil Subzone of Lake Zone.

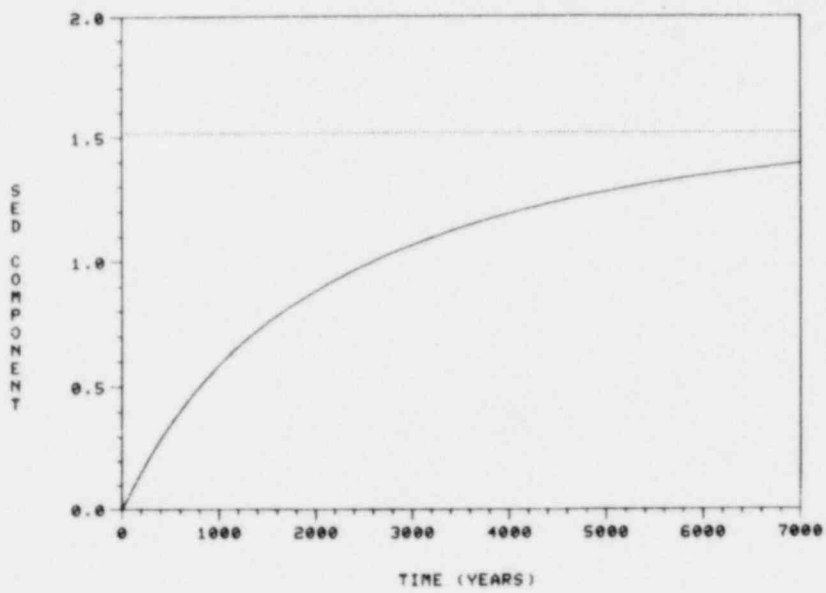
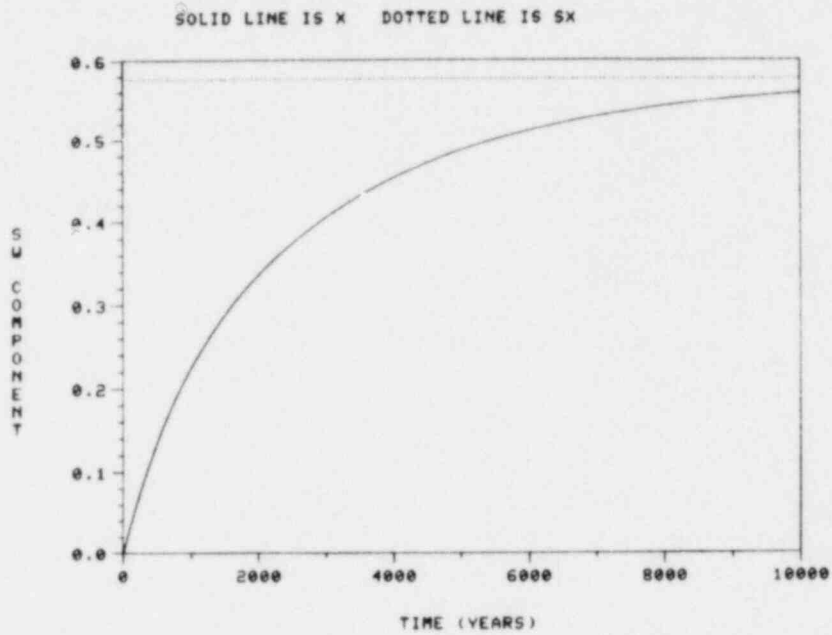


Figure 3-14. Continued

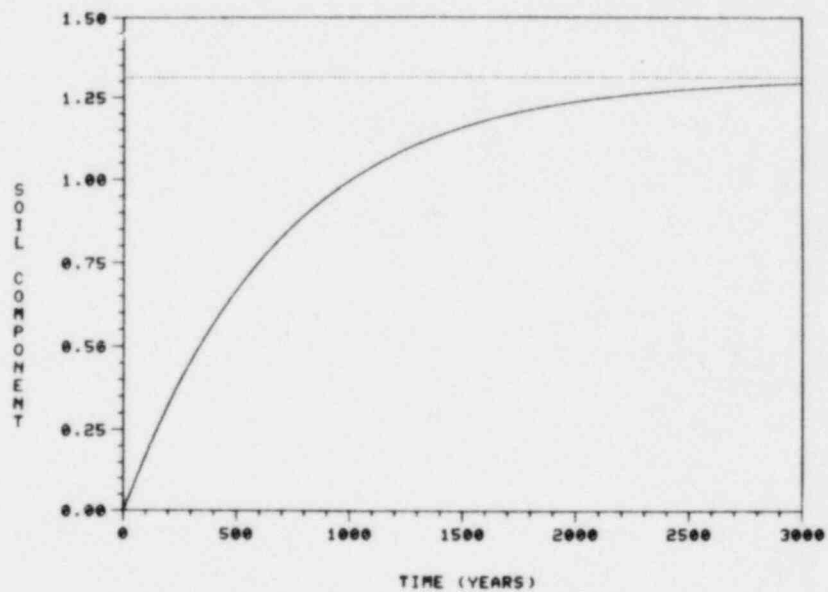
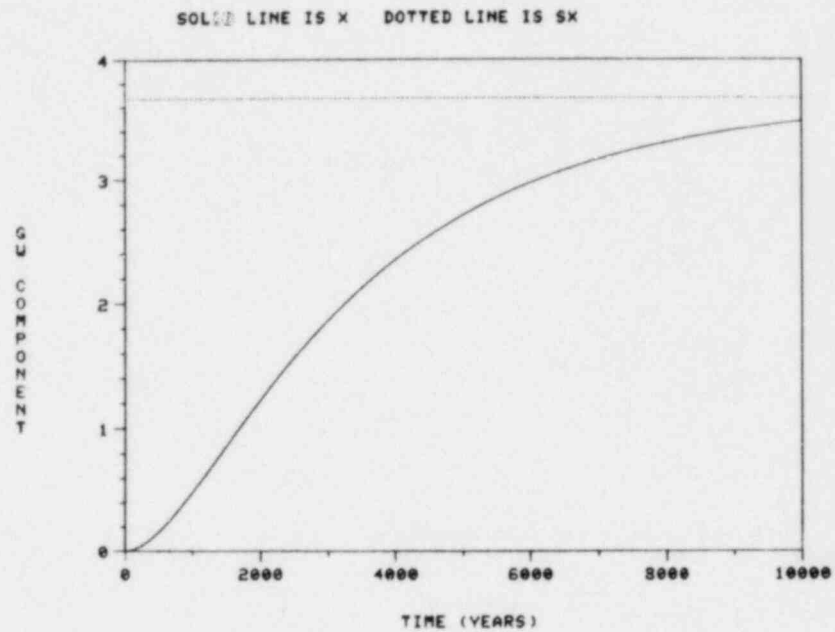


Figure 3-15. Asymptotic Behavior of X (Units: Atoms) for Radionuclide Input to Surface Water Subzone of Lake Zone.

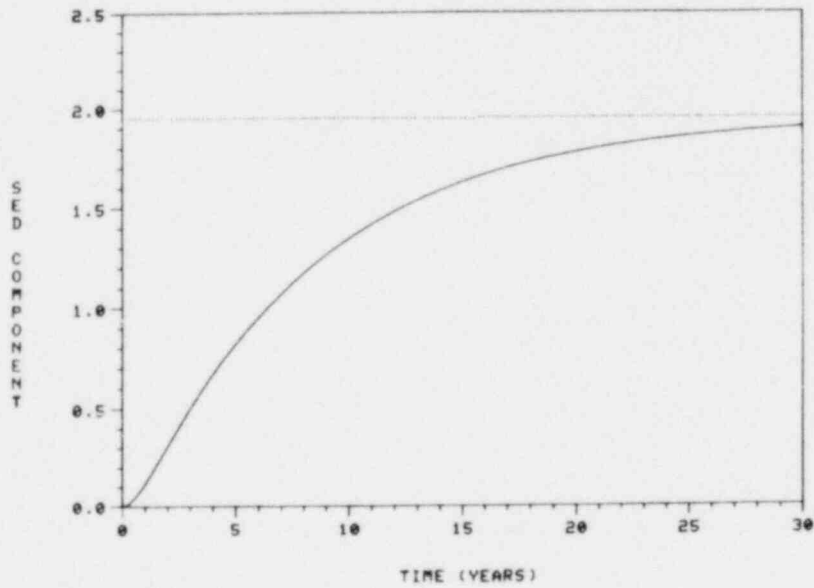
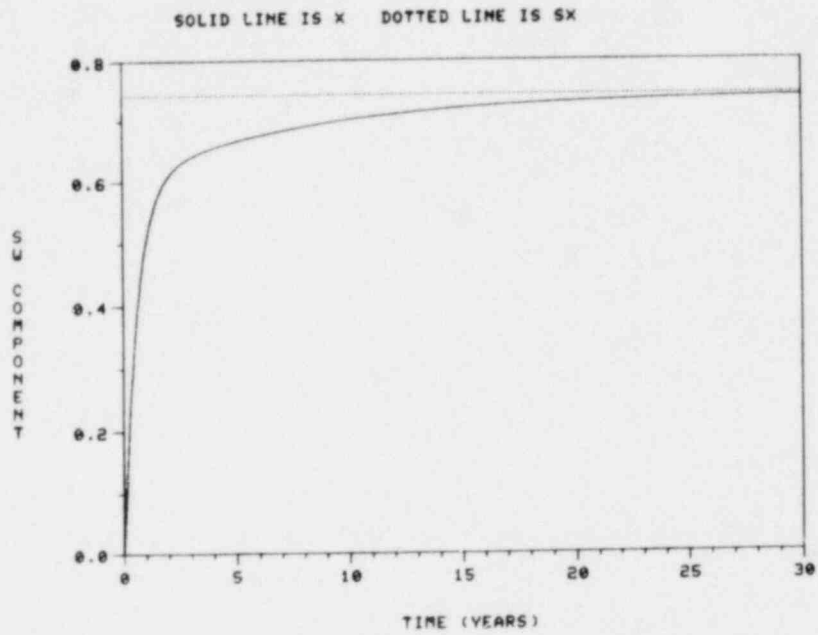


Figure 3-15. Continued

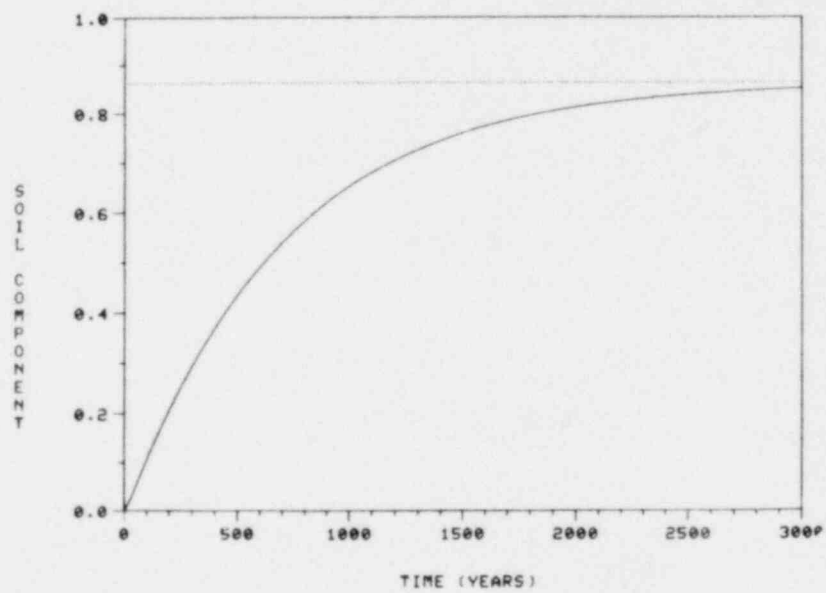
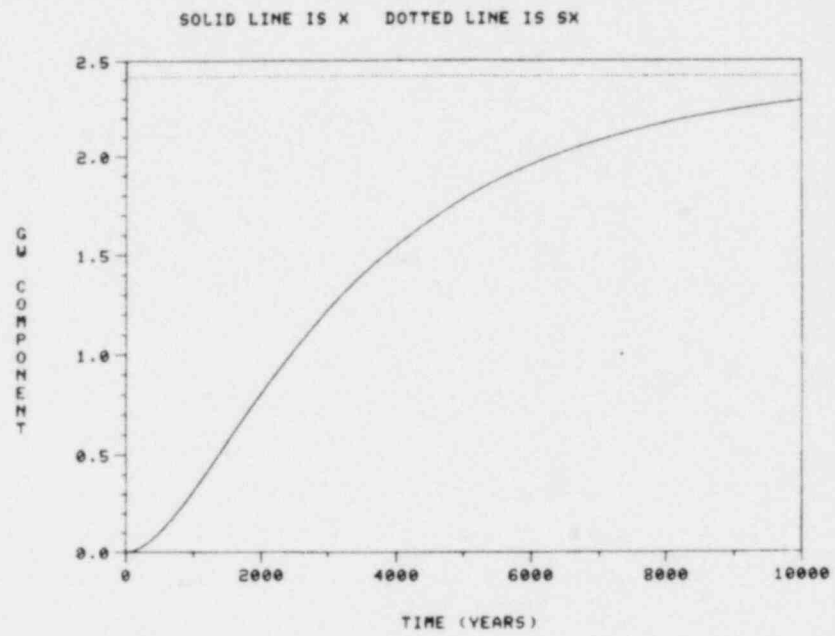


Figure 3-16. Asymptotic Behavior of X (Units: Atoms) for Radionuclide Input to Sediment Sub-zone of Lake Zone.

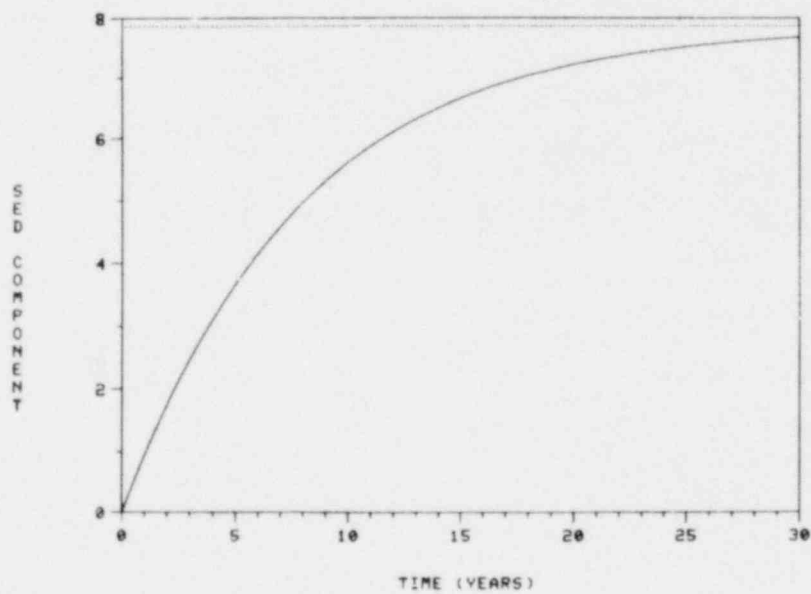
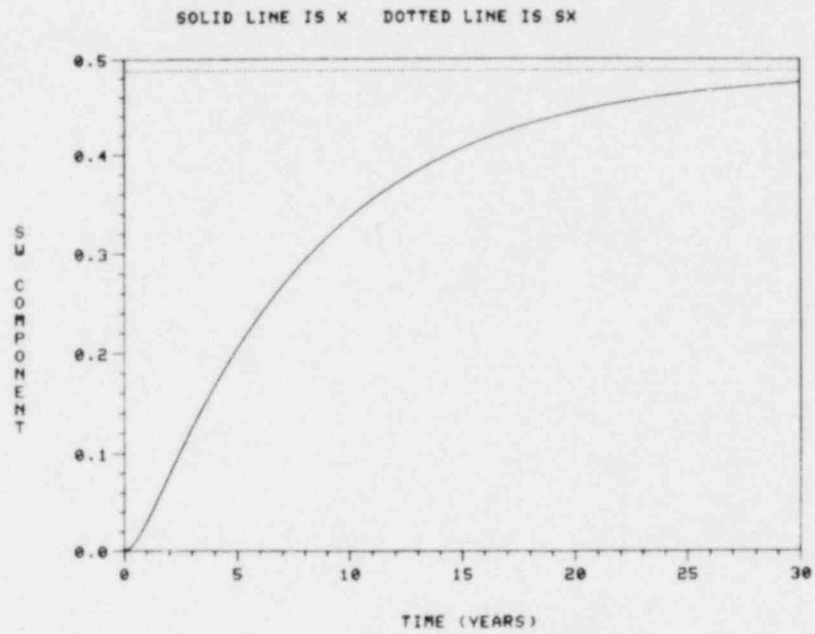


Figure 3-16. Continued

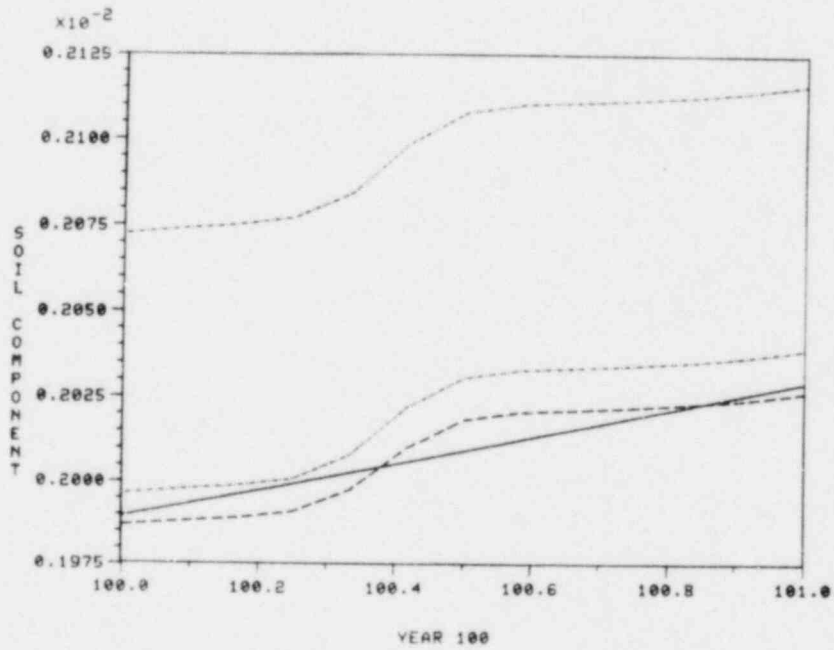
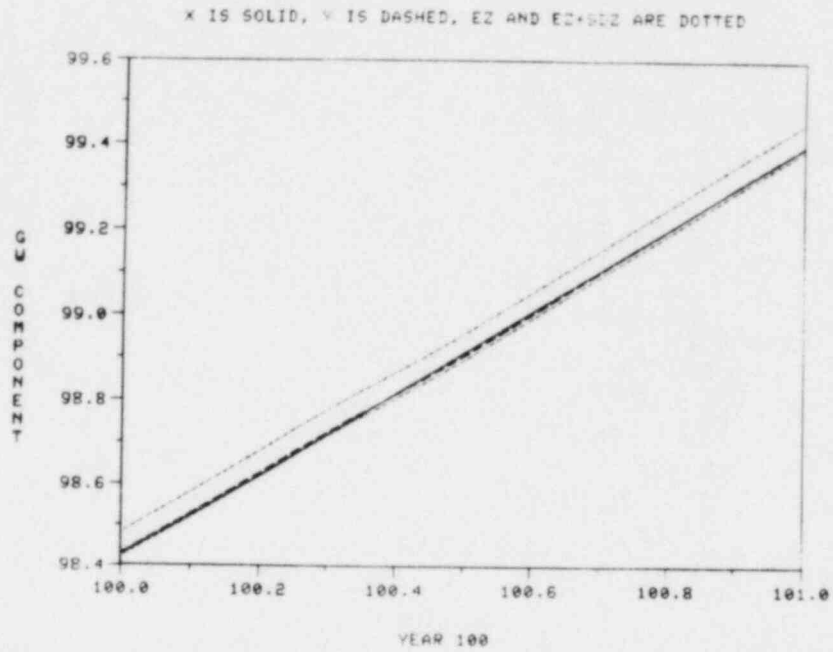


Figure 3-17. Behavior of X, Y, EZ, and EZ + SDZ (Units: Atoms) for Year 100 With Radionuclide Input to Groundwater Subzone of Lake Zone.

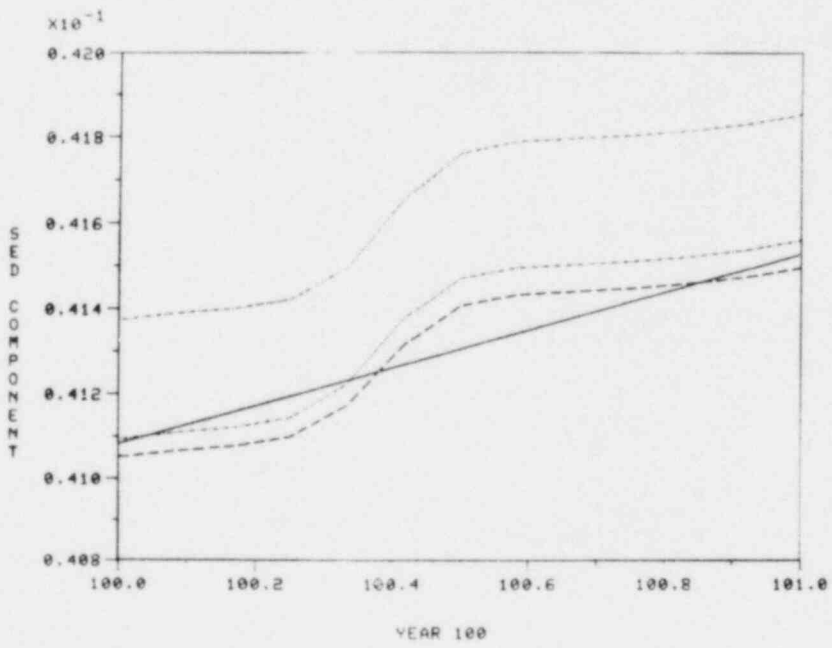
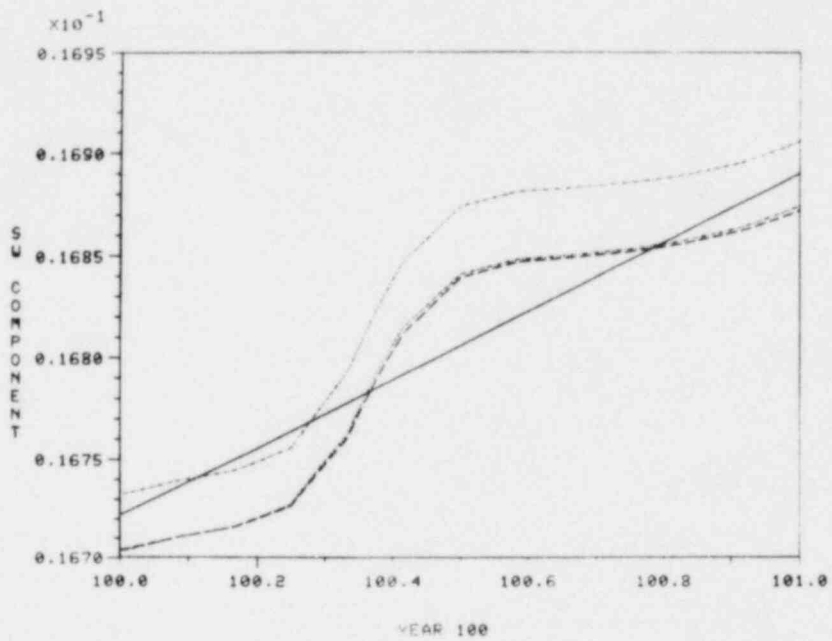


Figure 3-17. Continued

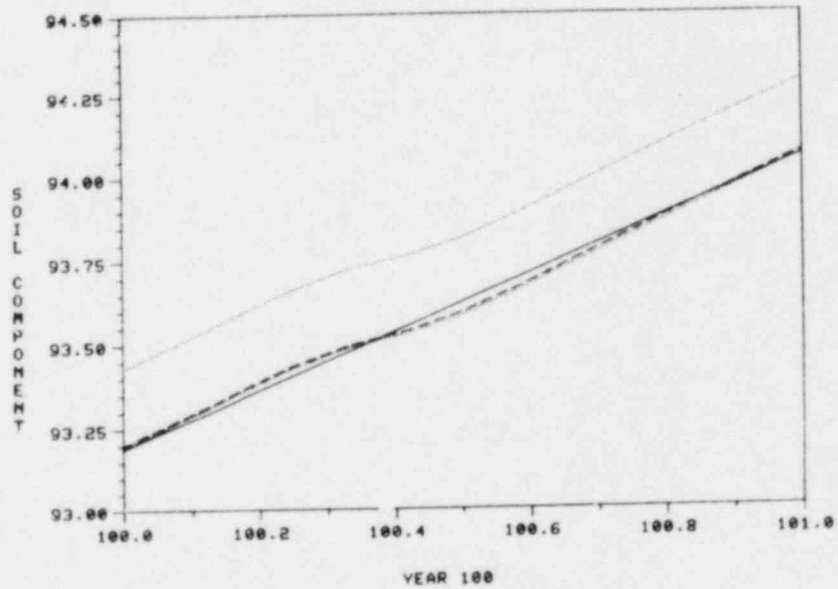
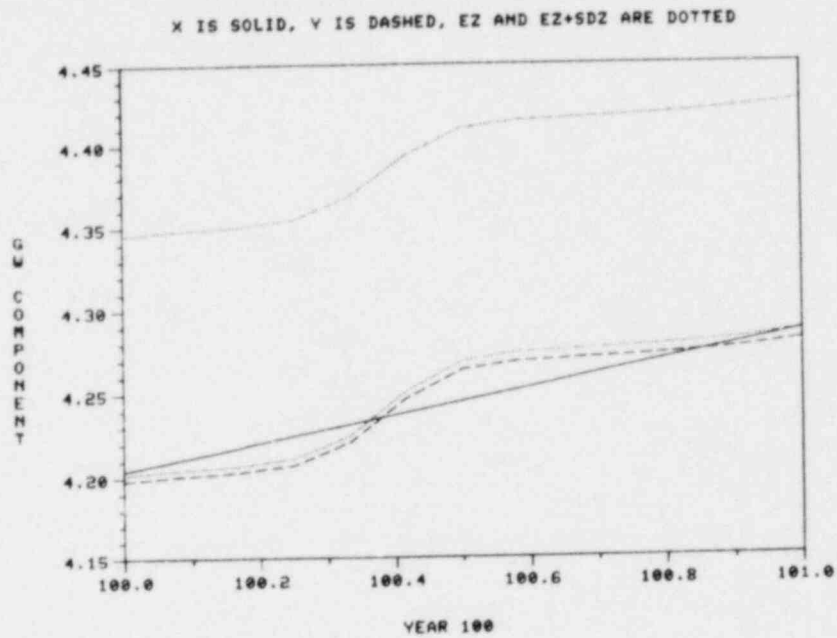


Figure 3-18. Behavior of X, Y, EZ, and EZ + SDZ (Units: Atoms) for Year 100 With Radionuclide Input to Soil Subzone of Lake Zone.

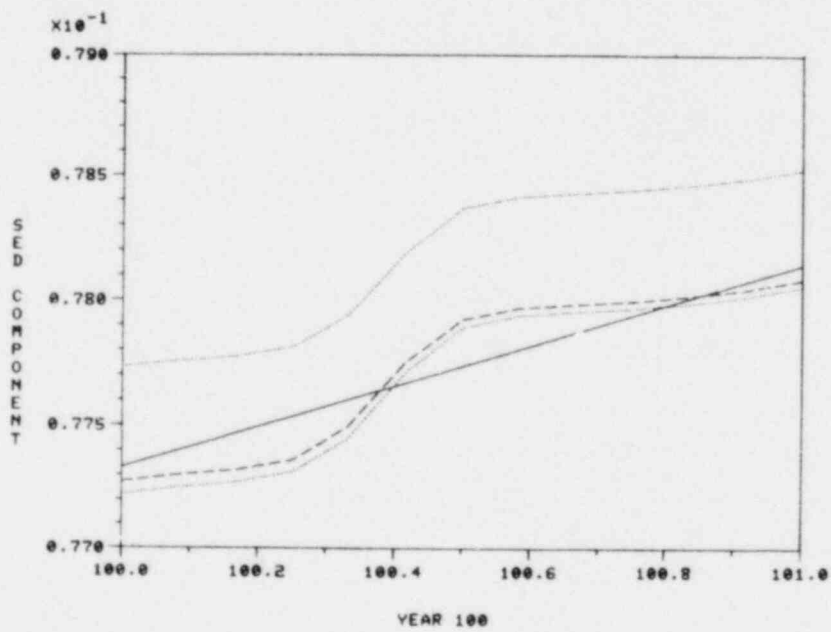
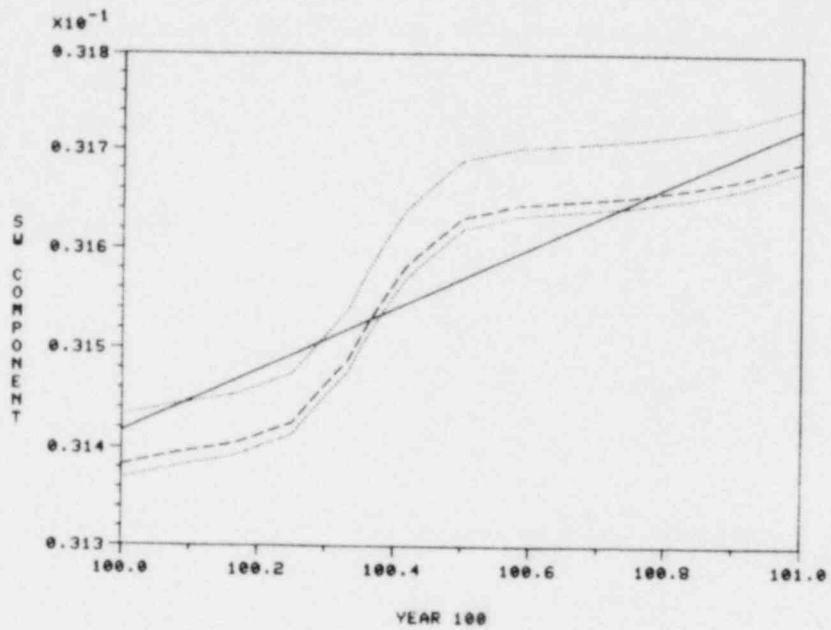


Figure 3-18. Continued

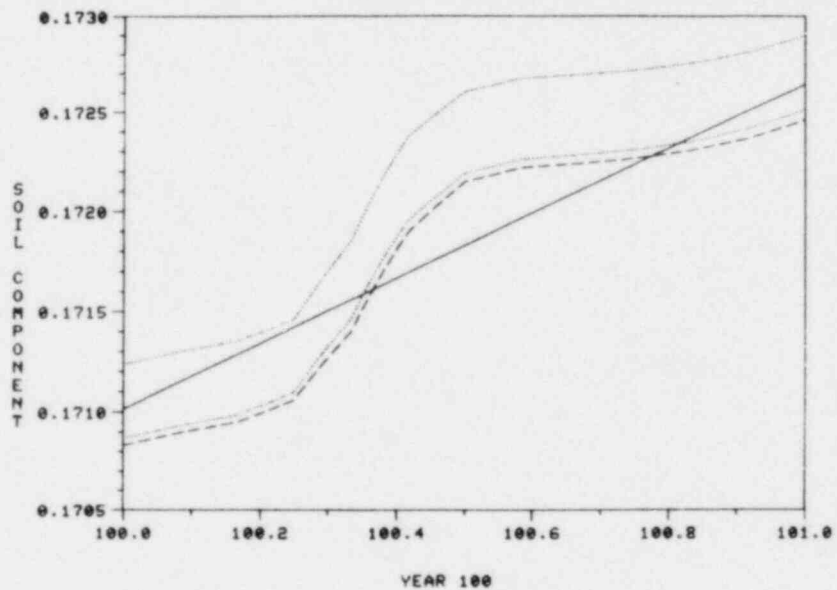
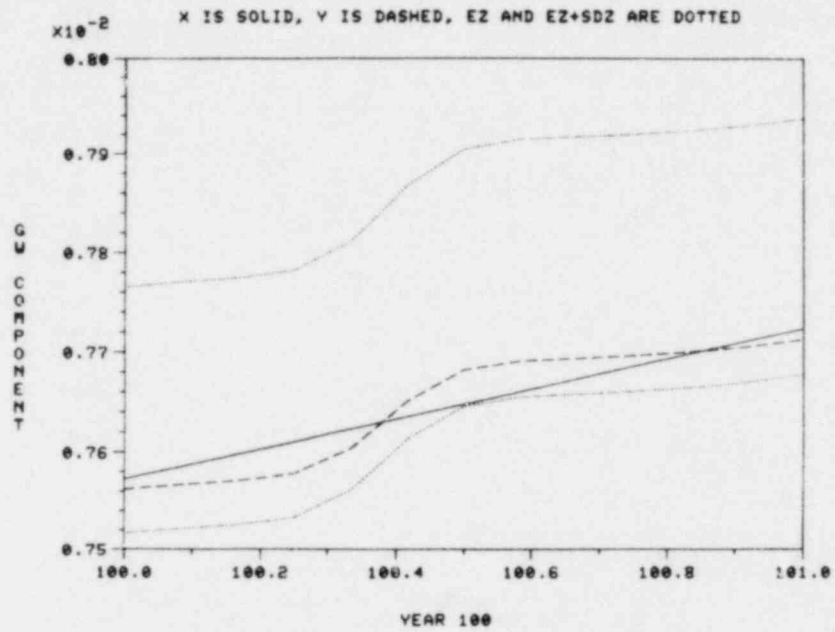


Figure 3-19. Behavior of X, Y, EZ, and EZ + SDZ (Units: Atoms) for Year 100 With Radionuclide Input to Surface Water Subzone of Lake Zone.

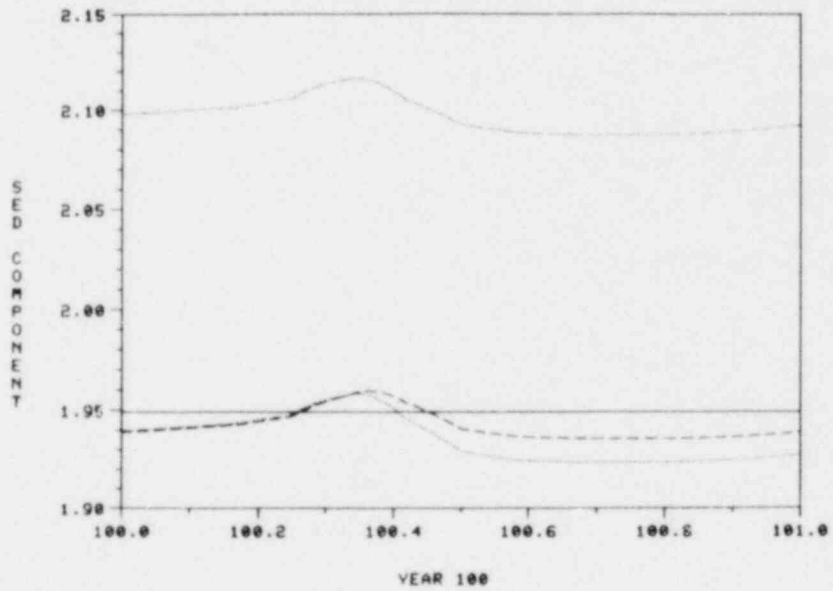
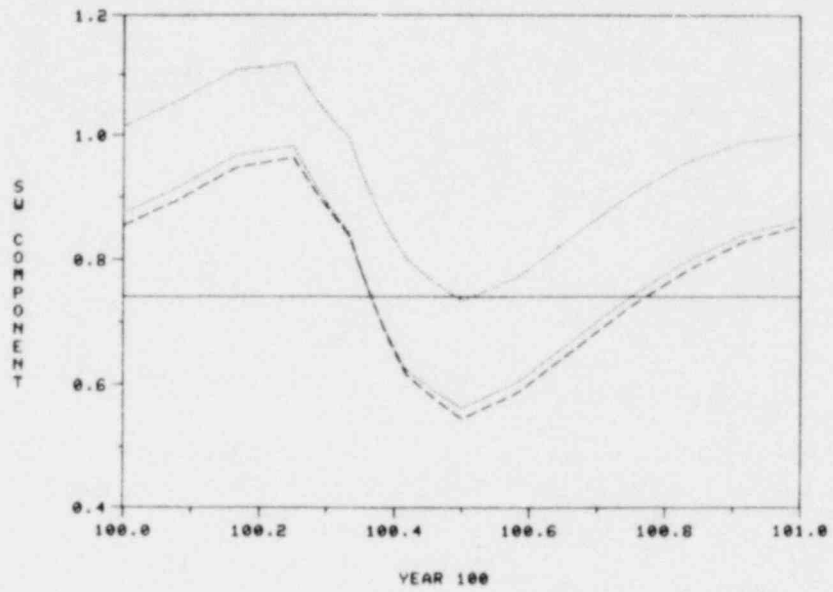


Figure 3-19. Continued

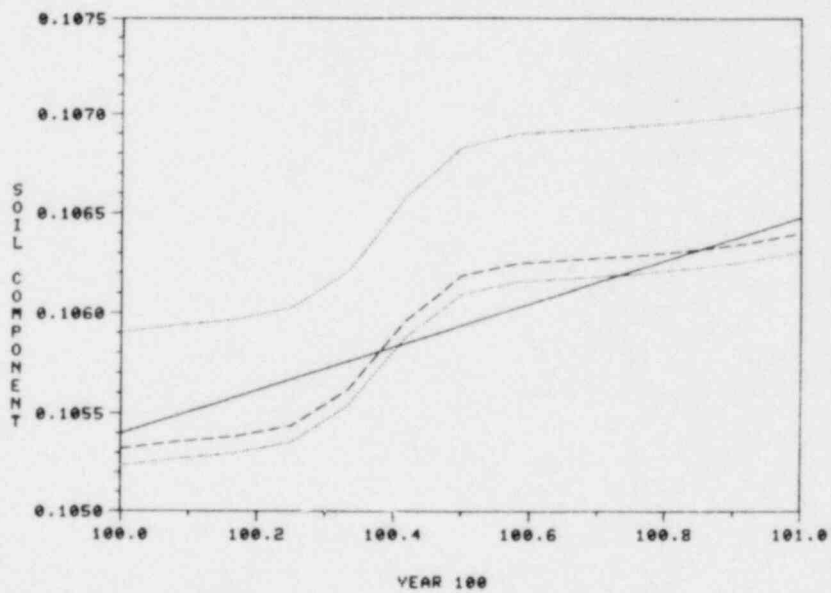
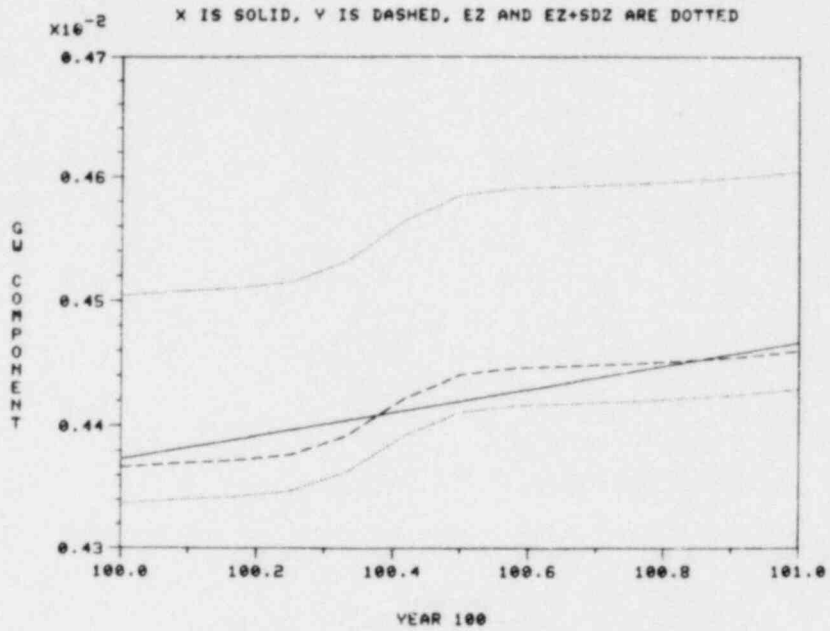


Figure 3-20. Behavior of X, Y, EZ, and EZ + SDZ (Units: Atoms) for Year 100 With Radionuclide Input to Sediment Subzone of Lake Zone.

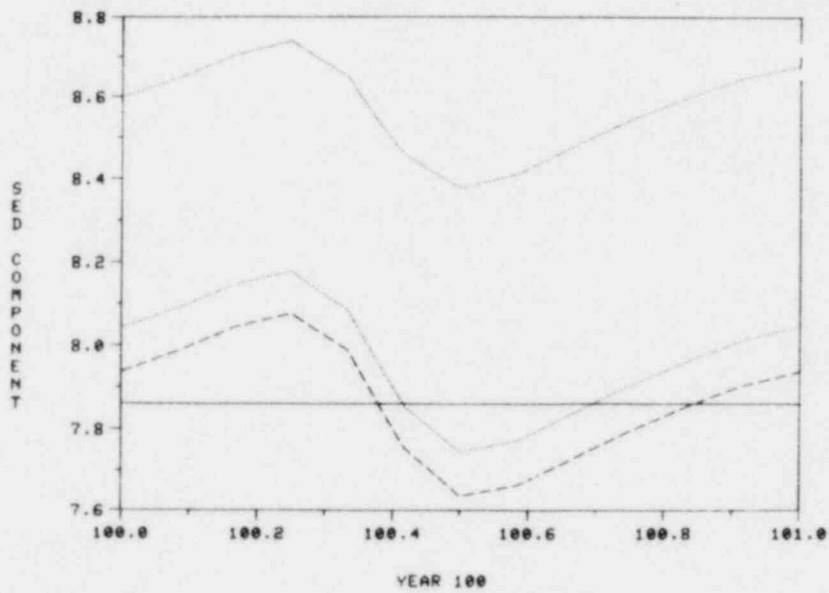
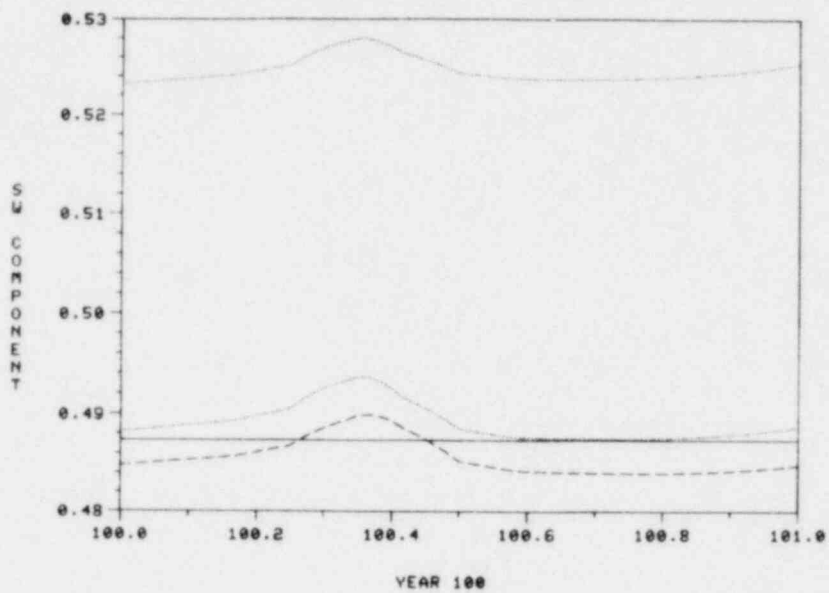


Figure 3-20. Continued

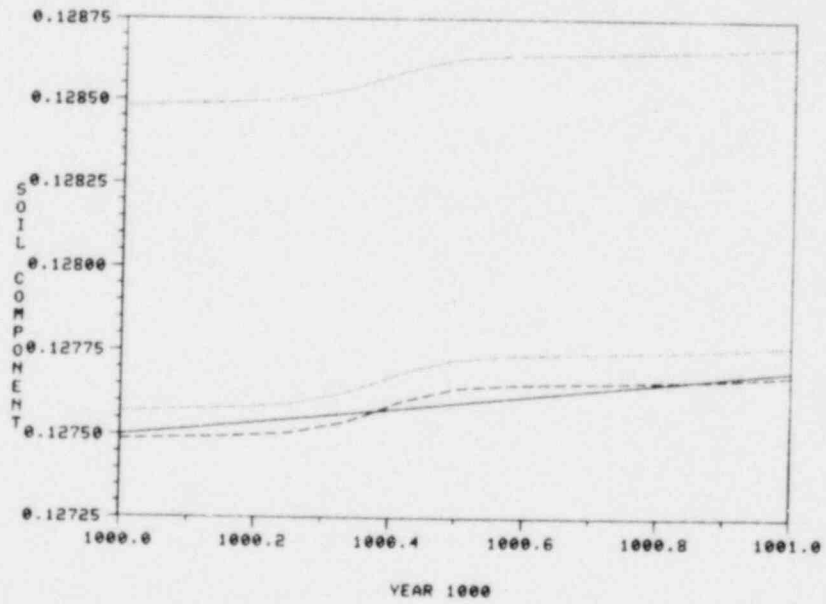
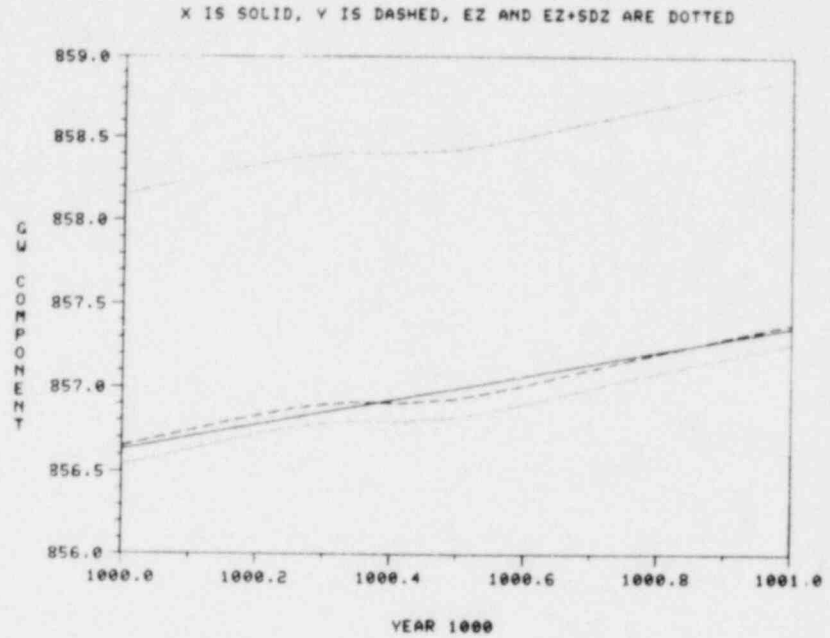


Figure 3-21. Behavior of X, Y, EZ, and EZ + SDZ (Units: Atoms) for Year 1000 With Radionuclide Input to Groundwater Subzone of Lake Zone.

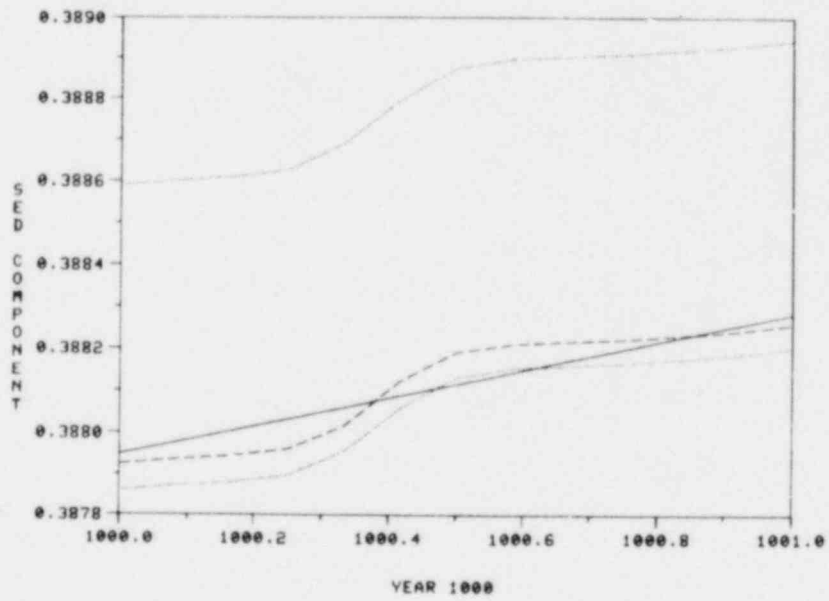
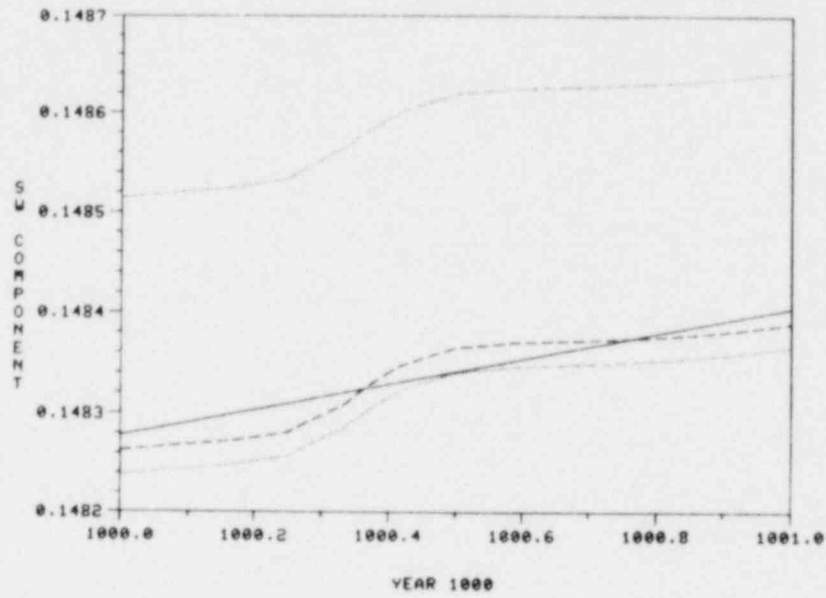


Figure 3-21. Continued

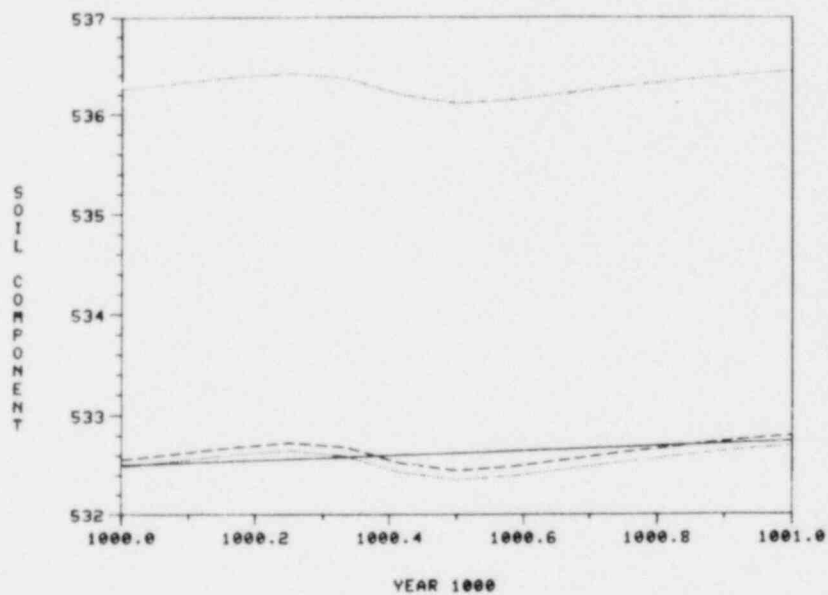
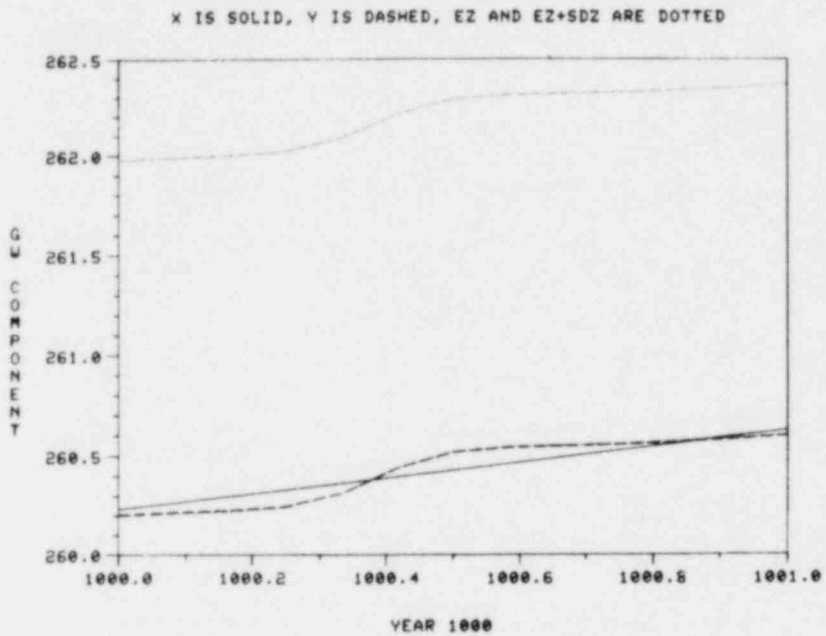


Figure 3-22. Behavior of X, Y, EZ, and EZ + SDZ (Units: Atoms) for Year 1000 With Radionuclide Input to Soil Subzone of Lake Zone.

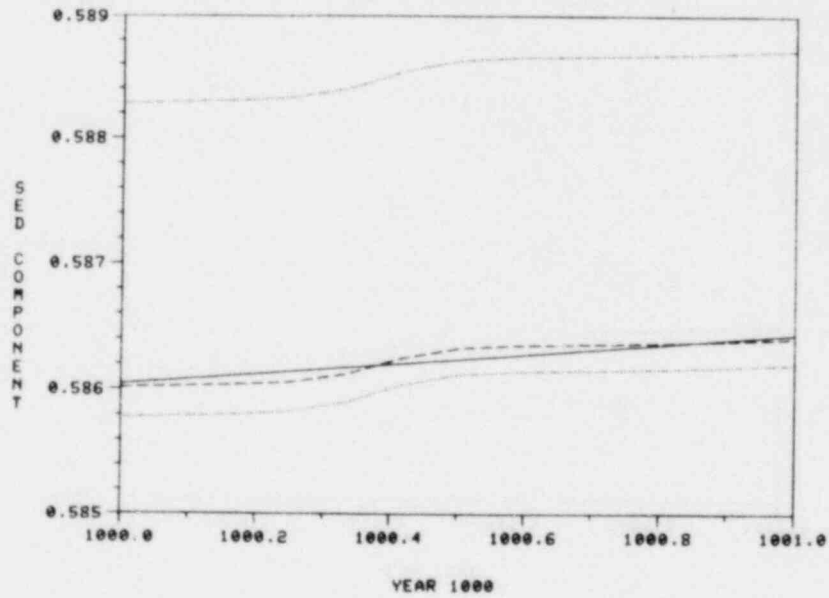
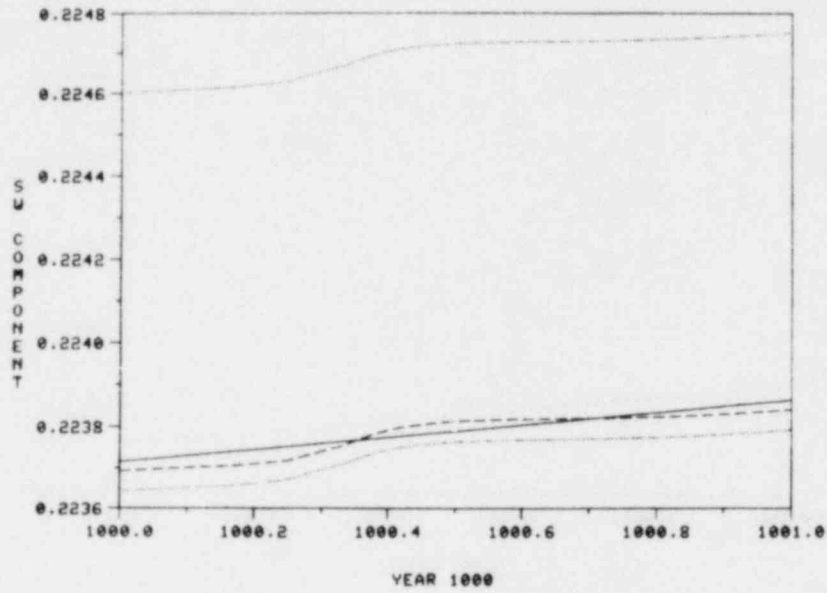


Figure 3-22. Continued

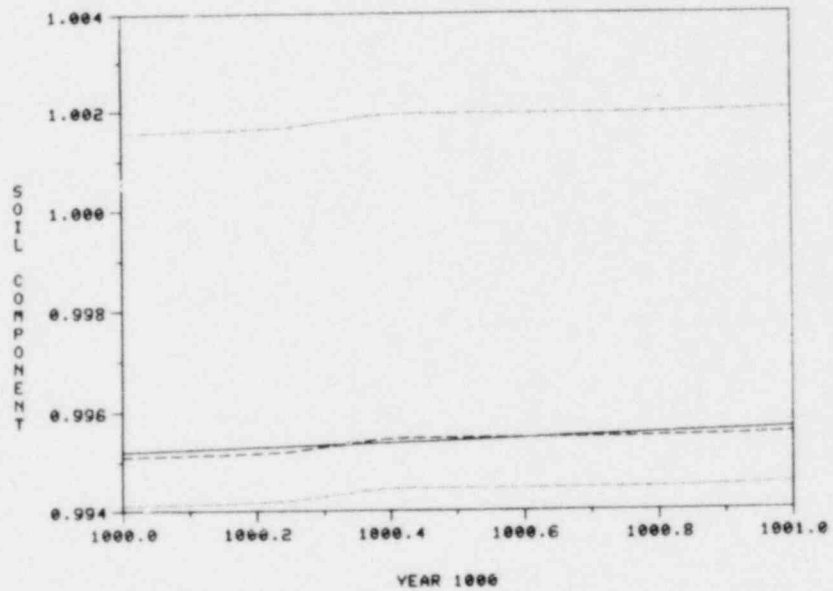
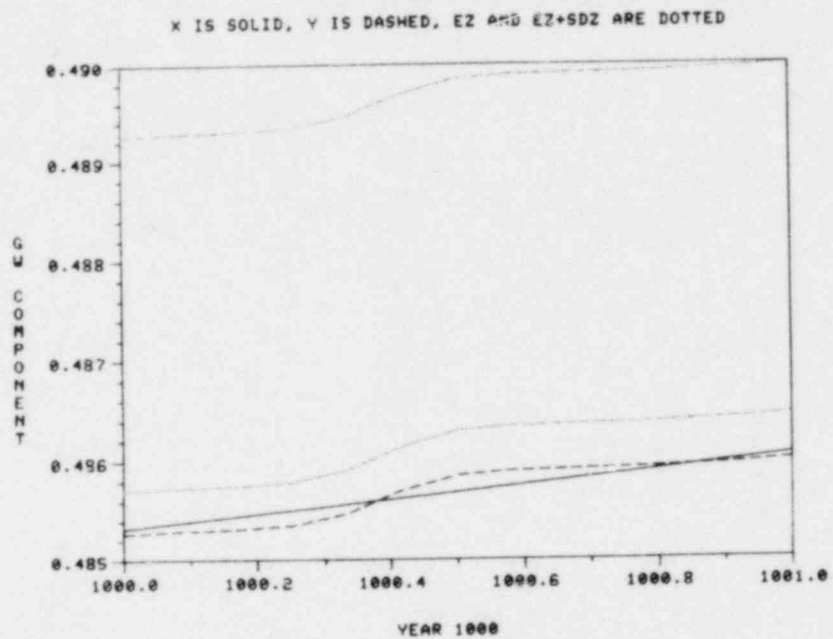


Figure 3-23. Behavior of X, Y, EZ, and EZ + SDZ (Units: Atoms) for Year 1000 With Radionuclide Input to Surface Water Subzone of Lake Zone.

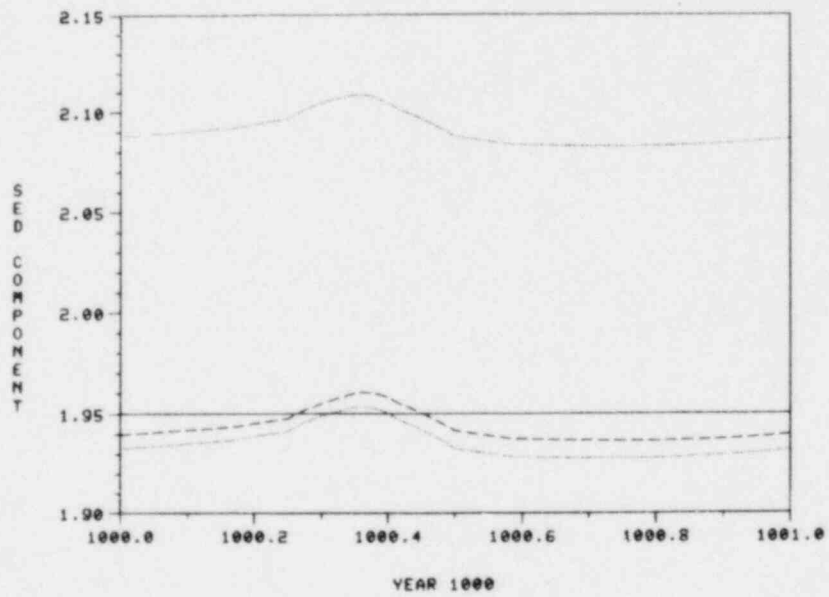
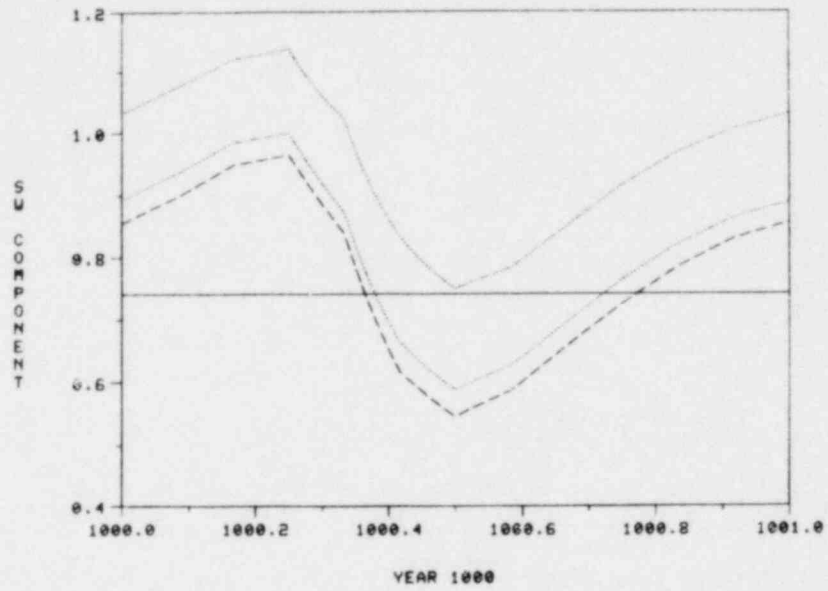


Figure 3-23. Continued

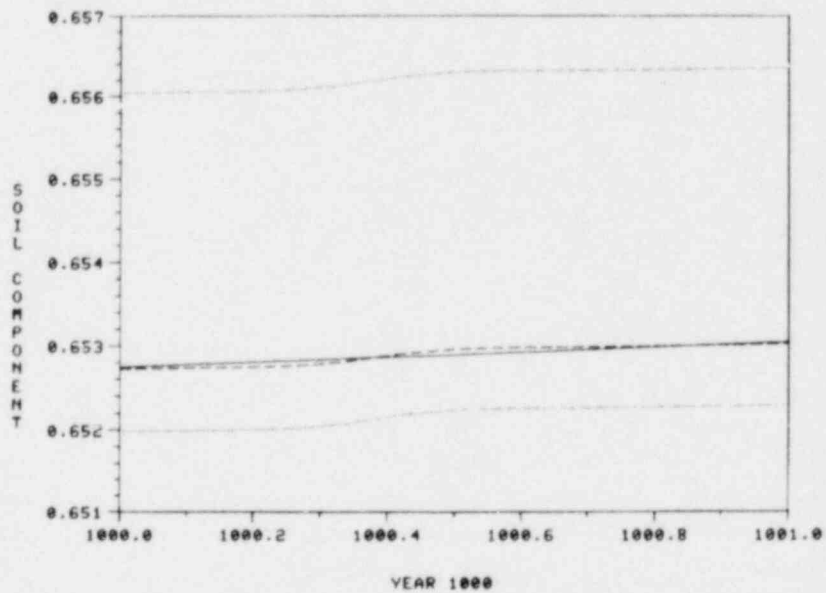
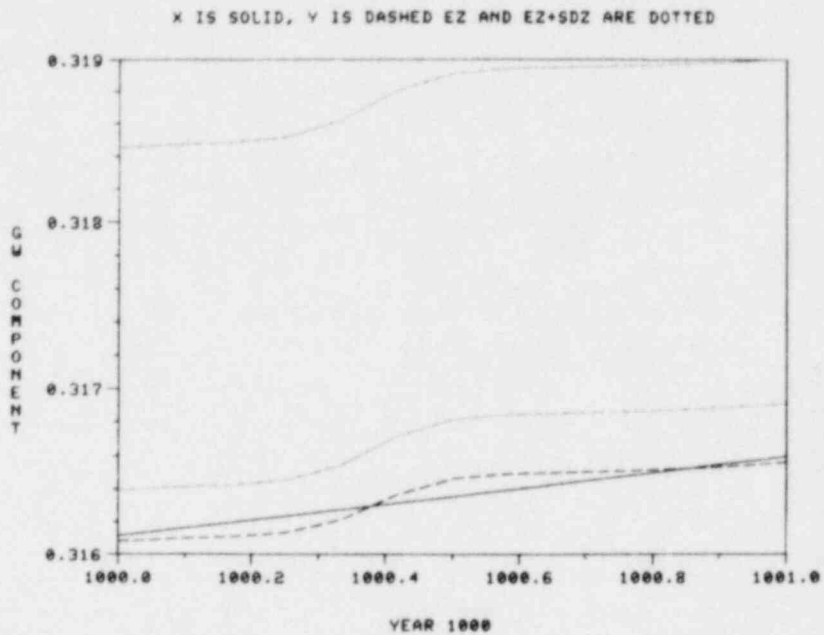


Figure 3-24. Behavior of X, Y, EZ, and EZ + SDZ (Units: Atoms) for Year 1000 With Radionuclide Input to Sediment Subzone of Lake Zone.

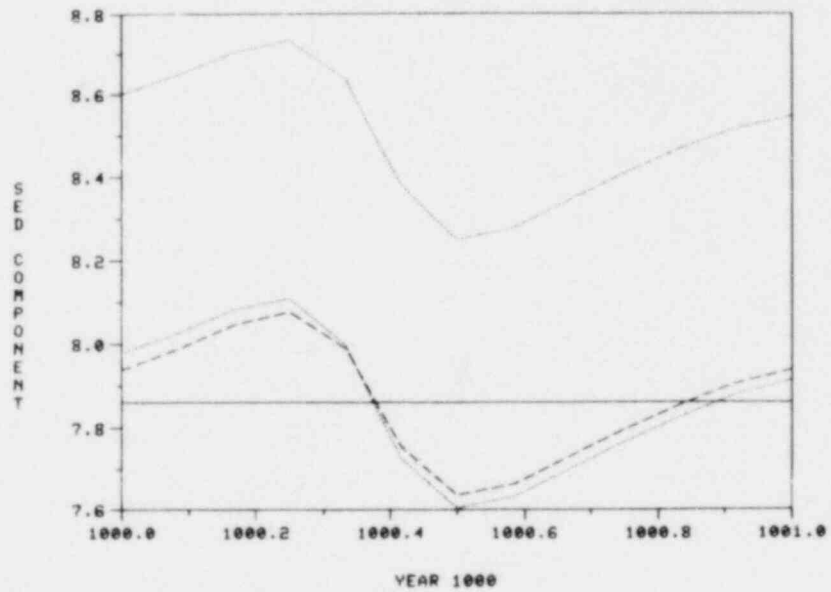
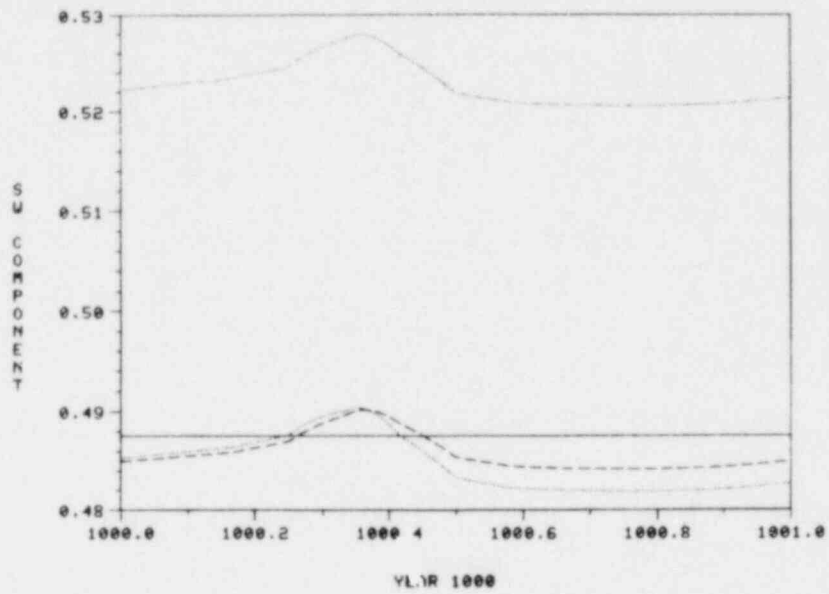


Figure 3-24. Continued

Table 3-1

$$\text{Max} [EZ_k(t) + 2 \cdot \text{SDZ}_k(t) - X_k(t)] / X_k(t)$$

Expressed as a Percentage

		RIVER ZONE		LAKE ZONE	
		<u>Year 100</u>	<u>Year 1000</u>	<u>Year 100</u>	<u>Year 1000</u>
Input to GW	GW	.15%	.11%	.3%	.4%
	SOIL	8.4 %	2.2 %	9.0%	1.6%
	SW	.15%	.3 %	.6%	.4%
	SED	1.8 %	.4 %	2.1%	.4%
Input to SOIL	GW	7.4 %	.9 %	7.1%	1.5%
	SOIL	.9 %	2.1 %	.6%	1.5%
	SW	.7 %	1.5 %	.6%	.9%
	SED	1.7 %	1.7 %	1.6%	.9%
Input to SW	GW	9.2 %	1.0 %	7.2%	1.7%
	SOIL	.8 %	2.0 %	.7%	1.4%
	SW	1200. %	1200. %	80.0%	80.0%
	SED	20. %	20. %	17.0%	16.4%
Input to SED	GW	7.8 %	1.3 %	8.3%	1.6%
	SOIL	1.4 %	1.9 %	1.7%	1.2%
	SW	16.0 %	17.3 %	16.4%	16.4%
	SED	15.0 %	16.2 %	20.0%	20.0%

Chapter 4

Comparison of X and Y

In this chapter, the solutions X and Y to the differential equations in (1.1) and (1.2), respectively, are discussed. In Section 4.1, a heuristic discussion of the similarities and differences between X and Y is given. This discussion is based on the comparison of components of X and Y to solutions of scalar differential equations. Then, in Section 4.2, several results are presented which provide exact comparisons between X and Y.

4.1 Heuristic Comparison of X and Y

To provide a basis for a heuristic discussion of the graphs appearing in Chapter 3, the following two scalar differential equations are introduced:

$$dx/dt = -ax(t) + r, \quad x(0) = 0 \quad (4.1)$$

and

$$dy/dt = -p(t)ay(t) + r, \quad y(0) = 0, \quad (4.2)$$

where a and r are positive numbers and p is a positive-valued, periodic function with period 1 such that

$$\int_0^1 p(t)dt = 1.$$

The solutions to the two preceding equations are given by

$$x(t) = \frac{r}{a} [1 - e^{-ta}] \quad (4.3)$$

and

$$y(t) = \int_0^t r \left[\exp\left(\int_s^t -adu\right) \cdot \exp\left(\int_s^t -h(u)du\right) \right] ds, \quad (4.4)$$

where the function h is defined by

$$h(u) = p(u)a - a. \quad (4.5)$$

It follows from the properties of p that h is periodic with period 1 and that

$$\int_s^{s+1} h(u)du = 0.$$

A bound for solutions to (4.2) is now established. This will help to explain the limited variation which appears in some of the solutions graphed in Chapter 3. Suppose $u < v$ are two nonnegative numbers; further, suppose n is the largest integer such that $u \leq u + n < v$. Then,

$$\begin{aligned} \exp\left(-\int_u^v h(w)dw\right) &= \exp\left(-\int_{u+n}^v h(w)dw\right) \\ &\geq \exp\left(-\int_{u+n}^v (\max h) dw\right) \\ &\geq \exp(-\max h) \\ &= \exp(1 - \max p)a, \end{aligned} \quad (4.6)$$

and similarly,

$$\begin{aligned}
 \exp\left(-\int_u^v h(w)dw\right) &= \exp\left(-\int_{u+n}^v h(w)dw\right) \\
 &\leq \exp\left(-\int_{u+n}^v (\min h) dw\right) \\
 &\leq \exp(-\min h) \\
 &= \exp(1 - \min p)a. \quad (4.7)
 \end{aligned}$$

Suppose t is an arbitrary positive number. Then, by using the two preceding inequalities, it follows that

$$\begin{aligned}
 y(t) &= \int_0^t r \left[\exp\left(\int_s^t -adu\right) \cdot \exp\left(\int_s^t -h(u)du\right) \right] ds \\
 &\quad \text{[From (4.4)]} \\
 &\geq \int_0^t r \left[\exp\left(\int_s^t -adu\right) \cdot \exp(1 - \max p)a \right] ds \\
 &\quad \text{[From (4.6)]} \\
 &= x(t) \exp(1 - \max p)a \\
 &\quad \text{[From (4.3)]}
 \end{aligned}$$

and also that

$$y(t) = \int_0^t r \left[\exp\left(\int_s^t -adu\right) \cdot \exp\left(\int_s^t -h(u)du\right) \right] ds \quad [\text{From (4.4)}]$$

$$\leq \int_0^t r \left[\exp\left(\int_s^t -adu\right) \cdot \exp(1 - \min p)a \right] ds \quad [\text{From (4.7)}]$$

$$= x(t) \exp(1 - \min p)a. \quad [\text{From (4.3)}]$$

Thus,

$$x(t) \exp[(1 - \max p)a]$$

$$\leq y(t) \leq x(t) \exp[(1 - \min p)a]. \quad (4.8)$$

It is now shown that the solutions of (4.1) and (4.2) intersect in every interval of length 1. Suppose s is a positive number. Further, let Q be defined as in (2.5); then,

$$\begin{aligned} \int_u^v h(t)dt &= \int_u^v [p(t)a - a]dt \\ &= a \int_u^v [p(t) - 1]dt = a[Q(v) - Q(u)]. \end{aligned}$$

As noted in Chapter 2, $Q(0) = 0$ and Q is periodic with period 1. Since Q is continuous, there exist t_1 and t_2 in $[s, s+1]$ such that Q assumes its maximum and minimum at t_1 and t_2 , respectively. It now follows from the representation for y given in (4.4) that

$$y(t_1) = \int_0^{t_1} r \left\{ \exp \left[\int_v^{t_1} -adu \right] \cdot \exp[-aQ(t_1) + aQ(v)] \right\} dv$$

$$\leq \int_0^{t_1} r \left\{ \exp \left[\int_v^{t_1} -adu \right] \right\} dv = x(t_1)$$

and

$$y(t_2) = \int_0^{t_2} r \left\{ \exp \left[\int_v^{t_2} -adu \right] \cdot \exp[-aQ(t_2) + aQ(v)] \right\} dv$$

$$\geq \int_0^{t_2} r \left\{ \exp \left[\int_v^{t_2} -adu \right] \right\} dv = x(t_2).$$

Thus, it follows from the continuity of x and y that there must exist a number t between t_1 and t_2 such that $x(t) = y(t)$. Hence, the solutions of (4.1) and (4.2) intersect in every interval of length 1.

In the following, three aspects of the graphs appearing in Chapter 3 are discussed: (1) the limited difference in the solutions to (1.1) and (1.2) for the groundwater subzone when radionuclide input is to the groundwater subzone, (2) the noticeable difference in the solutions to (1.1) and (1.2) for the surface water subzone when radionuclide input is to the surface water subzone, and (3) the limited difference in the solutions to (1.1) and (1.2) for the surface water subzone when radionuclide input is to the groundwater subzone.

In this paragraph, we consider the limited difference in the solutions to (1.1) and (1.2) for the groundwater subzone when radionuclide input is to the groundwater subzone. That is, the differences in X_1 and Y_1 are considered. For this situation, the amount of radionuclide in the groundwater subzone is represented by equations which are similar to, but slightly different from, the equations appearing in (4.1) and (4.2). The difference is that, in addition to the constant radionuclide inflow r , there is also a radionuclide inflow from the soil subzone. However, this inflow is small in comparison to r and thus has a limited effect on the solution. The result is that Y_1 is bounded by X_1 in a manner similar to that shown in (4.8) for the scalar equations. As the value corresponding to a in (1.1) and (1.2) is 3.2×10^{-4} and the values for $\max p$ and $\min p$ are 3.8 and 0.2, respectively, this bound should be reasonably tight. As indicated in the figures contained in Chapter 3, such is the case. Further, as previously shown, the solutions to (4.1) and (4.2) intersect in every interval of length l . Again, similar behavior can be expected from X_1 and Y_1 and such is indicated to be the case in Chapter 3. Although only the behavior of X_1 and Y_1 with radionuclide input to the groundwater subzone has been discussed, similar behavior is also exhibited by X_2 and Y_2 with radionuclide input to the soil subzone and by X_4 and Y_4 with radionuclide input to the sediment subzone.

We now consider the noticeable difference in the solutions to (1.1) and (1.2) for the surface water subzone when radionuclide input is to the surface water subzone. That is, the differences between X_3 and Y_3 are considered. Again, the amount of radionuclide in the surface water subzone is represented by equations which are similar to, but slightly different from, the equations appearing in (4.1) and (4.2). The difference is that, in addition to the constant radionuclide inflow r , there are also radionuclide inflows from the groundwater, soil and sediment subzones. However, these inflows are small in comparison to r and thus have a limited effect on the solution. Thus, X_3 and Y_3 tend to behave as indicated in (4.3) and (4.4). The difference in behavior X_3 and Y_3 from the cases considered in the preceding paragraph is due to the large rate constant (i.e., 960 for River Zone and 1.6 for Lake Zone) for flow out of the surface water subzone. The effects of this can be realized by considering (4.3), where a corresponds to the rate constant for flow out of the surface water subzone. With a large, the solution

to (4.1) moves very quickly to its asymptotic value r/a . That this is the case can be seen by considering Figures 3-3 and 3-15. Replacement of a in (4.1) by the product $p_1 a$ changes the asymptotic value to $r/p_1 a$. The differences in X_3 and Y_3 result from the tendency of these solutions to behave as indicated in (4.3); the relatively large values associated with $p_1 a$ tends to keep Y_3 close to $r/p_1 a$. This pattern is more pronounced for the surface water subzone of the River Zone than the surface water subzone of the Lake Zone as it has a larger rate constant for radionuclide outflow.

We now consider the limited difference in the solutions to (1.1) and (1.2) for the surface water subzone when radionuclide input is to the groundwater subzone. That is, the similarity between X_3 and Y_3 is considered. This similarity is much greater than one would expect. Specifically, there is almost no difference between X_3 and Y_3 when input is to the groundwater subzone while, as already discussed, there is noticeable difference when input is to the surface water subzone. This behavior results from the introduction of variation in (1.2) by the multiplication of the coefficient matrix A by the scalar hydrologic pattern $p(t)$, which causes all flow rates in the system to vary up and down together. For the situation under consideration, this causes more variation in the discharge of the groundwater subzone than is physically appropriate and in turn this discharge cancels out the effects of increased discharge from the surface water subzone.

The manner in which this occurs can be realized by considering X_3 and Y_3 as solutions to equations of the form given in (4.1) and (4.2). There will be inflows to the surface water subzone from the groundwater, soil and sediment subzones. As initial radionuclide input is to the groundwater subzone, the largest radionuclide inflow to the surface water subzone will be from this subzone. Further, as indicated in the two preceding paragraphs, the amount of radionuclide in the groundwater subzone will change very slowly relative to the changes in the surface water subzone and further will be little affected by the hydrologic pattern. The result is that X_3 and Y_3 will behave similarly to solutions for (4.1), where a is the rate constant for outflow from the surface water subzone and r is the rate of inflow from the groundwater subzone. The reason for this is indicated in the next paragraph.

Although multiplication of A by the hydrologic pattern $p(t)$ has little effect on Y_1 , it does have the effect of multiplying the radionuclide flow r from the groundwater subzone to the surface water subzone by p . The result is that X_3 and Y_3 can be approximated in each month by solutions to equations of the form

$$dX_3/dt = -aX_3(t) + r$$

and

$$dY_3/dt = -p_i a Y_3(t) + p_i r.$$

In turn, these equations have asymptotic solutions given by

$$r/a \text{ and } p_i r/p_i a = r/a,$$

respectively. Thus, due to the large rate constant associated with the surface water subzone which results in rapid attainment of equilibrium, the effects of the increased outflow from the surface water subzone which result from multiplication of A by the hydrologic pattern $p(t)$ are canceled by the increased inflow from the groundwater subzone. This is not a normal situation; one would not expect groundwater discharge to vary so directly with surface water discharge. The indicated patterns for direct radionuclide input to the surface water subzone are probably the most meaningful (i.e., revealing) of those presented. Similar behavior to that of X_3 and Y_3 with radionuclide input to the groundwater subzone is also exhibited by X_3 and Y_3 for input to the soil subzone and for input to the sediment subzone.

4.2 Analytic Comparison of X and Y

In the preceding section, a heuristic discussion of the similarities and differences between X and Y is provided. This section contains several results which provide analytic comparisons between X and Y.

We start by reminding the reader that Y is the solution of (1.2). In this equation, variation is introduced by multiplying the coefficient matrix A by the hydrologic

pattern $p(t)$. In contrast to the situation represented by (1.3), such a procedure results in a variation in the decay constants for the radionuclides involved. The relationship in (1.2) is more convenient to deal with than that in (1.3) as a suitable change of variable transforms (1.2) into an equation of the form

$$dW/dt = AW + h(t)R, \quad (4.9)$$

where $h(t)$ is another hydrologic pattern (i.e., a piecewise continuous, periodic, positive-valued function with a period of one year and

$$\int_0^1 h(t)dt = 1).$$

Specifically, let

$$W(t) = Y(P^{-1}(t)), \quad (4.10)$$

with $P(t)$ defined as in (2.5). Then,⁴

$$\begin{aligned} dW/dt &= \left[\frac{d}{du} Y(u) \Big|_{u=P^{-1}(t)} \right] \left[\frac{d}{dt} P^{-1}(t) \right] \\ &= [p(P^{-1}(t)) AY(P^{-1}(t)) + R] [1/p(P^{-1}(t))] \\ &= AY(P^{-1}(t)) + [1/p(P^{-1}(t))]R \\ &= AW(t) + h(t)R, \end{aligned} \quad (4.11)$$

⁴The reader is reminded of the following result on the existence of inverses and their derivatives: Suppose F is a one-to-one function with domain $[a,b]$ and range $[F(a),F(b)]$ whose derivative exists and is positive on (a,b) . Then, F has an inverse q ; and if $y = F(x)$, then $q'(y) = 1/F'(x)$ for $a < x < b$.

where

$$h(t) = 1/p(p^{-1}(t)) \quad (4.12)$$

is a hydrologic pattern such that

$$H(t) = \int_0^t h(s)ds = p^{-1}(t). \quad (4.13)$$

A result is now established which indicates the similarity between the solutions to (1.2) and (1.3). In essence, this result states that, when the decay constant for a radionuclide is "small," the difference between the solutions to (1.2) and (1.3) is "small." Although the following theorem is stated and proved for the 1-radionuclide case, it should be possible to obtain similar results for multi-radionuclide cases. The 1-radionuclide case is particularly tractable due to the commutativity of certain matrices.

Theorem 4.1. Suppose Y_1 and Y_2 are solutions to (1.2) and (1.3), respectively, in the 1-radionuclide case with decay constant λ and with initial values $Y_1(0) = Y_2(0) = 0$. Then,

$$e^{-2\lambda} Y_1(t) \leq Y_2(t) \leq e^{2\lambda} Y_1(t)$$

for $t \geq 0$.

Proof. Suppose t is a nonnegative number. Then,

$$\begin{aligned} Y_2(t) &= \int_0^t e^{[P(t)F+tD-P(s)F-sD]} R ds && \text{[From (2.7)]} \\ &= \int_0^t e^{[P(t)-P(s)] [F+D]} e^{[t-P(t)-s+P(s)] D} R ds. \end{aligned} \quad (4.14)$$

Now, since

$$e^{[t-P(t)-s+P(s)]D} = e^{[t-P(t)-s+P(s)][-\lambda]I}$$

where I denotes the identify matrix, it follows that

$$e^{-2\lambda} \leq e^{[t-P(t)-s+P(s)]D} \leq e^{2\lambda}. \quad (4.15)$$

The desired result can now be obtained from the relations in (4.14) and (4.15) and the following representation for Y_1 :

$$Y_1(t) = \int_0^t e^{[P(t)-P(s)]A_R} ds. \quad [\text{From (2.6)}]$$

This completes the proof of Theorem 4.1.

Next, a result is established which places conservative bounds on the difference between X and Y . These bounds are related to the extremes of the hydrologic pattern $p(t)$.

Theorem 4.2. Suppose X and Y are solutions to (1.1) and (1.2), respectively, with initial values $X(0) = Y(0) = V_0$. Then,

$$[1/\max p] X[P(t)] \leq Y(t) \leq [1/\min p] X[P(t)]$$

for $t \geq 0$.

Proof. Suppose t is a nonnegative number. Then,

$$\begin{aligned} Y(t) &= e^{P(t)A} V_0 + \int_0^t e^{[P(t)-P(s)]A_R} ds \\ &= e^{P(t)A} V_0 + \int_0^t [1/p(s)] p(s) e^{[P(t)-P(s)]A_R} ds. \end{aligned} \quad [\text{From (2.6)}]$$

Thus,

$$Y(t) \leq e^{P(t)A} V_0 + (1/\min p) \int_0^{P(t)} e^{[P(t)-z]A} R dz$$

and

$$Y(t) \geq e^{P(t)A} V_0 + (1/\max p) \int_0^{P(t)} e^{[P(t)-z]A} R dz.$$

The desired result now follows from the two preceding inequalities and the representation for X given in (2.1). This completes the proof of Theorem 4.2.

The implications of Theorem 4.2 are now discussed. For a hydrologic pattern with $\min p = .2$ and $\max p = 3.8$ (such as was assumed for the computer simulations presented in Chapter 3), Theorem 4.2 implies that within any interval $[s, s+1]$ each component of Y becomes no more than five times as large as the maximum of the corresponding component of X and no less than 1/4 as small as the minimum of the corresponding component of X. For the simulation results presented in Chapter 3, this is very close to the situation observed in the surface water subzone when radionuclide input is to that subzone. In this case, the component Y_3 of Y tends to oscillate between $(1/\max p) SX_3$ and $(1/\min p) SX_3$. As discussed in the preceding section, there are often other processes involved which result in less variation in Y than indicated by the bounds in Theorem 4.2.

If Y is the solution to (1.3) for the 1-radionuclide case with decay constant λ , then the combined application of Theorems 4.1 and 4.2 yields

$$[e^{-2\lambda/\max p}] X[P(t)] \leq Y(t) \leq [e^{2\lambda/\min p}] X[P(t)].$$

For this case when the decay constant λ is small, the implication is that similar bounds exist for the solutions to (1.2) and (1.3).

As indicated by the simulation results presented in Chapter 3, the similarity between solutions to (1.1) and (1.2) is often much greater than that indicated by Theorem 4.2. Early in the investigation, it became clear that a satisfactory explanation of this behavior would result if it could be proved that in each interval $[n, n+1]$, each component of Y agrees with the corresponding component of X for at least one t . If this is true, a proof has thus far eluded the authors. However, a proof to establish that such behavior does eventually occur was obtained. This result is presented as Theorem 4.3. After the proof of this result, it is shown how it can be used to construct bounds on the differences between the asymptotic solutions SX and SY to (1.1) and (1.2), respectively.

Theorem 4.3. Suppose X and Y are solutions to (1.1) and (1.2), respectively, with initial values $X(0) = Y(0) = 0^5$. Then,

$$\lim_{n \rightarrow \infty} \min_{t \in [n, n+1]} |X_k(t) - Y_k(t)| = 0$$

for corresponding components X_k and Y_k of X and Y . Further, each component of SY equals the corresponding component of SX for at least one t in every time interval $[n, n+1]$.

Proof. For convenience, the result is established for $W(t) = Y(P^{-1}(t))$. Since $P^{-1}(t)$ is a continuous, increasing function, $P^{-1}(n) = n$ for every positive integer n and X has a constant asymptotic solution, a proof that the limit equals zero with Y replaced by W will imply that the limit equals zero as stated in the theorem.

If n is a positive integer and z is a number between 0 and 1, then

⁵Theorem 4.3 remains true for the initial values $X(0) = X_0$ and $Y(0) = Y_0$.

$$\begin{aligned}
W(n+z) &= \int_0^{n+z} e^{(n+z-s)Ah(s)} R ds && \text{[From (4.11) and (2.1)]} \\
&= \int_0^z e^{(n+z-s)Ah(s)} R ds + \int_z^{n+z} e^{(n+z-s)Ah(s)} R ds \\
&= \int_0^z e^{(n+z-s)Ah(s)} R ds + \int_0^n e^{(n-u)Ah(u+z)} R du,
\end{aligned}
\tag{4.16}$$

where the last equality follows from the change of variables $u = s-z$ in the second integral. Further, since

$$\int_0^n e^{(n-u)Ah(u+z)} R du$$

is continuous in z and

$$\begin{aligned}
&\int_0^1 \left[\int_0^n e^{(n-u)Ah(u+z)} R du \right] dz \\
&= \int_0^n e^{(n-u)A} \left[\int_0^1 h(u+z) dz \right] R du \\
&= \int_0^n e^{(n-u)A} R du = X(n),
\end{aligned}$$

it follows from the mean value theorem for integrals that, for the k th element X_k of X and each positive integer n ,

there exists a choice z_{kn} of z , $0 \leq z_{kn} \leq 1$, such that

$$\left[\int_0^n e^{(n-u)A_h(u+z_{kn})R} du \right]_k = X_k(n). \quad (4.17)$$

It now follows by combining (4.16) and (4.17) that

$$W_k(n+z_{kn}) - X_k(n) = \left[\int_0^{z_{kn}} e^{(n+z_{kn}-s)A_h(s)R} ds \right]_k. \quad (4.18)$$

It is next shown that

$$\lim_{n \rightarrow \infty} \int_0^z e^{(n+z-s)A_h(s)R} ds = 0, \quad (4.19)$$

with the convergence being uniform for $z \in [0, 1]$. This result in combination with the equality indicated in (4.18) is sufficient to establish the limit in the theorem. For $0 \leq z \leq 1$ and any positive integer n ,

$$\begin{aligned} \int_0^z e^{(n+z-s)A_h(s)R} ds &= e^{nA} \int_0^z e^{(z-s)A_h(s)R} ds \\ &= e^{nA} W(z), \end{aligned}$$

where the second equality follows from the relations in (4.11) and (2.1). Further,

$$\|e^{nA} W(z)\| \leq \|e^{nA}\| \cdot \|W(z)\| \leq \|e^{nA}\| \mu, \quad (4.20)$$

where $\|\cdot\|$ indicates the Euclidean vector or matrix norm, as appropriate, and

$$\mu = \max_{0 \leq z \leq 1} \|W(z)\|.$$

As noted in (2.2), it follows that

$$\lim_{n \rightarrow \infty} \|e^{nA}\| = 0 \quad (4.21)$$

because all eigenvalues of A have negative real part. The inequality in (4.19) can now be established from the relations in (4.20) and (4.21). As already noted, this result is sufficient to establish the desired limit in the conclusion of the theorem.

It is now shown that each component of SY equals the corresponding component of SX for at least one t in every time interval $[n, n+1]$. Let X_k and Y_k be corresponding components of X and Y . It follows from the previously established limit that there exists a sequence

$$\{s_n\}_{n=1}^{\infty}$$

such that $n \leq s_n \leq n + 1$ for each positive integer n and also such that

$$\lim_{n \rightarrow \infty} |X_k(s_n) - Y_k(s_n)| = 0.$$

Further, there exists a number $t \in [0, 1]$ and a subsequence

$$\{s'_n\}_{n=1}^{\infty}$$

of

$$\{s_n\}_{n=1}^{\infty}$$

such that

$$\lim_{n \rightarrow \infty} \text{mod}(s_n', 1) = t.$$

Now, since

$$\lim_{n \rightarrow \infty} Y_k(s_n') = SY_k(t) \quad \text{and} \quad \lim_{n \rightarrow \infty} X_k(s_n') = SX_k(t),$$

it follows that $SX_k(t) = SY_k(t)$. This completes the proof of Theorem 4.3.

It is now shown how use of Theorem 4.3 in conjunction with Theorem 4.2 can yield tighter bounds on the difference between corresponding elements of SX and SY than use of Theorem 4.2 alone. This technique is applicable to a particular subzone when the rate constant d_k for movement out of that subzone is "small." Specifically, it is established that

$$\begin{aligned} & [1 - (\max p/\min p)d_k] SX_k \\ & \leq SY_k(t) \leq [1 + (\max p/\min p)d_k] SX_k \quad (4.22) \end{aligned}$$

for $t \geq 1$.

Suppose the k th components of SX and SY are under consideration and d_k is the unperturbed (i.e., not multiplied by a hydrologic pattern $p(t)$) rate constant associated with that component. For example, as indicated in (3.1) and (3.2) the unperturbed rate constant d_1 associated with the groundwater subzones of both the River Zone and the Lake Zone used in the simulation studies is 3.2×10^{-4} . An inequality involving the derivative of SY_k is established first. Since $-p(t)d_kSY_k$ is the only negative term in the differential equation involving SY_k , it follows that

$$\begin{aligned}
dSY_k/dt &\geq -p(t)d_kSY_k \\
&\geq -(\max p)d_kSY_k \\
&\geq -(\max p/\min p)d_kSX_k, \qquad (4.23)
\end{aligned}$$

where the last inequality is obtained from Theorem 4.2.

Suppose $t \geq 1$. The left inequality in (4.22) is established first. It follows from Theorem 4.3 that there exists $t_0 \leq t$ such that $SX_k = SY_k(t_0)$ and also such that $t - t_0 \leq 1$. Now,

$$\begin{aligned}
SY_k(t) - SY_k(t_0) &\geq \int_{t_0}^t -(\max p/\min p)d_kSX_k ds && \text{[From (4.23)]} \\
&= -(\max p/\min p)d_kSX_k(t - t_0) \\
&\geq -(\max p/\min p)d_kSX_k,
\end{aligned}$$

and thus from the equality $SX_k = SY_k(t_0)$,

$$SY_k(t) \geq [1 - (\max p/\min p) d_k] SX_k. \qquad (4.24)$$

The right inequality in (4.22) is established next. It follows from Theorem 4.3 that there exists $t \leq t_0$ such that $SX_k = SY_k(t_0)$ and also such that $t_0 - t \leq 1$. Now,

$$\begin{aligned}
SY_k(t_0) - SY_k(t) &\geq \int_t^{t_0} -(\max p/\min p)d_kSX_k ds \\
&= -(\max p/\min p)d_kSX_k(t_0 - t) \\
&\geq -(\max p/\min p)d_kSX_k,
\end{aligned}$$

and thus from the equality $SX_k = SY_k(t_0)$,

$$[1 + (\max p / \min p) d_k] SX_k \geq SY_k(t). \quad (4.25)$$

The expression in (4.22) now follows by combining the inequalities in (4.24) and (4.25).

As already noted, the value used for d_1 in the simulation studies is 3.2×10^{-4} . Further, for these simulations, $\max p = 3.8$ and $\min p = .2$. With these values, (4.22) yields the following relationship between SX_1 and SY_1 for $t \geq 1$:

$$\begin{aligned} [1 - (19.0)(3.2 \times 10^{-4})] SX_1 &\leq SY_1(t) \\ &\leq [1 + (19.0)(3.2 \times 10^{-4})] SX_1, \end{aligned}$$

or equivalently,

$$(1 - .006) SX_1 \leq SY_1(t) \leq (1 + .006) SX_1.$$

In contrast, use of Theorem 4.2 alone yields

$$.26 SX_1 \leq SY_1(t) \leq 5.0 SX_1.$$

However, use of Theorem 4.3 to improve bounds is dependent on d_k being small. When this is not the case, Theorem 4.2 will produce sharper bounds.

At present, the tight bounds on solutions to (1.1) and (1.2) obtainable through use of Theorem 4.3 are applicable only to the steady state solutions SX and SY . However, as is clear from the computer simulations presented in Chapter 3, there may be little difference between the corresponding groundwater, soil and sediment components of X and Y in the time period before steady state is reached. As an examination of the arguments which establish the inequalities in (4.24) and (4.25) will reveal, the bounds indicated in (4.22) for steady state solutions can be extended to solutions $X_k(t)$ and

$Y_k(t)$ if Theorem 4.3 can be generalized to show that the corresponding components of X and Y have a common value (i.e., $X_k(t) = Y_k(t)$) in every interval of length 1.). As already noted, a proof for this has thus far eluded the authors. Should it be possible to establish such a result, then it would follow that the corresponding components of X and Y are practically indistinguishable as long as the associated rate constant for movement out of that component is small.

Chapter 5

Further Discussion of the Stochastic Case

For linear stochastic differential equations of the type

$$dz/dt = AZ + R, \quad z(0) = z_0 \quad (5.1)$$

if the randomness occurs only in the initial condition z_0 or in the inhomogeneous part R , it is usually possible to treat the derivative as a mean square derivative, and the theory is much the same as for deterministic equations. Additional discussion is given by T. T. Soong (So73, Chapter 7). In such situations, the expected value of the stochastic solution $E[z(t, \cdot)]$ will be the same as the deterministic solution of (5.1) with the stochastic parameters replaced by their expected values.

Analysis of equations of type (5.1) where the randomness occurs in the coefficients of A is much more complicated. The reader is referred to the paper by J. L. Strand (St70), where relationships between the mean square theory and the "sample path" theory (or "SP" approach, as Strand calls it) are explored. We have taken the "sample path" approach in this report because the paths of the process $S(t, \omega)p(t)$ are well-behaved enough to allow this. Indeed, all sample path solutions exist for the numerical example considered in Chapter 3. However, there can sometimes be a problem with trying to apply the mean square theory to a linear model when the distribution of $A(t, \cdot)$ is taken to be log normal. For example, Strand states that "if $A(\omega) \geq 0$, $x' = A(\omega)x$, $x(0) = 1$ has a 'mean square' solution on $[0, b]$ if, and only if, the Laplace transform of A is analytic for $s \leq 2b$ ".⁶ He is considering the scalar case here and A is just a random variable. If the Laplace transform of a distribution is analytic on $|s| \leq 2b$, then the moment generating function exists on the real part of that interval. However, we are dealing with the log normal distribution, which has no moment generating function.

⁶The Laplace transform is a function of the variable s ; see Strand (St70) for the exact form of the Laplace transformation under consideration.

We now try to apply Strand's criteria for the existence and uniqueness of a mean square solution to our equation

$$dZ(t, \omega)/dt = S(t, \omega)p(t)AZ(t, \omega) + R, \quad Z(0) = 0 \quad (5.2)$$

on the first one-month interval $[0, 1/12]$. As $S(t, \omega)$ is just a log normal random variable V which is not dependent on t , we will just need to show that condition (a') of Strand's Corollary 10 holds. In our case, this condition reduces to showing that

$$\sum_{k=1}^{\infty} \sqrt{E(V^{2k})} \cdot t^k < \infty \text{ for } t = p_1 \|A\|,$$

where $\|A\| = \sup_i \sum_k |a_{ik}|$ and p_1 is the value of p on the first one-month interval. However, for a log-normal variable V , the indicated summation turns out to be of the form

$$\sum_{k=1}^{\infty} e^{(k\mu + 4k^2\sigma^2)} \cdot t^k,$$

which diverges for any $t \neq 0$. Thus, it cannot be concluded from application of Corollary 10 that (5.2) has a unique mean square solution.

The preceding test for the existence of a mean square solution is mainly useful for linear equations $dZ/dt = A(t, \omega)Z + R$, where A has eigenvalues with positive real part. Our equation is much better behaved than this, so we are assured of the existence of a mean square solution by Theorem 3(a) of Strand's paper. To obtain this result, it is only necessary to verify that the integral

$$\int_0^b \|S(t, \omega)p(t)AZ(t, \omega) + R\|_2 dt$$

is finite for all $b > 0$. The integrand is less than or equal to

$$\|S(t, \omega)\|_2 \cdot p(t) \cdot \|A\| \cdot \|Z(t, \omega)\|_2 + 1$$

since $R > 0$ and $\sum R_i = 1$. Hence, the integrand is bounded for $0 < t < b$ since $\|S(t, \omega)\|_2 = 1$ for all t and $Z(t, \omega) < 1 \cdot t$ for all t and ω . Thus, the integral is finite for all $b > 0$ and so a mean square solution exists. However, this solution is not unique.

The dependence properties of the process $S(t, \omega)$ make it very difficult to obtain analytical expressions for the moments $E(Z_k(t, \cdot))$ and $SD(Z_k(t, \cdot))$. A search of the literature has failed to locate an analytical treatment of a problem as complicated as (5.1). The closest thing found was a paper by Becus (Bec79), which yields formulas for $E(Z_k(t, \cdot))$ to an equation of type (5.1). In this paper, the matrix A can assume only finitely many states (ours can assume a continuum of states and the coefficients $a_{ij}(t, \omega)$ for a given t are unbounded in ω in a very strong way), with Poisson "switching times" (at least our switching times are deterministic).

We know that the expected value $E(Z(t, \cdot))$ will not be the same as $Y(t)$, which is the deterministic solution to (5.1) with all stochastic parameters replaced by their expected values. In fact, it is surprising that in many of the plots $EZ(t)$ is running below $Y(t)$. Matis and Wehrly in their excellent survey paper (Mati79) on stochastic compartment systems point out that in the one compartment model $dZ/dt = az + r$, where a and r are independent random variables, it is necessarily true that "the mean of the stochastic model exceeds the deterministic model evaluated at the mean rates."

The problem of an analytical determination of the nature of $E(Z_k(t, \cdot))$ and $SD(Z_k(t, \cdot))$ under various assumptions concerning the distribution of $S(t, \omega)$ is deserving of further study. However, the Monte Carlo simulation study indicated that there is probably not enough difference between Z and X to warrant any real concern about the practice of using X as the model.

The greatest difference between Z and X occurs between the surface water components X_3 and Z_3 of the River Zone for radionuclide input to the surface water subzone. As already noted, $Z_3(t, \omega)$ behaves approximately like $SX_3/S(t, \omega)p(t)$ in this case. It would be interesting to investigate further just how much like the process

$$Q(t, \omega) = SX_3/S(t, \omega)p(t)$$

the component Z_3 behaves. For fixed t , $S(t, \omega)$ is a log-normal variable with mean 1 and variance .25, so $1/S(t, \omega)$ is a log-normal variable with mean 1.255 and variance .3906 or standard deviation .625. This implies that $E(Q(t, \cdot)) = 1.25 SX_3/p(t)$, and this is almost exactly what the plots $EZ(t)$ look like in this case (see Figures 3.7 and 3.11). Also,

$$\text{Max}\{E[Q(t, \cdot)] + 2 \cdot \text{SD}[Q(t, \cdot)] - SX_3\} / SX_3$$

will occur for $p(t) = .2$, where it equals $11.5 SX_3$. This agrees almost exactly with the information derived from the plots, reinforcing our suggestion that the process $Q(t, \cdot)$ is a good approximation to $Z_3(t, \cdot)$.

Chapter 6

Summary and Conclusion

The purpose of this investigation was to develop an understanding of the effects that variable hydrologic patterns have on predictions made by the Environmental Transport Model. Specifically, it was desired to gain insight as to whether it was appropriate to use "average" annual water and sediment flow rates in the derivation of model input parameters or whether such parameters should be represented as periodic functions of time or, more generally, as stochastic processes.

The investigation proceeded in the following manner. First, the asymptotic behavior of the Environmental Transport Model was determined for transport equation coefficients derived with average yearly values for flow rates. It was found that the model runs to a steady state condition in time periods that are often short with respect to the time periods considered in geologic waste disposal. Then, comparisons were made between steady state solutions and solutions obtained by perturbing the system in periodic and periodic-stochastic manners. Specifically, the coefficient matrix for the radionuclide transport equations was multiplied by a periodic function and a periodic stochastic process. The results of such perturbations were investigated both analytically and numerically. In performing the perturbations, the intent was not to produce an exact reproduction of the behavior of a natural system; rather, the intent was to develop a system whose variation would be amenable to both analytical and numerical analysis and which would, at the same time, provide a feeling as to how a real system might behave.

The result of such perturbations was to cause the predicted radionuclide concentrations to vary above and below the predicted values for the unperturbed system of equations. However, even in the most extreme cases, the transient variations were at most about one order of magnitude larger than the values for the unperturbed system. Most of the time, the variations were smaller. On the basis of the material contained in this report, it is felt that it is reasonable to continue to use "average" yearly values in defining flow rates for the Environmental Transport Model. The decision is made for several reasons: (1) to some extent the variations are offsetting in that

concentrations observed when variable hydrologic patterns are considered are both above and below those obtained when average rates are considered, (2) the highest concentrations occur for only part of a year, and (3) in the context of the geologic disposal of radioactive waste, much greater uncertainty in surface radionuclide concentrations will result from variation in potential discharge rates to the surface environment and in the actual nature of the surface environment. However, the concentrations obtained with average rates may be somewhat higher than the expected concentrations which result when additional variability is taken into account. It is emphasized that such observations are not "proved" in this report. Rather, a collection of simulation and analytic results is presented which help give credence to the acceptance of this modeling approach.

APPENDIX

The PROGRAM XYZ1 was used to generate the data points which were used in plotting the graphs of Figures 3-1 through 3-24. It is listed here in the form used to generate the graphs X, Y, AVEZ and AVEZ+SDZ of Figure 3-10 for the 1000th year, where the input is into the soil subzone of the base case River Zone. The data points $(t, X_i(t))$ for $1000 < t < 1001$ in increments of $DDT = 1/120$ are computed for $i = 1, 2, 3, 4$ and placed on permanent files "TAPE51" - "TAPE54". Similarly, the data points $(t, Y_i(t))$ are written onto tapes 61-64. After 100 simulations of the stochastic process $Z(t)$ from time $T = 0$ to $T = 1001$, the data points $(t, AVEZ_i(t))$ and $(t, AVEZ+SDZ_i(t))$ are written onto tapes 71-74 and 81-84, respectively. Then, the data points in these permanent files are used to generate the graphs in Figure 3-10. The plotting was actually done using the plotting routine PLOTIT designed by H. E. Anderson of Division 1223.

Certain functions and subroutines used in the program are special to the Sandia National Laboratories computing system. NORDEV is a standard normal variable generator and UDSET and RANDSET initialize the generator. SAXB is a subroutine for solving a linear system of equations $AX = B$, and RNAA is a subroutine for computing the eigenvalues and eigenvectors of a matrix.

P*

```
PROGRAM XYZ1(INPUT,OUTPUT,TAPE51,TAPE52,TAPE53,TAPE54,TAPE61,  
1 TAPE62,TAPE63,TAPE64,TAPE71,TAPE72,TAPE73,TAPE74,TAPE81,TAPE82,  
1 TAPE83,TAPE84)
```

C

C

C

C

```
PROGRAM FOR COMPUTING SOLUTIONS X, Y, AND Z TO DE'S  $X' = AX + R$ ,  
 $Y' = P(T)AY + R$ , AND  $Z' = RU(T,W)P(T)AY + R$  AND COMPARING VALUES
```

```
REAL KD,MS,NORDEV  
DIMENSION A(5,4),R(4),IN(4),EUR(4),EVI(4),UEC(4,4),X(4),  
1AA(4,4),B(4),SX(4),UU(4,4),UW(4),RW(5,4),MS(4),RS(5,4),S(4),  
1KD(4),EU(4),Y(4),SY(4),P(12),Z(4),AVEZ(4,121),SDZ(4,121),  
1W(4)
```

```
CALL KILL(115) $ NYR=1000 $ TYR=1000. $ DT=1/12. $ DDT=1/120.
```

```
PRINT 19
```

```
19 FORMAT(* ENTER RANDOM STARTER*)
```

```
READ*,NST
```

```
CALL UDSET(NST)
```

```
CALL RANSET(NST)
```

C

C

C

```
DEFINE HYDROLOGIC PATTERN
```

```
P(1)=.4$P(2)=.3$P(3)=.6$P(4)=2.0$P(5)=3.8$P(6)=2.5
```

```
P(7)=.7$P(8)=.2$P(9)=.2$P(10)=.3$P(11)=.4$P(12)=.6
```

```
PRINT 81
```

```
PRINT*, "THE HYDROLOGIC PATTERN P(I), I=1,12 IS"
```

```
PRINT 11,P
```

```
11 FORMAT(12F6.1/)
```

C

C

C

```
GIVE NONVARIABLE VOLUMES, MASSES, AND FLOW RATES
```

```
UW(1)=1.4E12 $ MS(1)=9.4E12 $ RW(3,1)=2.2E12
```

```
UW(2)=2.0E10 $ MS(2)=1.1E11 $ RW(1,2)=9.8E10
```

```
UW(3)=2.2E10 $ RW(5,3)=1.9E13
```

```
UW(4)=8.7E9 $ MS(4)=2.3E10
```

```
KD(1)=1000.$KD(2)=1000.$KD(3)=1000.$KD(4)=1000.
```

```
RW(3,2)=4.E10 $ RS(3,2)=1.1E8
```

```
MS(3)=3.5E6 $ RW(2,3)=RW(3,2) $ RS(2,3)=RS(3,2)
```

RW(4,3)=8.7E8 \$ RS(4,3)=2.3E9
RS(5,3)=3.0E9 \$ RU(3,4)=RU(4,3) \$ RS(3,4)=RS(4,3)

C
C
C

GENERATE MATRIX A

DO 3 J=1,4
S(J)=(KD(J)*MS(J))/(KD(J)*MS(J)+UW(J))
DO 3 I=1,5
IF(I.EQ.J)GO TO 3
A(I,J)=(1.-S(J))*(RW(I,J)/UW(J))+S(J)*(RS(I,J)/MS(J))
3 CONTINUE
A(1,1)=-A(3,1)-A(4,1)-.000084
A(2,2)=-A(1,2)-A(3,2)-.000084
A(3,3)=-A(2,3)-A(4,3)-A(5,3)-.000084
A(4,4)=-A(3,4)-.000084

C
C
C

DEFINE INPUT VECTOR

R(1)=0.\$R(2)=1.\$R(3)=0.\$R(4)=0.

C
C
C

COMPUTE STEADY STATE VALUES SX(I),I=1,2,3,4

DO 5 I=1,4 \$ DO 5 J=1,4
5 AA(I,J)=A(I,J)
CALL SAXB(4,4,1,AA,R,0,IN,KER)
DO 6 I=1,4
6 SX(I)=-R(I)

C
C
C

GET MAIN EIGEN VALUES AND EIGEN VECTORS

DO 15 I=1,4 \$ DO 15 J=1,4
15 AA(I,J)=A(I,J)
CALL RNAA(4,4,AA,EVR,EVI,VEC,IERR)

C
C
C

GET COEFFICIENTS B(I) USED IN COMPUTATION OF X(I)

DO 17 I=1,4 \$ B(I)=-SX(I) \$ DO 17 J=1,4
17 UV(I,J)=VEC(I,J)

```

CALL SAXB(4,4,1,UU,B,0,IN,KER)
KK=2 $ KN=121
WRITE(51,*)KK,KN $ WRITE(52,*)KK,KN $ WRITE(53,*)KK,KN
WRITE(54,*)KK,KN
WRITE(61,*)KK,KN $ WRITE(62,*)KK,KN $ WRITE(63,*)KK,KN
WRITE(64,*)KK,KN
WRITE(71,*)KK,KN $ WRITE(72,*)KK,KN $ WRITE(73,*)KK,KN
WRITE(74,*)KK,KN
WRITE(81,*)KK,KN $ WRITE(82,*)KK,KN $ WRITE(83,*)KK,KN
WRITE(84,*)KK,KN

```

C
C
C

```
RUN Y OUT TO YEAR NYR
```

```

DO 50 N=1,NYR
DO 50 M=1,12
Q=P(M)
DO 35 I=1,4 $ S(I)=SX(I)/Q $ EU(I)=EUR(I)*Q $ W(I)=Y(I)-S(I)
DO 35 J=1,4
35 UU(I,J)=VEC(I,J)
CALL SAXB(4,4,1,UU,W,0,IN,KER)
DO 41 I=1,4
41 Y(I)=W(1)*VEC(I,1)*EXP(EU(1)*DT)+W(2)*VEC(I,2)*EXP(EU(2)*DT)
1+S(I) +W(3)*VEC(I,3)*EXP(EU(3)*DT)+W(4)*VEC(I,4)*EXP(EU(4)*DT)
50 CONTINUE

```

C
C
C

```
COMPUTE Y(I) IN INCREMENTS OF DDT FOR YEAR NYR AND PUT ON TAPE6I
```

```

T=TYR $ WRITE(61,*)T,Y(1) $ WRITE(62,*)T,Y(2)
WRITE(63,*)T,Y(3) $ WRITE(64,*)T,Y(4)
DO 100 M=1,12
Q=P(M)
DO 65 I=1,4 $ S(I)=SX(I)/Q $ EU(I)=EUR(I)*Q $ W(I)=Y(I)-S(I)
DO 65 J=1,4
65 UU(I,J)=VEC(I,J)
CALL SAXB(4,4,1,UU,W,0,IN,KER)
DO 80 J=1,10 $ T=J*DDT
DO 82 I=1,4
82 Y(I)=W(1)*VEC(I,1)*EXP(EU(1)*T)+W(2)*VEC(I,2)*EXP(EU(2)*T)

```

```

1+S(I) +W(3)*VEC(I,3)*EXP(EU(3)*T)+W(4)*VEC(I,4)*EXP(EU(4)*T)
L=M-1
WRITE(61,*)TYR+L*DT+J*DDT,Y(1) $ WRITE(62,*)TYR+L*DT+J*DDT,Y(2)
WRITE(63,*)TYR+L*DT+J*DDT,Y(3) $ WRITE(64,*)TYR+L*DT+J*DDT,Y(4)
100 CONTINUE
ENDFILE 61 $ ENDFILE62 $ ENDFILE63 $ ENDFILE64
DO 200 NREP=1,100

```

C
C
C

```

RUN Z OUT TO YEAR NYR

```

```

RU=EXP(.47238074*NORDEV(0))
Z(1)=0. $ Z(2)=0. $ Z(3)=0. $ Z(4)=0.
DO 250 N=1,NYR
DO 250 M=1,12
Q=P(M)*RU$RU=EXP(.40121505*NORDEV(0)-.05268026)*(RU**52783527)
DO 135 I=1,4 $ S(I)=SX(I)/Q $ EU(I)=EUR(I)*Q $ W(I)=Z(I)-S(I)
DO 135 J=1,4
135 UU(I,J)=VEC(I,J)
CALL SAXB(4,4,1,UU,W,0,IN,KER)
DO 141 I=1,4
141 Z(I)=W(1)*VEC(I,1)*EXP(EU(1)*DT)+W(2)*VEC(I,2)*EXP(EU(2)*DT)
1+S(I) +W(3)*VEC(I,3)*EXP(EU(3)*DT)+W(4)*VEC(I,4)*EXP(EU(4)*DT)
250 CONTINUE

```

C
C
C
C

```

COMPUTE Z(I) IN INCREMENTS OF DDT FOR YEAR NYEAR, AT EACH STAGE
SET AVEZ(I,J)=AVEZ(I,J)+Z(I) AND SDZ(I,J)=SDZ(I,J)+Z(I)**2

```

```

DO 161 I=1,4 $ AVEZ(I,1)=AVEZ(I,1)+Z(I)
161 SDZ(I,1)=SDZ(I,1)+Z(I)**2 $ JJ=2
DO 200 M=1,12
Q=P(M)*RU$RU=EXP(.40121505*NORDEV(0)-.05268026)*(RU**5278527)
DO 165 I=1,4 $ S(I)=SX(I)/Q $ EU(I)=EUR(I)*Q $ W(I)=Z(I)-S(I)
DO 165 J=1,4
165 UU(I,J)=VEC(I,J)
CALL SAXB(4,4,1,UU,W,0,IN,KER)
DO 200 J=1,10 $ T=J*DDT
DO 181 I=1,4
181 Z(I)=W(1)*VEC(I,1)*EXP(EU(1)*T)+W(2)*VEC(I,2)*EXP(EU(2)*T)

```

```

1+S(I) +W(3)*UEC(I,3)*EXP(EU(3)*T)+W(4)*UEC(I,4)*EXP(EU(4)*T)
DO 182 I=1,4 $ AVEZ(I,JJ)=AVEZ(I,JJ)+Z(I)
182 SDZ(I,JJ)=SDZ(I,JJ)+Z(I)**2 $ JJ=JJ+1
200 CONTINUE $ T=TYR-DDT

```

```

C
C CONVERT AVEZ AND SDZ TO ACTUAL AVERAGES AND STANDARD DEVIATIONS
C AND WRITE AVEZ(I,JJ) ON TAPE7I AND AVEZ(I,JJ)+SDZ(I,JJ) ON
C TAPE8I FOR JJ=1,121
C

```

```

DO 201 JJ=1,121 $ T=T+DDT
DO 202 I=1,4 $ AVEZ(I,JJ)=AVEZ(I,JJ)/100.
202 SDZ(I,JJ)-=((SDZ(I,JJ)/100.)-(AVEZ(I,JJ))**2)**.5
WRITE(71,*)T,AVEZ(1,JJ) $ WRITE(72,*)T,AVEZ(2,JJ)
WRITE(73,*)T,AVEZ(3,JJ) $ WRITE(74,*)T,AVEZ(4,JJ)
WRITE(81,*)T,AVEZ(1,JJ)+SDZ(1,JJ)
WRITE(82,*)T,AVEZ(2,JJ)+SDZ(2,JJ)
WRITE(83,*)T,AVEZ(3,JJ)+SDZ(3,JJ)
WRITE(84,*)T,AVEZ(4,JJ)+SDZ(4,JJ)
201 CONTINUE $ ENDFILE 81 $ ENDFILE 82 $ ENDFILE 83 $ ENDFILE 84
ENDFILE 71 $ ENDFILE 72 $ ENDFILE 73 $ ENDFILE 74

```

```

C
C COMPUTE X(I) IN INCREMENTS OF DDT FOR YEAR NYEAR AND PUT ON TAPES I
C

```

```

T=TYR-DDT
DO 400 J=1,121 $ T=T+DDT
DO 381 I=1,4
381 X(I)=B(1)*UEC(I,1)*EXP(EUR(1)*T)+B(2)*UEC(I,2)*EXP(EUR(2)*T)
1+SX(I) +B(3)*UEC(I,3)*EXP(EUR(3)*T)+B(4)*UEC(I,4)*EXP(EUR(4)*T)
WRITE(51,*)T,X(1) $ WRITE(52,*)T,X(2)
WRITE(53,*)T,X(3) $ WRITE(54,*)T,X(4)
400 CONTINUE
ENDFILE 51 $ ENDFILE 52 $ ENDFILE 53 $ ENDFILE 54

```

```

C
C PRINT OUT R AND A
C
PRINT 70
70 FORMAT(* THE INPUT VECTOR R IS*)
R(1)=0.$R(2)=1.$R(3)=0.$R(4)=0.

```

```
PRINT 80,R
PRINT 81
81 FORMAT(/)
PRINT 76
76 FORMAT(* THE A MATRIX IS*)
PRINT 83,((A(I,J),J=1,4),I=1,5)
PRINT 81
80 FORMAT(4E12.2)
83 FORMAT(4E12.6)
STOP $ END
SUBROUTINE KILL(NN)
DIMENSION IE(6)
DATA IE/-0,-0,-0,0,-0,-0/
CALL SYSTEMC(NN,IE)
RETURN
END
```


REFERENCES

- Ap77 Apps, J. A., Lucas, J., Mather, H. K. and Tsao, L., 1977, "Theoretical and Experimental Evaluation of Waste Transport in Selected Rocks: 1977 Annual Report of LBL Contract No. 45901AK," Report No. LBL-7022, Lawrence Berkeley Laboratory, Berkeley, CA.
- Bec79 Becus, G. A., 1979, "Random Evolutions and Stochastic Compartments," Math. Biosciences 44, pp. 241-254.
- Bel70 Bellman, R., 1970, Introduction to Matrix Analysis (McGraw-Hill, NY).
- Br69 Brauer, F. and Noel, J. A., 1969, The Qualitative Theory of Differential Equations (W. A. Benjamin Inc., NY).
- Ca78 Campbell, J. E., Dillon, R. T., Tierney, M. S., Davis, H. T., McGrath, P. E., Pearson, F. J., Shaw, H. R., Helton, J. C., and Donath, F. A., 1978, "Risk Methodology for Geologic Disposal of Radioactive Waste: Interim Report," Report No. SAND78-0029, Sandia Laboratories, Albuquerque, NM.
- Do79 Dollard, J. D. and Friedman, C. N., 1979, Product Integration (Addison-Wesley, Reading, MA).
- Fr68 Franklin, J. N., 1968, Matrix Theory (Prentice Hall, Englewood Cliffs, NJ).
- Ha67 Harms, A. A. and Campbell, T. H., 1967, "An Extension of the Thomas-Fiering Model for the Sequential Generation of Streamflow," Water Resour. Res. 3, pp. 653-661.
- Hea73 Heathcote, H. W., 1973, "Asymptotic Behavior in a Deterministic Epidemic Model," Bull. Math. Biol. 35, pp. 607-613.
- Hel80 Helton, J. C. and Iman, R. L., 1980, "Risk Methodology for Geologic Disposal of Radioactive Waste: Sensitivity Analysis of the Environmental Transport Model," Report No. NUREG/CR-1636 (Vol. 2), SAND79-1393, Sandia National Laboratories, Albuquerque, NM.

Hel81a Helton, J. C., Brown, J. B., and Iman R. L., 1981, "Risk Methodology for Geologic Disposal of Radioactive Waste: Asymptotic Properties of the Environmental Transport Model," Report No. NUREG/CR-1636 (Vol. 3), SAND79-1908, Sandia National Laboratories, Albuquerque, NM.

Hel81b Helton, J. C. and Kaestner, P. C., 1981, "Risk Methodology for Geologic Disposal of Radioactive Waste: Model Description and User Manual for Pathways Model," Report No. NUREG/CR-1636 (Vol. 1), SAND78-1711, Sandia National Laboratories, Albuquerque, NM.

Im78 Iman, R. L., Helton, J. C., and Campbell, J. E., 1978, "Risk Methodology for Geologic Disposal of Radioactive Waste: Sensitivity Analysis Techniques," Report No. SAND78-0912, Sandia Laboratories, Albuquerque, NM.

Mata67 Matalas, N. C., 1967, "Mathematical Assessment of Synthetic Hydrology," Water Resour. Res. 3, pp. 937-945.

Mati79 Matis, J. H. and Wehrly, T. E., 1979, "Stochastic Models of Compartmental Systems," Biometrics 35, pp. 199-220.

Mo70 Moreau, D. H. and Pyatt, E. E., 1970, "Weekly and Monthly Flows in Synthetic Hydrology," Water Resour. Res. 6, pp. 53-61.

Ry71 Rykiel, E. J., Jr. and Kuenzel, N. T., 1971, "Analog Computer Models of 'The Wolves of Isle Royale,'" in Systems Analysis and Simulation in Ecology, Vol. I (edited by Patten, B. C.) (Academic Press, NY).

So73 Soong, T. T., 1973, Random Differential Equations in Science and Engineering (Academic Press, NY).

St70 Strand, J. L., 1970, "Random Ordinary Differential Equations," J. Diff. Eq. 7, pp. 538-553.

Tho62 Thomas, H. A. and Fiering, M. D., 1962, "Mathematical Synthesis of Streamflow Sequences for the Analysis of River Basins by Simulation." Ch. 12 of Design of Water Resource Systems (edited by Arthur Maass, et al.) (Harvard Univ. Press, Cambridge, MA).

- Thr72 Thron, C. D., 1972, "Structure and Kinetic Behavior of Linear Multicompartment Systems," Bull. Math. Biophysics 34, pp. 277-298.
- Ti78 Tiwari, J. L., Hobbie, J. E., Reed, J. P., Stanley, D. W., and Miller, M. C., 1978, "Some Stochastic Differential Equation Models of an Aquatic Ecosystem," Ecological Modelling 4, pp. 3-27.
- To79 Towse, D., 1979, "Geoscience Parameter Data Base Handbook," Report No. UCRL-52557 (Draft), Lawrence Livermore Laboratory, Livermore, CA.
- Ye72 Yevdjevich, V. M., 1972, Stochastic Processes in Hydrology, (Water Resources Publications, Ft. Collins, CO).

DISTRIBUTION:

U.S. NRC Distribution Contractor (CDSI)
7300 Pearl Street
Bethesda, MD 20014
375 copies for GF
25 copies for NTIS

Author selected distribution - 148 copies
(List available from author.)

400 C. Winter
1223 R. L. Iman
1223 M. Shortencarrier
4000 A. Narath
4400 A. W. Snyder
4410 D. J. McCloskey
Attn: J. W. Hickman
G. V. Varnado
L. D. Chapman
4413 D. C. Aldrich
4413 M. Chu
4413 R. M. Cranwell
4413 N. C. Finley
4413 J. C. Helton (25)
4413 J. Johnson
4413 D. Longsine
4413 A. Muller
4413 N. R. Ortiz (5)
4413 R. M. Ostmeyer
4413 R. Pepping
4413 L. T. Ritchie
4413 G. Runkle
4413 M. Siegel
4413 J. Sprung
4510 W. D. Weart
4511 G. E. Barr
4511 L. R. Hill
4514 M. L. Merritt
4514 M. S. Tierney
4530 R. W. Lynch
4536 D. M. Talbert
5521 M. G. Marietta
3141 L. J. Erickson (5)
3151 W. L. Garner (3)
8214 M. A. Pound

